AD-A083 010 SMITHSONIAN ASTROPHYSICAL OBSERVATORY CAMBRIDGE MASS F/G 4/1
CALCULATIONS PERTAINING TO THE ENERGY BALANCE AND PLASMA MOTION--ETC(U)
NOV 79 A DALGARNO, E CONSTANTINIDES F19628-78-C-0047
UNCLASSIFIED AFGL-TR-79-0270 NL

1 OF 2
AD A083 010

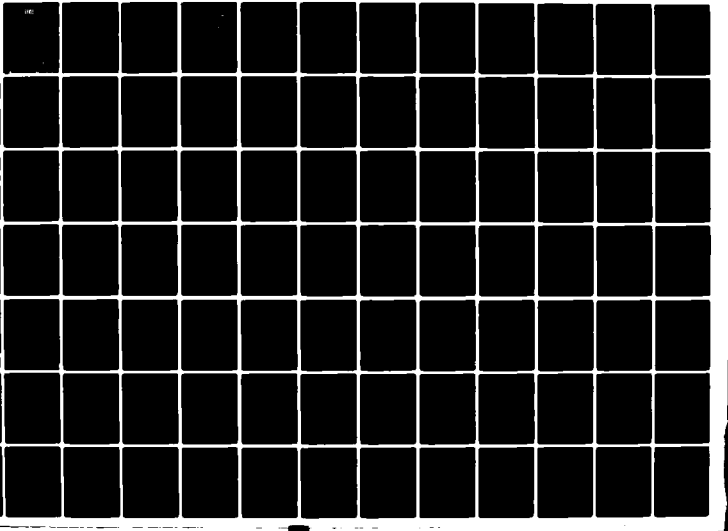

LEVEL II

12 5

AFGL-TR-79-0270

CALCULATIONS PERTAINING TO THE ENERGY BALANCE AND PLASMA MOTIONS IN THE IONOSPHERE

Alexander Dalgarno
Eustratios Constantinides

Smithsonian Astrophysical Observatory
60 Garden Street
Cambridge, Massachusetts 02138

November 1979

Final Report

1 January 1978 - 30 September 1978

AD A083010

Approved for public release; distribution unlimited

AIR FORCE GEOPHYSICS LABORATORY
AIR FORCE SYSTEMS COMMAND
UNITED STATES AIR FORCE
HANSCOM AFB, MASSACHUSETTS 01731

Qualified requestors may obtain additional copies from the Defense Documentation Center. All others should apply to the National Technical Information Service.

Unclassified

SECURITY CLASSIFICATION OF THIS PAGE (When Data Entered)

REPORT DOCUMENTATION PAGE	READ INSTRUCTIONS BEFORE COMPLETING FORM
1. REPORT NUMBER (19) (18) AFGL-TR-79-0270	2 GOVT ACCESSION NO.
3. RECIPIENT'S CATALOG NUMBER (Rept.)	
4. TITLE (and Subtitle) (6) CALCULATIONS PERTAINING TO THE ENERGY BALANCE AND PLASMA MOTIONS IN THE IONOSPHERE	5. TYPE OF REPORT & PERIOD COVERED (9) Final 1 Jan [redacted] 30 Sep [redacted] 78
	6 PERFORMING ORG. REPORT NUMBER
7. AUTHOR(s) (10) Alexander Dalgarno [redacted] Eustratios Constantinides	8. CONTRACT OR GRANT NUMBER(s) (15) F19628-78-C-0047
9. PERFORMING ORGANIZATION NAME AND ADDRESS Smithsonian Astrophysical Observatory 60 Garden Street Cambridge, Massachusetts 02138	10. PROGRAM ELEMENT, PROJECT, TASK AREA & WORK UNIT NUMBERS (16) 61102F 2311G2 AP (17) 02
11. CONTROLLING OFFICE NAME AND ADDRESS Air Force Geophysics Laboratory Hanscom AFB, Massachusetts 01731 Monitor: Rita Sagalyn/PHG	(11) 12. REPORT DATE Nov [redacted] 79
	13. NUMBER OF PAGES 148
14. MONITORING AGENCY NAME & ADDRESS (if different from Controlling Office) (12) 142	15. SECURITY CLASS. (of this report) Unclassified
	15a. DECLASSIFICATION/DOWNGRADING SCHEDULE

16. DISTRIBUTION STATEMENT (of this Report)

Approved

DISTRIBUTION STATEMENT A
Approved for public release;
Distribution Unlimited

17. DISTRIBUTION STATEMENT (of the abstract entered in Block 20, if different from Report)

Approved for public release; distribution unlimited

18. SUPPLEMENTARY NOTES

19. KEY WORDS (Continue on reverse side if necessary and identify by block number)

Ionosphere, Plasma Motions, Electric Fields, Transport Properties

20. ABSTRACT (Continue on reverse side if necessary and identify by block number)

Plasma motions in the upper atmosphere have been investigated with the aid of satellite data. It is shown that the major ion, O^+, moves in response to the sum of the forces on itself and on electrons. Minor ions follow the motion of the major ion. The observed plasma velocity in the vertical direction is in harmony with the assumption of an eastward electric field of between 3 and 5 millivolts per meter. The

DD FORM 1 JAN 73 1473 EDITION OF 1 NOV 65 IS OBSOLETE

SECURITY CLASSIFICATION OF THIS PAGE (When Data Entered)

044850

(block 20, cont.)

present investigation demonstrates clearly the need for measurements of electric fields and plasma drifts.

1. INTRODUCTION AND SUMMARY

Knowledge of the energy balance and plasma motions in the atmosphere is essential for the accurate prediction of atmospheric effects on radio communications under both normal and disturbed conditions. A substantial portion of the variable content of atmospheric energy is stored in charged particles. Previous investigations have demonstrated that the concentrations of atomic ions are controlled by transport. Electric fields play an important part in determining transport properties. Section 2 reviews some aspects of the photochemistry of atmospheric ions and assesses the magnitude of transport effects on atomic ions.

The effort undertaken under the present investigation has focused on formulating procedures to utilize satellite measurements in order to obtain a self-consistent model of charged particle motions. Such a formulation is presented in Section 3. Section 4 deals with the simpler situation of one ionic species in addition to electrons for the purpose of illustrating several features of the general theory. Results utilizing satellite data are presented in Section 5. It is shown, generally, that the major ion moves in response to the sum of the forces on itself and on electrons, and that minor ions follow the motion of the major ion. It is further shown that the observed vertical plasma drift velocity can be accounted

for by an eastward electric field of between 3 and 5 millivolts per meter. Calculations based on the assumption that horizontal variations are negligible cannot account for the transport term in the equation of continuity, probably because the data pertains to the (magnetically) equatorial region. Application of the present approach to midlatitude data is suggested.

Appendix A lists the data used in the calculations. Appendix B reviews the definition of momentum transfer collision frequencies, and presents collision frequencies for electrons and O^+ ions. An updated version of atomic and molecular cross sections is presented in Appendix F. A procedure for the calculation of the spectrum of secondary electrons produced by energetic precipitating particles is given in Section 6, and Appendices C, D, and E.

2. ION CONCENTRATIONS IN THE DAYTIME IONOSPHERE

The altitude profiles of ionic species in the upper atmosphere are determined by photochemical processes and by transport. In order to assess the effects of transport, it is necessary to have knowledge of the relative importance of the photochemical effects. Using data from an Atmosphere Explorer orbit (see Appendix A for details) we show that the altitude profiles of molecular ions are determined by photochemical processes under the assumption of local equilibrium, i.e. that transport effects are negligible for molecular ions. For atomic ions, on the other hand, transport processes play the dominant part in determining altitude profiles, particularly at the upper altitudes.

Fig. 1 is a plot of the concentration of the molecular ions (O_2^+, NO^+, N_2^+) versus altitude. The observed concentrations are in harmony with theoretical values calculated under the assumption of local photochemical equilibrium. The agreement between theory and observations is due to the short chemical lifetimes of the molecular ions. Fig. 2 is a plot of the chemical lifetime of each ion vs. altitude. The primary sink for molecular ions is dissociative recombination. Accordingly chemical lifetimes for these ions tend to decrease with increasing altitude, following the increase with altitude of the electron concentration. Under daytime conditions, the

sources are balanced by the sink from dissociative recombination in the equation of continuity. At night, both of these terms are reduced significantly, and transport terms become of comparable magnitude.

Fig. 2 further shows that chemical lifetimes increase rapidly with altitude for the atomic ions. The increase is particularly rapid for He^+, for which the only significant sink is the reaction with molecular nitrogen. Thus the chemical lifetime of He^+ is inversely proportional to the N_2 concentration, and therefore transport effects dominate the He^+ profile at the upper altitudes. This is apparent in Fig. 3, which shows the observed and calculated altitude profiles for the atomic ions.

Fig. 3 contains three profiles for each of the other atomic ions (O^+, H^+, and N^+). At the upper altitudes, the significant sources for these ions are photoionization and charge transfer from other atomic ions. The solid line profile for each ion is a purely theoretical calculation under the assumption of local photochemical equilibrium (i.e. no transport effects are included) and the concentrations of the ions are determined by solving the coupled equations of continuity. Fig. 3 shows that these purely theoretical profiles are increasingly at variance with the observed concentrations above 250 km, reflecting the neglect of transport on all the coupled species. Fig. 3 also displays a second theoretical

profile, calculated under the assumption of photochemical equilibrium but utilizing observed concentrations for all ions except the ion of interest. In this instance the agreement between calculated and observed values is very good. This latter result indicates that the model of photochemical reactions utilized is an accurate one. It does not follow, however, that the atomic ions are in local photochemical equilibrium. In what follows we indicate why the agreement between observed ion concentrations and those calculated by the photochemical model (without transport) improves if, in computing the concentration of a particular ion, the observed concentrations of all other ions are used. The improvement is very substantial in the case of O^+, H^+ and N^+. The improvement results from the fact that the observed concentrations implicitly contain the effects of transport. We demonstrate this idea by considering two ions whose photochemistry is coupled.

The equation of continuity states that the rate of production minus the rate of loss equals the divergence of the flux:

$$P - L = \nabla \cdot \vec{F} \ .$$

For the example under consideration, we have

$$P_1 = Q_1 + k_2 X_2 \qquad L_1 = (\ell_1 + k_1) X_1 \qquad \nabla \cdot \vec{F}_1 \equiv t_1 X_1$$

$$P_2 = Q_2 + k_1 X_1 \qquad L_2 = (\ell_2 + k_2) X_2 \qquad \nabla \cdot \vec{F}_2 \equiv t_2 X_2$$

where the Q's represent production rates not involving the ions of interest, the ℓ's represent loss rates not involving the ions of interest, the X's represent the ion concentrations, and the t's are defined by the equations. The equations of continuity may then be written as

$$Q_1 + k_2X_2 - (\ell_1+k_1)X_1 = t_1X_1$$

$$Q_2 + k_1X_1 - (\ell_2+k_2)X_2 = t_2X_2 \ .$$

The solution is

$$X_1 = [(\ell_2+k_2+t_2)\ Q_1 + k_2Q_2] \ / \ [(\ell_2+k_2t_2)(\ell_1+k_1+t_1) - k_1k_2]$$

with an analogous expression for X_2. This is the exact solution and therefore represents the observed value of X_1. If we neglect transport ($t_1 = t_2 = 0$) the solution is

$$Y_1 = [(\ell_2+k_2)\ Q_1 + k_2Q_2] \ / \ [(\ell_2+k_2)(\ell_1+k_1) - k_1k_2]$$

where a different symbol (Y) has been used to indicate that this is an approximate value. We compare this with the exact (observed) value X_1:

$$Y_1 = X_1 \ \{ \ 1 + [(\ell_2+k_2)t_1 + k_2t_2(X_2/X_1)] \ / \ (\ell_1\ell_2+\ell_1k_2+\ell_2k_1) \ \}$$

We note first that the difference is of order t/ℓ. This is a ratio that increases rapidly with altitude, since transport effects increase with altitude whereas ℓ decreases in proportion to the neutral density. Secondly, the difference involves,

in general, the transport of both ions. Thirdly, the difference can be of either sign, since the t's can be of either sign. Finally, if the ratio of concentrations (X_2/X_1) is very large, the inaccuracy in the concentration of the minor ion depends on the transport characteristics of the major ion. This observation indicates that the use of observed concentrations is particularly beneficial to the calculation of minor ion concentrations.

Using observed concentrations in a pure photochemical calculation (without transport) yields the solutions

$$Z_1 = X_1 \left[1 + t_1/(\ell_1+k_1)\right]$$

We have used a different symbol (Z) for the computation that neglects transport but uses observed concentrations for ions other than the ion of interest. The error, in this instance, involves only the transport properties of the ion of interest. Further, the error is proportional to $t/(\ell+k)$. This is of practical interest forthe concentrations of O^+, H^+, and N^+ because ℓ is proportional to the molecular densities, whereas k is proportional to atomic densities. Thus the error in Z_1 is of order (ℓ/k) compared to the error in Y_1, i.e. in the ratio of molecular to atomic densities. Since this ratio decreases rapidly with altitude, the ratio of the error in Z_1 compared to the error in Y_1 decreases rapidly with altitude. Finally, it should be noted that transport effects are needed to reconcile the difference between the observed value (X_1)

and Z_1, not the difference between X_1 and Y_1.

It is useful to discuss the definition of chemical lifetimes. If the equation of continuity does not involve coupling to other ions, the chemical lifetime is uniquely defined as the reciprocal of the factor multiplying the ion concentration in the loss term. When ions are coupled in the equation of continuity, there are two lifetimes that can be defined. In the conventional definition, $1/(\ell_1+k_1)$ in the equation for X_1 is the lifetime for an individual ion. To discuss the second definition, we write the equation for X_1 in the form

$$Q_1 + Q_2/(\ell_2+k_2+t_2) - [(\ell_1+k_1) - k_1k_2 / (\ell_2+k_2+t_2)] X_1 = \nabla\cdot\vec{F}_1 .$$

It can be argued that the reciprocal of the factor multiplying X_1 in this expression is the physically meaningful lifetime. In the absence of transport, and if $k_2 \gg \ell_2$, the lifetime then becomes $1/\ell_1$, which is much larger than $1/(\ell_1+k_1)$ in the upper atmosphere for the species of interest (H^+,O^+, H^+).

3. GENERAL THEORY OF IONOSPHERIC MOTIONS

A. Determination of Particle Velocities

The drift velocity for each species in a gas mixture is determined by the momentum transfer equations which may be written as (cf. Schunk 1977)

$$\nabla p_s - n_s m_s \vec{g} - n_s e_s (\vec{E} + \frac{1}{c}\vec{v}_s \times \vec{B}) = -\sum_t n_s m_s \nu_{st} (\vec{v}_s - \vec{v}_t)$$

where $\vec{E}$ and $\vec{B}$ are the electric and magnetic fields, respectively, p_s, n_s, m_s, e_s are the partial pressure, concentration, mass, and charge, respectively, $\vec{g}$ is the gravitational acceleration, and ν_{st} is the collision frequency of species s with species t. For the charged species it is convenient to deal with drift velocities relative to the neutral medium:

$$\vec{u}_i = \vec{v}_i - \vec{V}$$

where $\vec{V}$ is a suitably defined velocity for the neutrals. Let

$$\vec{F}_i = m_i \vec{g} + e_i (\vec{E} + \frac{1}{c}\vec{V} \times \vec{B}) - \nabla p_i / n_i + m_i \sum_n \nu_{in} (\vec{v}_n - \vec{V})$$

where the sum over n indicates that the summation extends over neutral species only. Then

$$\sum_j m_i \nu_{ij} (\vec{u}_i - \vec{u}_j) + \sum_n m_i \nu_{in} \vec{u}_i - e_i \vec{u}_i \times \vec{B}/c = \vec{F}_i$$

where the sum over j extends over charged species only. Finally, let

$$\bar{\nu}_i = \sum_j \nu_{ij} + \sum_n \nu_{in}$$

$$\omega_i = e_i B/m_i C$$

$$\hat{b} = \vec{B}/B$$

where B is the magnitude of the magnetic field, and ω_i is the gyrofrequency. Then

$$m_i \bar{\nu}_i \vec{u}_i - m_i \sum_{j \neq i} \nu_{ij} \vec{u}_j + m_i \omega_i (\hat{b} \times \vec{u}_i) = \vec{F}_i$$

To solve this system of coupled vector equations, define the matrix D as follows:

$$D^{-1}_{ii} = m_i \bar{\nu}_i \ , \quad D^{-1}_{ij} = -m_i \nu_{ij} \quad (j \neq i)$$

Then

$$\sum_j D^{-1}_{ij} \vec{u}_j + m_i \omega_i (\hat{b} \times \hat{u}_i) = \vec{F}_i$$

The solution for the parallel (to $\vec{B}$) components) follows immediately:

$$\hat{b} \cdot \vec{u}_i = \sum_j D_{ij} \hat{b} \cdot \vec{F}_j$$

To obtain a solution for the transverse components, let $\hat{i}_2$ be an arbitrary unit vector normal to $\hat{b}$, and $\hat{i}_3 = \hat{b} \times \hat{i}_2$. Equating the coefficients of $\hat{i}_2$, $\hat{i}_3$ in the equation of motions.

$$\sum_j D^{-1}_{ij} u_{j2} - m_i \omega_i u_{i3} = F_{i2}$$

$$\sum_j D^{-1}_{ij} u_{j3} + m_i \omega_i u_{i2} = F_{i3}$$

These equations can be combined to give

$$\sum_j \left(\sum_k D_{ik}^{-1} \frac{1}{m_k\omega_k} D_{kj}^{-1}\right) u_{j2} + m_i\omega_i u_{i2} = F_{i3} + \sum_k D_{ik}^{-1} \frac{1}{m_k\omega_k} F_{k2}$$

$$\sum_j \left(\sum_k D_{ik}^{-1} \frac{1}{m_k\omega_k} D_{kj}^{-1}\right) u_{j3} + m_j\omega_i u_{i3} = -F_{i2} + \sum_k D_{ik}^{-1} \frac{1}{m_k\omega_k} F_{k3}$$

Let $$H_{ij}^{-1} = \sum_k D_{ik}^{-1} \frac{1}{m_k\omega_k} D_{kj}^{-1} + \delta_{ij}\, m_i\omega_i$$

Then

$$u_{i2} = \sum_j H_{ij}F_{i3} + \sum_j P_{ij}\, F_{j2}$$

$$u_{i3} = \sum_j H_{ij}\, F_{j2} + \sum_j P_{ij}\, F_{j3}$$

where $$P_{ij} = \left(\sum_k H_{ik}\, D_{kj}^{-1}\right)/m_j\omega_j$$

The total transverse component is

$$\hat{i}_2 u_{i2} + \hat{i}_3 u_{i3} = \sum_j H_{ij}(\hat{i}_2 F_{j3} - \hat{i}_3 F_{j2}) + \sum_j P_{ij}(\hat{i}_2 F_{j2} + \hat{i}_3 F_{j3})$$

or

$$\hat{b} \times (\vec{u}_i \times \hat{b}) = \sum_j H_{ij}(\vec{F}_j \times \hat{b}) + \sum_j P_{ij}\, \hat{b} \times (\vec{F}_j \times \hat{b})$$

$$= \left(\sum_j H_{ij}\vec{F}_j\right) \times \hat{b} + \hat{b} \times \left[\left(\sum_j P_{ij}\vec{F}_j\right) \times \hat{b}\right]$$

which is a form that makes no reference to any particular coordinate system.

The definition of $\vec{F}_i$,

$$\vec{F}_i = m_i\vec{g} + e_i\vec{\mathcal{E}} - \nabla p_i/n_i + m_i \sum_n \nu_{in}(\vec{v}_n - \vec{V})$$

indicates that contributions to the drift velocity come from the gravitational acceleration g, the total electric field

$$\vec{\varepsilon} = \vec{E} + \frac{1}{c}\vec{V} \times \vec{B} ,$$

gradients in the partial pressures, and contributions arising from differences in the velocities of the neutral species. The last-named contributions are small and will be neglected hereinafter. It is useful to distinguish the different contributions to the velocity $\vec{u}_i$ by writing

$$\vec{u}_i = \vec{u}_i(g) + \vec{u}_i(\varepsilon) + \vec{U}_i(\nabla)$$

For the parallel components:

$$\hat{b}\cdot\vec{u}_i(g) = (\hat{b}\cdot\vec{g}) \sum_j D_{ij}m_j$$

$$\hat{b}\cdot\vec{u}_i(\varepsilon) = (\hat{b}\cdot\vec{\varepsilon}) \sum_j D_{ij}e_j$$

$$\hat{b}\cdot\vec{u}_i(\bar{v}) = -\sum_j D_{ij}(\nabla p_j/n_j) \cdot \hat{b}$$

For the transverse components:

$$\hat{b} \times [\vec{u}_i(g) \times \hat{b}] = (\vec{g} \times \hat{b}) \sum_j H_{ij}m_j + \hat{b} \times (\vec{g} \times \hat{b}) \sum_j P_{ij}m_j$$

$$\hat{b} \times [\vec{u}_i(\varepsilon) \times \hat{b}] = (\vec{\varepsilon} \times \hat{b}) \sum_j H_{ij}e_j + \hat{b} \times (\vec{\varepsilon} \times \hat{b}) \sum_j P_{ij}e_j$$

$$\hat{b} \times [\vec{u}_i(\nabla) \times \hat{b}] = -\sum_j H_{ij} (\nabla p_j/n_j) \times \hat{b} - \hat{b} \times [\sum_j P_{ij}(\nabla p_j/n_j) \times \hat{b}]$$

B. Current Density

The current density $\vec{J}$ is given by

$$\vec{J} = \frac{1}{c} \sum_i n_i e_i \vec{v}_i = \frac{1}{c} \sum_i n_i e_i \vec{u}_i + \frac{1}{c} \sum_i n_i e_i \vec{V}$$

It is useful to write

$$\vec{J} = \vec{J}(V) + \vec{J}(g) + \vec{J}(\epsilon) + \vec{J}(\nabla)$$

where, owing to the condition of local neutrality,

$$\vec{J}(V) = \vec{V} \frac{1}{c} \sum_i n_i e_i = 0$$

The other contributions may again be split into parallel and transverse components. For the parallel components:

$$\hat{b} \cdot \vec{J}(g) = (\hat{b} \cdot \vec{g}) \frac{1}{c} \sum_i n_i e_i \sum_j D_{ij} m_j$$

$$\hat{b} \cdot \vec{J}(\epsilon) = (\hat{b} \cdot \vec{\epsilon}) \frac{1}{c} \sum_i n_i e_i \sum_j D_{ij} e_j$$

$$\hat{b} \cdot \vec{J}(\bar{v}) = -\frac{1}{c} \sum_i n_i e_i \sum_j D_{ij} (\nabla p_j / n_j) \cdot \hat{b}$$

For the transverse components

$$\hat{b} \times [\vec{J}(g) \times \hat{b}] = (\vec{g} \times \hat{b}) \frac{1}{c} \sum_i n_i e_i \sum_j H_{ij} m_j + \hat{b} \times (\vec{g} \times \hat{b}) \frac{1}{c} \sum_i n_i e_i \sum_j P_{ij} m_j$$

$$\hat{b} \times [\vec{J}(\epsilon) \times \hat{b}] = (\vec{\epsilon} \times \hat{b}) \frac{1}{c} \sum_i n_i e_i \sum_j H_{ij} e_j + \hat{b} \times (\vec{\epsilon} \times \hat{b}) \frac{1}{c} \sum_i n_i e_i \sum_j P_{ij} e_j$$

$$\hat{b} \times [\vec{J}(\nabla) \times \hat{b}] = \frac{1}{c} \sum_i n_i e_i \sum_j H_{ij} (\nabla p_j / n_j) \times \hat{b} + \hat{b} \times \left[\frac{1}{c} \sum_i n_i e_i \sum_j P_{ij} (\nabla p_j / n_j) \times \hat{b}\right]$$

The conventional electrical conductivities, which determine the contribution to the current density from electric fields, are seen to be

$$\text{Parallel:} \quad \sigma_D = \frac{1}{c} \sum_i n_i e_i \sum_j D_{ij} e_i$$

$$\text{Hall:} \quad \sigma_H = \frac{1}{c} \sum_i n_i e_i \sum_j H_{ij} e_j$$

$$\text{Petersen:} \quad \sigma_p = \frac{1}{c} \sum_i n_i e_i \sum_j P_{ij} e_j$$

In terms of the electrical conductivities, we may write

$$\vec{J}(\varepsilon) = \sigma_D(\vec{\varepsilon} \cdot \hat{b})\hat{b} + \sigma_H(\vec{\varepsilon} \times \hat{b}) + \sigma_p \hat{b} \times (\vec{\varepsilon} \times \hat{b}) \ .$$

C. Ion Drag

The force exerted on the neutral constituents by charged particles is commonly called ion drag. Neglecting differences in the neutral particle velocities, we may write the force (per unit volume) exerted on neutral species n by the charged species i as

$$\vec{f}_{ni} = -m_n n_n \nu_{ni} (\vec{V} - \vec{v}_i)$$

$$= + m_n n_n \nu_{ni} \vec{u}_i$$

$$= m_i n_i \nu_{in} \vec{u}_i$$

by the symmetry property of collision frequencies.

The force exerted by all charged particles on neutral species n is

$$\vec{f}_n = \sum_i \vec{f}_{ni} = \sum_i m_i n_i \nu_{in} \vec{u}_i$$

Finally, the total force exerted on all neutral species by all charged species is

$$\vec{f} = \sum_n \vec{f}_n = \sum_i n_i m_i \left(\sum_n \nu_{in}\right) \vec{u}_i$$

Let $\quad \vec{f} = \vec{f}(g) + \vec{f}(\varepsilon) + \vec{f}(\nabla)$

For the parallel components:

$$\hat{b}\cdot\vec{f}(g) = (\hat{b}\cdot\vec{g}) \sum_i n_i m_i \left(\sum_n \nu_{in}\right) \sum_j D_{ij} m_j$$

$$\hat{b}\cdot\vec{f}(\varepsilon) = (\hat{b}\cdot\vec{\varepsilon}) \sum_n n_i m_i \left(\sum_n \nu_{in}\right) \sum_j D_{ij} e_j$$

$$\hat{b}\cdot\vec{f}(\nabla) = \sum_i n_i m_i \left(\sum_n \nu_{in}\right) \sum_j D_{ij} (\nabla p_j/n_j)\cdot\hat{b}$$

For the transverse components:

$$\hat{b} \times [\vec{f}(g) \times \hat{b}] = (\hat{b} \times \vec{g}) \sum_i n_i m_i \left(\sum_n \nu_{in}\right) \sum_j H_{ij} m_j + \hat{b} \times (\vec{g} \times \hat{b}) \sum_i n_i m_i \left(\sum_n \nu_{in}\right) \sum_j P_{ij} m_j$$

$$\hat{b} \times [\vec{f}(\varepsilon) \times \hat{b}] = (\hat{b} \times \vec{\varepsilon}) \sum_i n_i m_i \left(\sum_n \nu_{in}\right) \sum_j H_{ij} e_j + \hat{b} \times (\vec{\varepsilon} \times \hat{b}) \sum_i n_i m_i \left(\sum_n \nu_{in}\right) \sum_j P_{ij} e_j$$

$$\hat{b} \times [\vec{f}(\nabla) \times \hat{b}] = \sum_i n_i m_i \left(\sum_n \nu_{in}\right) \sum_j H_{ij} (\nabla p_j/n_j) \times \hat{b} + \sum_i n_i m_i \left(\sum_n \nu_{in}\right) \sum_j P_{ij} \hat{b} \times [(\nabla p_j/n_j) \times \hat{b}]$$

D. Electric Fields

The expression relating the drift velocity of a charged species to the electric field may be inverted to yield an expression for the electric field. For the parallel component:

$$\hat{b}\cdot\vec{\varepsilon} = \hat{b}\cdot\vec{u}_i(\varepsilon)/(\sum_j D_{ij}e_j)$$

For the transverse components:

$$[(\sum_j H_{ij}e_j)^2 + (\sum_j P_{ij}e_j)^2]\ \hat{b} \times (\varepsilon \times \hat{b}) =$$

$$= -(\sum_j H_{ij}e_j)[\vec{u}_i(\varepsilon) \times \hat{b}] + (\sum_j P_{ij}e_j)\ \hat{b} \times [\vec{u}_i(\varepsilon) \times \hat{b}]$$

A vector measurement of the drift velocity $\vec{u}_i$, together with measurements required for the calculation of $\vec{u}_i(g)$ and $\vec{u}_i(\nabla)$, is required for the calculation of

$$\vec{u}_i(\varepsilon) = \vec{u}_i - \vec{u}_i(g) - \vec{u}_i(\nabla)\ ,$$

from which the electric field can be computed. This procedure appears to be feasible in regions of the atmosphere where one ionic species dominates.

4. THEORY: ONE IONIC SPECIES

Even though it is applicable only to a portion of the ionosphere, the theory for the case when only one ionic species and electrons are present helps illustrate several features of the general theory. The equations of motion are

$$m_i(\nu_{in} + \nu_{ie})\,\vec{u}_i - m_i\nu_{ie}\vec{u}_e + m_i\omega_i(\hat{b} \times \vec{u}_i) = \vec{F}_i$$

$$m_e(\nu_{en} + \nu_{ei})\,\vec{u}_e - m_e\nu_{ei}\vec{u}_i + m_e\omega_e(\hat{b} \times \vec{u}_e) = \vec{F}_e$$

where the forces $\vec{F}_i$, $\vec{F}_e$ are defined by

$$\vec{F}_s = -\nabla p_s/n_s + m_s\vec{g} + e_s\vec{\mathcal{E}}\ , \qquad s = i, e$$

and where the subscripts i, e, and n denote ions, electrons, and neutrals respectively. We note first that if collisions with neutrals are neglected ($\nu_{in} = \nu_{en} = 0$), then the equations of motion can only determine the velocity difference ($\vec{u}_i - \vec{u}_e$) and not the velocities of each species. This remains true when several ionic species are present.

Parallel Components

It is useful to examine the solution for the "uncoupled" case, i.e. when ion-electron collisions are neglected ($\nu_{ie} = \nu_{ei} = 0$):

$$\hat{b}\cdot\vec{u}_i \to (\hat{b}\cdot\vec{F}_i)/(m_i\nu_{in}) \equiv V_i$$
$$\hat{b}\cdot\vec{u}_e \to (\hat{b}\cdot\vec{F}_e)/(m_e\nu_{en}) \equiv V_e$$

Inasmuch as the forces F_i and F_e are of the same order of magnitude, it follows that

$$V_i/V_e \sim \alpha \equiv (m_e\nu_{en})/(m_i\nu_{in}) \ .$$

The "uncoupled" case also serves to define the "uncoupled" diffusion coefficient

$$D_S = kT_s/m_s\nu_{sn} \ .$$

In the presence of collisions, the solutions are

$$\hat{b}\cdot\vec{u}_i = [(m_e\nu_{en} + m_e\nu_{ei})(\hat{b}\cdot\vec{F}_i) + (m_i\nu_{ie})(\hat{b}\cdot\vec{F}_e)]/D$$

$$\hat{b}\cdot\vec{u}_e = [(m_e\nu_{ei})(\hat{b}\cdot\vec{F}_i) + (m_i\nu_{in} + m_i\nu_{ie})(\hat{b}\cdot\vec{F}_e)]/D$$

where

$$D = (m_i\nu_{in})(m_e\nu_{en}) + (m_i\nu_{in})(m_e\nu_{ei}) + (m_e\nu_{en})(m_i\nu_{ie})$$

Since $n_i = n_e$ in the present case, it follows from the symmetry property of collision frequencies that

$$m_i\nu_{ie} = m_e\nu_{ei} \ .$$

Accordingly

$$D = (m_i\nu_{in})(m_e\nu_{en}) + (m_e\nu_{ei})[(m_i\nu_{in}) + (m_e\nu_{en})]$$

$$= (m_i\nu_{in})\ [(m_e\nu_{en}) + (m_e\nu_{ei})(1 + \alpha)]$$

and

$$(\hat{b}\cdot\vec{u}_i) = (m_e\nu_{ei})[\hat{b}\cdot(\vec{F}_i + \vec{F}_e)]/D + (m_e\nu_{en})(\hat{b}\cdot\vec{F}_i)/D$$

$$(\hat{b}\cdot\vec{u}_e) = (m_e\nu_{ei})[\hat{b}\cdot(\vec{F}_i + \vec{F}_e)]/D + (m_i\nu_{in})(\hat{b}\cdot\vec{F}_e)/D$$

These expressions show that collisions between ions and electrons give rise to a velocity component that is common to both. It should be noted also that the electric field does not enter this component because it appears with opposite signs in $\vec{F}_i$ and $\vec{F}_e$. The "uncoupled" velocities V_i, V_e are still present, but they are divided by the factor

$$D/[(m_i\nu_{in})(m_e\nu_{en})] = 1 + (\nu_{ei}/\nu_{en})(1+\alpha).$$

It is useful to note that

$$\alpha \equiv (m_e\nu_{en})/(m_i\nu_{in}) < 10^{-2}$$

at all altitudes. The parameter α is a measure of the strength of electron-neutral coupling compared to ion-neutral coupling. A second useful parameter is

$$x \equiv \nu_{ei}/[\nu_{en} + (1+\alpha)\nu_{ei}] .$$

As the fractional ionization (n_i/n_n) increases, the ratio (ν_{ei}/ν_{en}) increases and so does x. It is convenient to refer to x as the (collisional) coupling parameter. The reason for this choice becomes apparent when the velocities are expressed as

$$(\hat{b}\cdot\vec{u}_i) = (1-\alpha x)\ V_i + \alpha x V_e = V_i + \alpha x(V_e - V_i)$$

$$(\hat{b}\cdot\vec{u}_e) = (1-x)\ V_e + xV_i = V_e - x(V_e - V_i)$$

where V_i and V_e are the uncoupled velocities previously defined. The collisional coupling changes both velocities, the change being proportional to the coupling parameter x and to the difference $(V_e - V_i)$ of the uncoupled velocities. The change in the ion velocity, however, is smaller than the change in the electron velocity by a factor of $\alpha(<10^{-2})$. This, of course, is the result of the fact that the coupling of the electrons to neutrals is weaker (by a factor of α) than the coupling of ions to neutrals. In fact, as the coupling parameter approaches unity, the electron velocity tends to a value unrelated to its "uncoupled" value.

Since collisions between particles do not constitute external forces, the total force per unit volume remains unchanged by collisions. In the present case, this force is

$$\begin{aligned} n_i(\hat{b}\cdot\vec{F}_i) + n_e(\hat{b}\cdot\vec{F}_e) &= n_i m_i \nu_{in}(\hat{b}\cdot\vec{u}_i) + n_e m_e \nu_{en}(\hat{b}\cdot\vec{u}_e) \\ &= n_i m_i \nu_{in}\,[(\hat{b}\cdot\vec{u}_i) + \alpha(\hat{b}\cdot\vec{u}_e)] \\ &= n_i m_i \nu_{in}\,(V_i + \alpha V_e) \\ &= n_i m_i \nu_{in} V_i + n_e m_e \nu_{en} V_e \end{aligned}$$

Thus, irrespective of the magnitude and nature of the collision frequencies,

$$(\hat{b}\cdot\vec{u}_i) + \alpha(\hat{b}\cdot\vec{u}_e) = V_i + \alpha V_e \ .$$

In some theoretical formulations (see for example Schunk and Walker 1970) it is assumed that $(m_e \nu_{en} \vec{u}_e)$ is

of order (m_e/m_i) compared to $(m_i \nu_{in} \vec{u}_i)$, and therefore negligible. This assumption is not correct in general. The ratio in question is in fact

$$|\alpha V_e - \alpha x(V_e - V_i)| / |V_i + \alpha x(V_e - V_i)| \xrightarrow[x \to 0]{} |\alpha V_e| / |V_i|$$

$$\xrightarrow[x \to 1]{} |\alpha V_i| / |V_i + \alpha V_e|$$

Since $|\alpha V_e| / |V_i| \sim 1$, as shown previously, the assumption is incorrect unless the collisional coupling parameter x is near unity. Data from daytime observations (listed in this report), indicates that $x > 0.95$ above 270 kilometers and $x > 0.99$ above 330 kilometers. At night, the fractional ionization is lower, and these values of the coupling parameter are reached above altitude limits which are ~100 kilometers higher than in the daytime.

It is interesting to consider the effects of ion-electron collisions on the parallel component of the current. This is proportional to

$$\hat{b} \cdot (\vec{u}_i - \vec{u}_e) = (V_i - V_e)(1 - x - \alpha x)$$

$$= (V_i - V_e) x \{\nu_{en} / [\nu_{en} + \nu_{ei}(1 + \alpha)]\}$$

As x approaches unity (which is equivalent to saying as electron-ion collisions dominate electron-neutral collisions) the effect of electron-ion collisions is to reduce the parallel conductivity by a factor of (ν_{en}/ν_{ei}) compared to the "uncoupled" case. This result further shows that as (ν_{en}/ν_{ei}) tends to zero, ions and electrons tend to move with the same velocity.

Transverse Components

By combining the equations for u_i and u_e we obtain uncoupled equations of the form

$$A_o \vec{u}_s + A_1(\hat{b}x\vec{u}_s) + A_2\,\hat{b} \times (\hat{b}x\vec{u}_s) = \vec{C}_s, \quad s=i,e$$

where

$$A_o = \alpha r^2(1 + f + \alpha f),\ A_1 = -r(1-\alpha),\ A_2 = -1$$

$$\vec{C}_i = [\alpha r(1+f)\ \vec{F}_i + \alpha rf\ \vec{F}_e + \vec{F}_i \times \hat{b}]/(m_i\omega_i)$$

$$\vec{C}_e = [r(1+\alpha f)\ \vec{F}_e + \alpha rf\ \vec{F}_i - \vec{F}_e \times \hat{b}]/(m_i\omega_i)$$

and

$$\alpha = (m_e\nu_{en}/m_i\nu_{in}),\ r = (\nu_{in}/\omega_i)\ ,\quad f = (\nu_{ei}/\nu_{en})\ .$$

The parameter α has been discussed before. It ranges from 3.3×10^{-3} at 650 km to 1.2×10^{-3} at 160 km in the data used in this report. The ratio r of the ion-neutral collision frequency to the ion gyrofrequency has the value 0.06 at 160 km and decreases with altitude essentially in proportion to the atmospheric density. Like α, r is insensitive to atmospheric conditions where its value is significant. The parameter f is a measure of the fractional ionization and ranges from 0.5 at 160 km to 4×10^3 at 657 km in our data. It is, of course, highly variable, and substantially lower at night than in the daytime. Inasmuch as f appears in a product with r, and rf is always a small number ($\lesssim$0.03), knowledge of the actual value of f is not needed. Taking into account the numerical

characteristics of the parameters, we may write the solutions in a simple form that is highly accurate at all altitudes:

$$(1+r^2)(m_i\omega_i)\ \hat{b}x(\vec{u}_i x\hat{b}) = [\vec{F}_i-\alpha r^2 f\vec{F}_e]\ x\ \hat{b} + r\ \hat{b}\ x\ (\vec{F}_i x\hat{b}) + \alpha r f\ \hat{b}\ x[(\vec{F}_i+\vec{F}_e)\ x\ \hat{b}]$$

$$(1+r^2)(m_i\omega_i)\ \hat{b}\ x\ (\vec{u}_e x\hat{b}) = -(1+r^2)\ (\vec{F}_e x\hat{b}) - \alpha r^2 f[\vec{F}_i+2\vec{F}_e]\ x\ \hat{b} + \alpha r\ \hat{b}\ x\ (\vec{F}_e x\hat{b}) + \alpha r f\ \hat{b}\ x\ [(\vec{F}_i+\vec{F}_e)x\hat{b}]$$

It should be noted that the "Hall" components (i.e. the components which involve a single vector product with $\hat{b}$) are are essentially diagonal, the off-diagonal elements being smaller by a factor $\alpha r^2 f(<10^{-4})$. The diagonal elements are essentially equal to $1/(m_i\omega_i) = c/eB$. The Hall components remain diagonal even when several ionic species are present.

On the other hand the "Pedersen" off-diagonal components are of order $\alpha f(=\nu_{ie}/\nu_{in})$ compared to diagonal components, and this product may be small or large. Finally, the magnitude of the Pedersen components is of order $r\ (=\nu_{in}/\omega_i)$ compared to the Hall components.

It is useful to examine the velocity difference, which is proportional to the current

$$(1+r^2)(m_i\omega_i)\ \hat{b}\ x\ [(\vec{u}_i-\vec{u}_e)\ x\ \hat{b}] =$$

$$(1+\alpha r^2 f)(\vec{F}_i+\vec{F}_e)\ x\ \hat{b} + r^2\ (\vec{F}_e x\hat{b}) + r\ \hat{b}\ x\ [(\vec{F}_i-\alpha\vec{F}_e)\ x\ \hat{b}]$$

The leading "Hall" component is independent of the electric field, since $\vec{F}_i$ and $\vec{F}_e$ contain the electric field with opposite signs. Thus the Hall electrical conductivity is proportional to $r^2/(1+r^2)$, and decreases very rapidly with increasing

altitude. On the other hand, the Pedersen electrical conductivity is linearly proportional to r, and decreases less rapidly with altitude. Finally, we note for convenience that

$$\alpha r f = (\nu_{ie}/\omega_i), \quad \alpha^2 r^2 f = (\nu_{ie}\nu_{in}/\omega_i^2) \ .$$

5. RESULTS AND DISCUSSION

In this section we present some results using the formalism of Section 3 and the data given in Appendix A.

A. General

It was shown in Section 3 that, when collisions between charged particles are taken into account, the velocity of a given charged particle species depends on the forces acting on all the charged species. Figures 4, 5, and 6 demonstrate this for the parallel component of the velocity of O^+ ions, electrons, and N^+ ions, respectively. More specifically, the various curves in each figure represent the velocity generated in the species of interest by a force on another species. Before discussing each figure separately, we note that these figures give the velocity (in cm/sec) generated by a force of 1.66×10^{-24} dyne.

Fig. 4 pertains to O^+, which is the major ion through most of the altitude region considered. The curve labeled "uncoupled" represents the response of O^+ ions to the force exerted on them in the absence of collisions with other charged particles. It is defined explicitly in Section A. The curve labeled O^+ represents the response of O^+ ions to the force exerted on them in the presence of collisions with other charged particles. We note, as in Section 4, that the introduction of collisions has a very small effect on this response

function, owing to the much higher mobility of the electrons. The curve labeled "electrons" represents the response of O^+ ions to the force exerted on electrons. Because O^+ is the major ion, this response function is nearly identical to the response function to the force exerted on O^+. Thus, as far as O^+ is concerned, the presence of collisions has the effect of subjecting O^+ to the sum of the forces on O^+ and electrons. The effect of the forces on the other (minor) ions is an order of magnitude smaller in the altitude range considered. This result remains valid even below 220 km, where O_2^+ and NO^+ have higher concentrations than O^+, because at these altitudes collisions with neutral particles play a major part, and the ions are not strongly coupled.

Fig. 5 shows the response of electrons to forces exerted on each charged species. As pointed out in Section 4, the introduction of collisions reduces drastically the response of electrons to the force exerted on them. This is evident in Fig. 5 from a comparison of the curves labeled "electrons" and "uncoupled" (no collisions). With increasing altitude, collisions with O^+ predominate over collisions with neutrals, and the motion of electrons is effectively governed by the sum of the forces on O^+ and on electrons. The effect of minor ions is an order of magnitude smaller.

Fig. 6 represents the respone of N^+ ions to forces exerted on each charged species. N^+ is a minor ion throughout the altitude range considered. Fig. 6 shows that the motion of N^+

ions is controlled by the sum of the forces on O^+ (the major ion) and electrons. The response to the force on N^+ is negligible compared to its value in the absence of collisions (as depicted by the curve labeled "uncoupled"), except at the lowest altitudes, where collisions with neutrals dominate. At the upper altitudes, where collisions with O^+ are dominant, the response functions of N^+ are identical to the response functions of O^+, which means that the motion of N^+ ions is identical to the motion of O^+ ions. This result is valid for all the minor ions.

We can summarize the results for the parallel components as follows:

- Where charged particle collisions dominate ion-neutral collisions, minor ions move with the same velocity as the major ion;

- Except as noted below, the velocity of the major ion and of electrons is proportional to the sum of the forces exerted on the major ion and on electrons;

- In the presence of parallel electric fields, the velocity of electrons may be substantially different from the velocity of the ions. The effect of electric fields on ions is of order $\alpha(=m_e\nu_{en}/m_i\nu_{in}<10^{-2})$ compared to the effect of electric fields on electrons.

For the transverse velocity components we note that the "Hall" contribution is negligible except for a force due to a transverse electric field, and that the "Pedersen" contribution is negligible in the altitude range considered.

B. Calculation of O^+ Drift Velocity.

We have calculated the drift velocity of O^+ ions using the equations of Section 3. In the expression for the force on species s

$$\vec{F}_s = m_s\vec{g} + e_s\vec{E} - \nabla p_s/n_s$$

we have assumed that the gradient of the partial pressure has a vertical component only. Further, in the absence of any data on electric fields, we have calculated separately the contribution from parallel (to the magnetic field) and eastward electric fields. The results are shown in Figures 7, 8, and 9.

Figure 7 shows the effect of the gravitational force on charged particles, and demonstrates that, in the region where collisions between charged particles dominate collisions with neutrals, the gravitational force affects all species equally.

Figure 8 shows the contribution to the velocity of O^+ from various terms. The vertical component of the velocity is given by $\sin^2 I$ times the value shown in the figure (where I is the magnetic inclination). Inasmuch as the magnitude of the velocity varies by 10^4 over the altitude range, a logarithmic plot has been used, and a dashed curve indicates negative contributions. The curve labeled -G represents the contribution from the gravitational force, as in Fig. 7. The curve labeled N (or -N) represents the contributions from gradients of the concentrations of charged particles. The curve labeled T (or -T) represents contributions from the gradients of electron and

ion temperatures. All ions were assumed to be at the same temperature. The curve labeled S represents the sum of the aforementioned contributions. Figure 8 indicates that the contribution from temperature gradients is relatively small, that the contribution from the gravitational force is the largest contribution over most of the altitude ranges and that the sum of the contributions is negative below about 590 km.

Fig. 9 displays various contributions to the vertical component of the O^+ drift velocity. As in Fig. 8, a logarithmic plot has been used, and dashedlines indicate negative values. The curve marked u_s represents the contributions to the vertical velocity from the gravitational force and from the gradients of partial pressures. u_s is proportional to $\sin^2 I$, where I is the magnetic inclination, and thus tends to zero at about 375 km, which occurs above the magnetic equator. Also shown in Fig. 9 by the curve labeled E_{11} is the contribution to the vertical velocity of a (constant) parallel electric field of 1 millivolt per meter. This contribution is proportional to sinI, and also vanishes at the magnetic equator. The curve labeled E_ϕ represents the "Hall" contribution to the vertical velocity of a geomagnetically eastward electric field of 3 millivolts per meter. It should be noted that, insofar as the calculation of drift velocities is concerned, this contribution is the same for all charged particles, including electrons. Finally, the filled circles represent the

vertical component of plasma drift, as measured by the RPA experiment on the AE-C satellite (Hanson, 1973). A comparison of the measurements with the various curves indicates that an eastward electric field of between 3 and 5 millivolts per meter is sufficient by itself to explain the observations. Further, it appears that if a parallel electric field is present, it must be less than $\sim$0.01 millivolts per meter over most of the altitude range. Up to about 500 km, the contribution from E_ϕ dominates u_s, and the calculated drift velocity can be said to be in harmony with observations. Above that altitude, however, the values of u_s dominate. It should be remembered that, in calculating gradients, it was assumed of necessity that variations occur only in the vertical direction, and that no (geomagnetically) north-south variations are present. It may very well be that this is not a valid assumption in the equatorial region.

C. The Equation of Continuity for O^+

To provide a satisfactory explanation of the observed altitude profile of O^+ ions, we must be able to calculate the divergence of the flux in the equation of continuity

$$P - L = \nabla \cdot (n\vec{u}),$$

in regions where transport is significant. This task requires knowledge of the variation of the concentration, and of the drift velocity, in a three-dimensional frame. Unfortunately, the data do not allow the calculation of horizontal derivatives,

and the assumption that only vertical variations are present is not consistent with the equation of continuity.

D. Conclusions

The motion of charged particles in the upper atmosphere has been investigated with the aid of satellite data. It has been shown that the major ion, O^+, determines the motion of all minor ions. The observed plasma drift velocity in the vertical direction is in harmony with the assumption of an eastward electric field of between 3 and 5 millivolts per meter. It appears that the assumption that horizontal variations are negligible is not valid in the present instance, owing probably to the fact that the altitude region where transport is important lies within 15° of the magnetic equator. The present investigation clearly demonstrates the need for electric field measurements and measurements of plasma drifts. The approach outlined in this investigation will be applied to midlatitude data, where the assumption that horizontal variations are negligible is valid.

6. ELECTRON VELOCITY DISTRIBUTION

Photoelectrons and secondary auroral electrons play an important role in the coupling of the solar ionizing ultraviolet flux and the fast primary particles to the upper atmosphere. Theoretical studies of the transport and thermalization of the photoelectrons and secondary auroral electrons are necessary to determine how the incident energy gets partitioned among heat, ionization, dissociation, luminosity and other modes in the atmosphere. The presence of a parallel electric field may influence the partitioning of the energy and therefore provide the possibility of developing diagnostics. Our preliminary effort to study the effects of electric fields on the electron velocity distribution has been to modify and generalize an accurate electron deposition code (Victor, Kirby-Docken and Dalgarno 1976). With these modifications we had hoped to develop a perturbation-iterative method to introduce the effects of weak electronic fields. Limits of time and funding have limited progress. The code takes explicit account of the discrete nature of the electron energy loss process and employs cross section data based on a recent critical reivew. Local deposition is assumed so that accurate results can be obtained only for altitudes below about 300 km.

The latest original version of the code was operational on a Σ9 computer system at NASA Goddard Space Flight Center. Minor modifications were made so that the code would run efficiently on CDC 6600 series computers such as those at AFGL.

The code was then generalized so that it would calculate the steady state velocity distribution for arbitrary initial velocity ($E \leq 200$ eV) distributions obtained from a file (TAPE4) read by subroutine SETPRO. A card copy of the source deck and the cross section data was supplied to AFGL. A listing of this deck is given in Appendix C. A listing of a typical production file (TAPE4) is given in Appendix D. A small code to produce an input file appropriate to an auroral secondary electron production distribution (using the energy distribution given by Opal, Peterson and Beaty 1971) has been written. A listing of the source code and sample output is shown in Appendix E.

REFERENCES

Banks, P. M., and G. Kockarts (1973), Aeronomy, vol. A, Academic Press (New York).

Barth, C. A., D. W. Rusch, and A. I. Stewart (1973), Radio Science 8, 379.

Brace, L. H., R. F. Theis, and A. Dalgarno (1973), Radio Science 8, 341.

Dalgarno, A., W. B. Hanson, N. W. Spencer, and E. R. Schwerling (1973), Radio Science 8, 263.

Hanson, W. B., D. R. Zuccaro, C. R. Lippincott, and S. Sanatani (1973), Radio Science 8, 333.

Hayes, P. B., G. Carignan, B. C. Kennedy, G. G. Shepard, and J. C. G. Walker (1973), Radio Science 8, 369.

Hedin, A. E., C. A. Reber, G. P. Newton, H. G. Mayr, and W. E. Potter (1977), J. Geophys. Res. 82, 2148.

Nier, A. O., W. E. Potter, D. R. Hickman, and K. Mausberger (1973) Radio Science 8, 271.

Opal, C. B., W. K. Peterson and E. C. Beaty (1971), J. Chem. Phys. 55, 4100.

Oppenheimer, M., E. R. Constantinides, K. Kirby-Docken, G. A. Victor and A. Dalgarno (1977), J. Geophys. Res. 82, 5485.

Schunk, R. W. (1977), Rev. Geophys. and Space Phys. 15, 429.

Schunk, R. W., and J. C. G. Walker (1970), Planet. Space Sci. 18, 535.

Victor, G. A., K. Kirby-Docken, and A. Dalgarno, "Calculations

of the equilibrium photoelectron flux in the thermosphere,"
(1976)Planet. Space Science 24, 679.

Walker, J. C. G. (1965), J. Atmos. Sci. 22, 462.

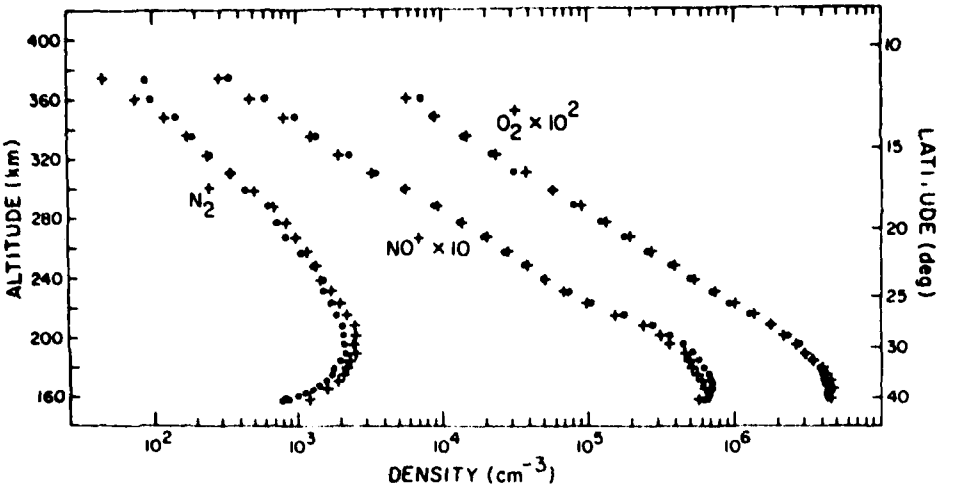

Fig. 1. The concentration of molecular ions plotted against altitude. Dots indicate measurements by the MIMS experiment (Hoffman 1973) on orbit 594 (uplet) of the AE-C satellite. Pluses indicate theoretical values.

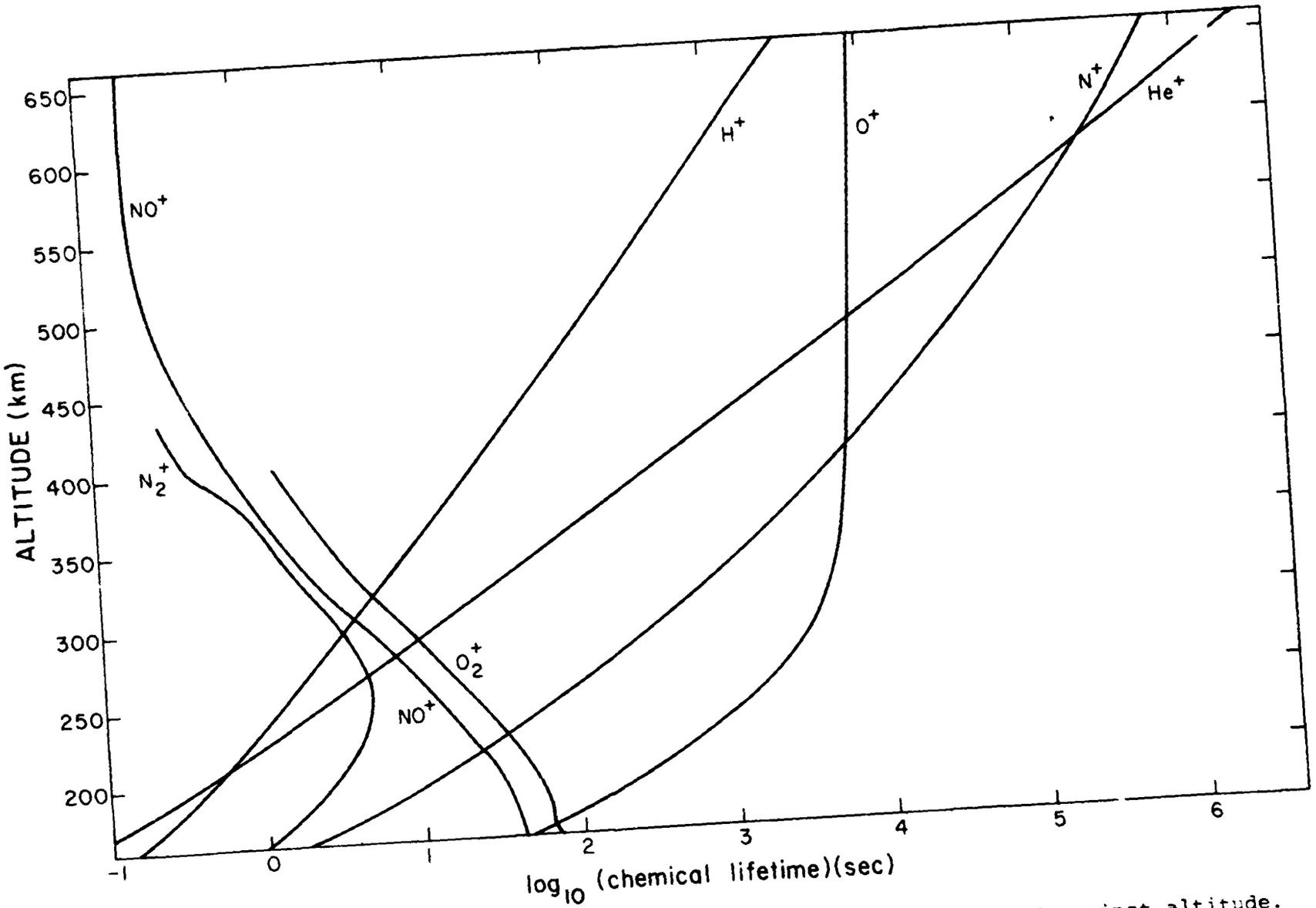

Figure 2. Chemical lifetimes of ionospheric ions plotted against altitude.

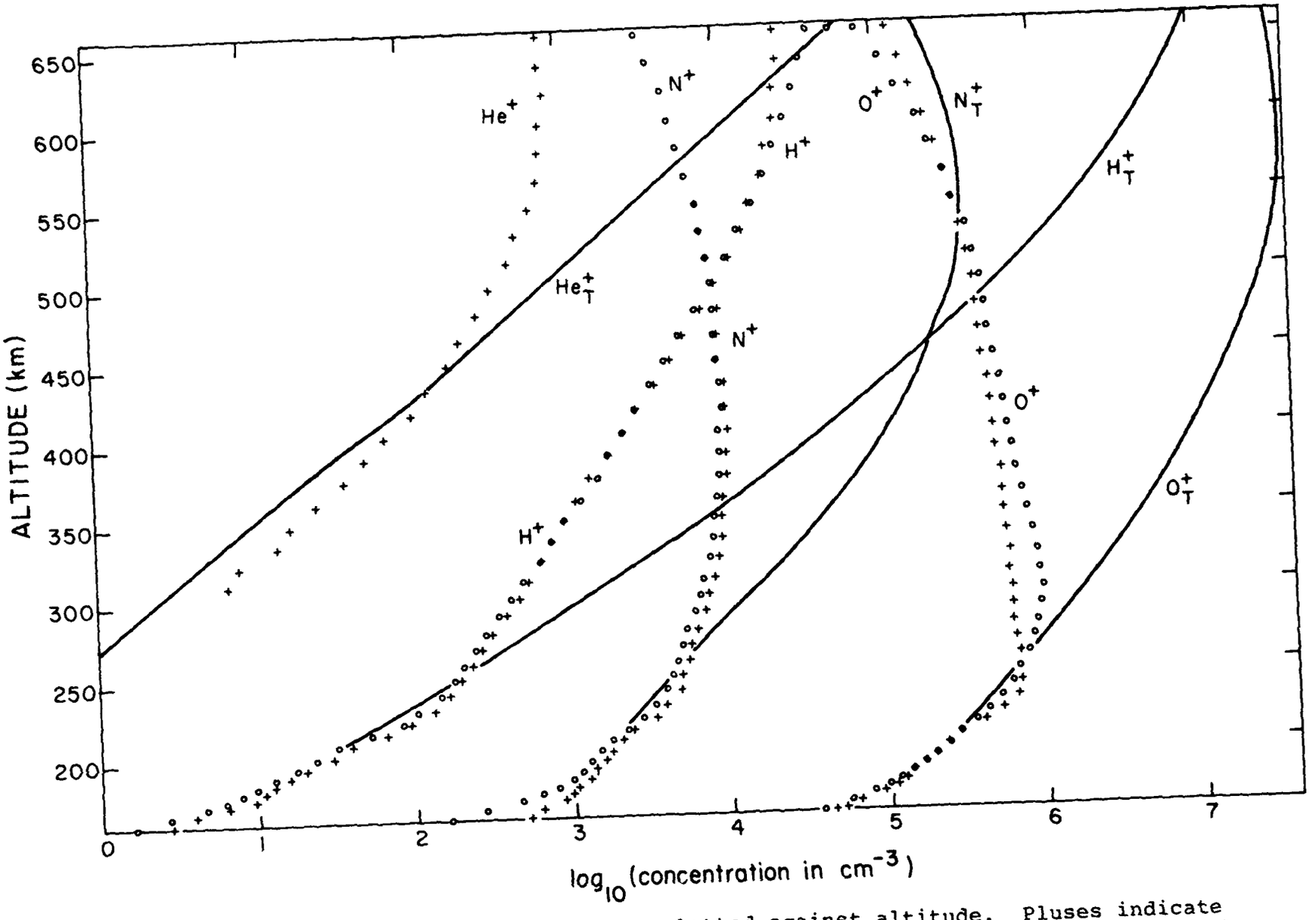

Fig. 3. The concentrations of atomic ions plotted against altitude. Pluses indicate measurements by the MIMS experiment (Hoffman 1973) on orbit 594 (upleg) of the AE-C satellite. Open circles indicate local photochemical equilibrium calculations but using observed ion concentrations for ions other than the ion of interest. Solid lines indicate local photochemical equilibrium theory.

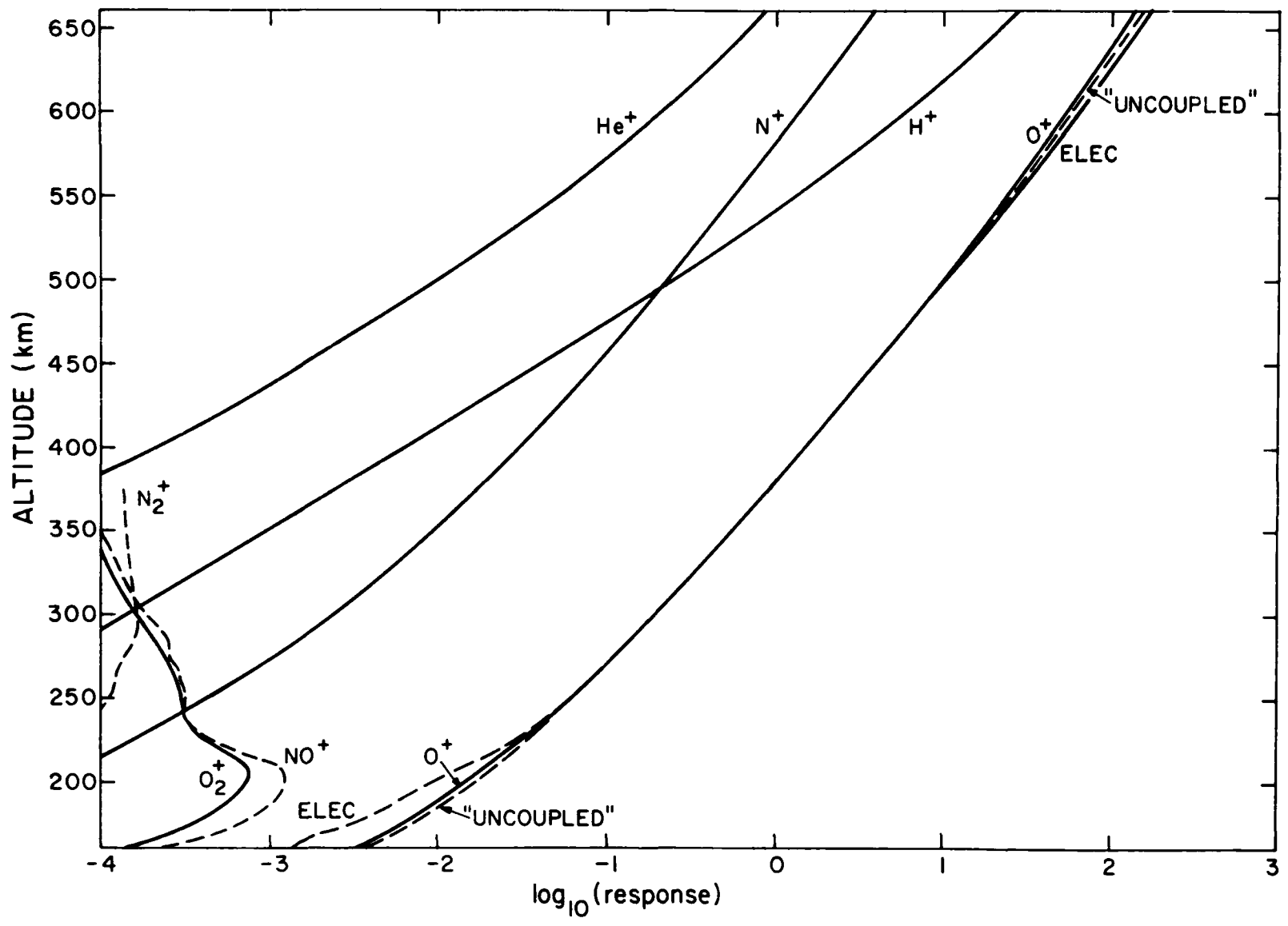

Fig. 4. Response of O^+ ions to forces on charged particles plotted against altitude (see text for units). Data from AE-C orbit 594 (upleg) has been used in the calculations. The curve labeled "uncoupled" refers to the response of O^+ ions to the force exerted on them by the absence of collisions.

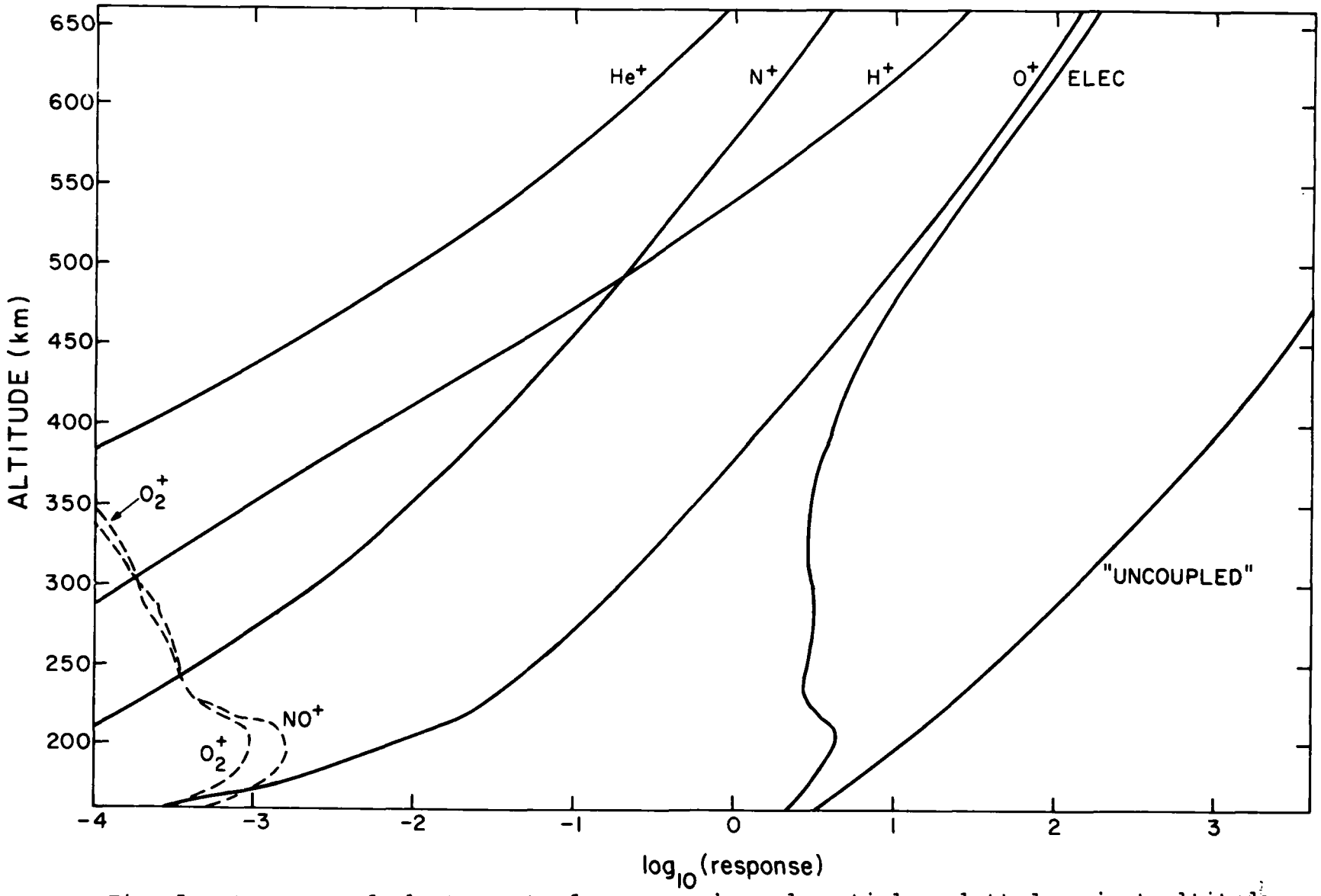

Fig. 5. Response of electrons to forces on charged particles plotted against altitude (see text for units). The curve labeled "uncoupled" refers to the response of electrons to the forces exerted on them in the absence of collisions.

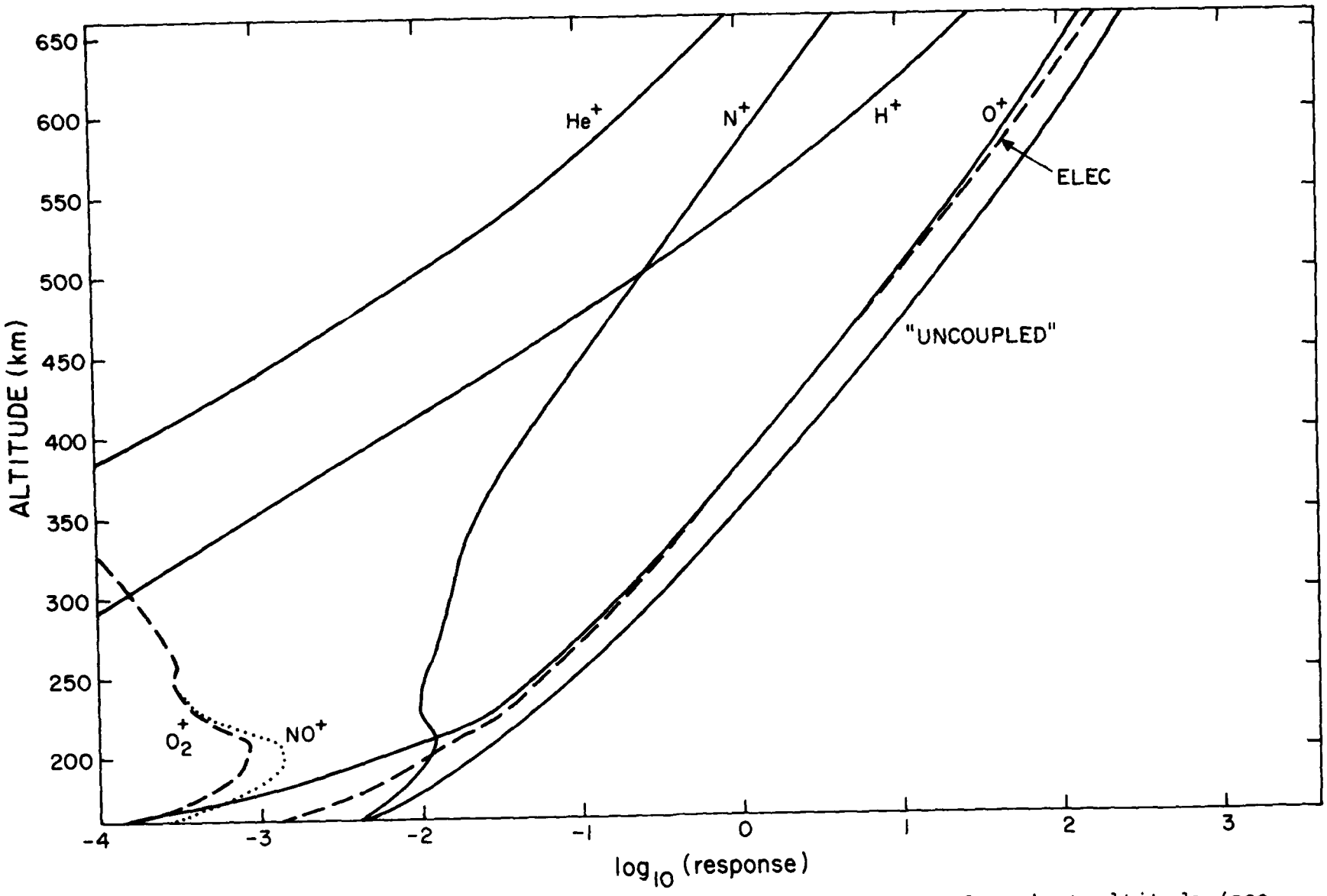

Fig. 6. Response of N^+ ions to forces on charged particles plotted against altitude (see text for units). The curve labeled "uncoupled" refers to the response of N^+ ions to the force exerted on them in the absence of collisions.

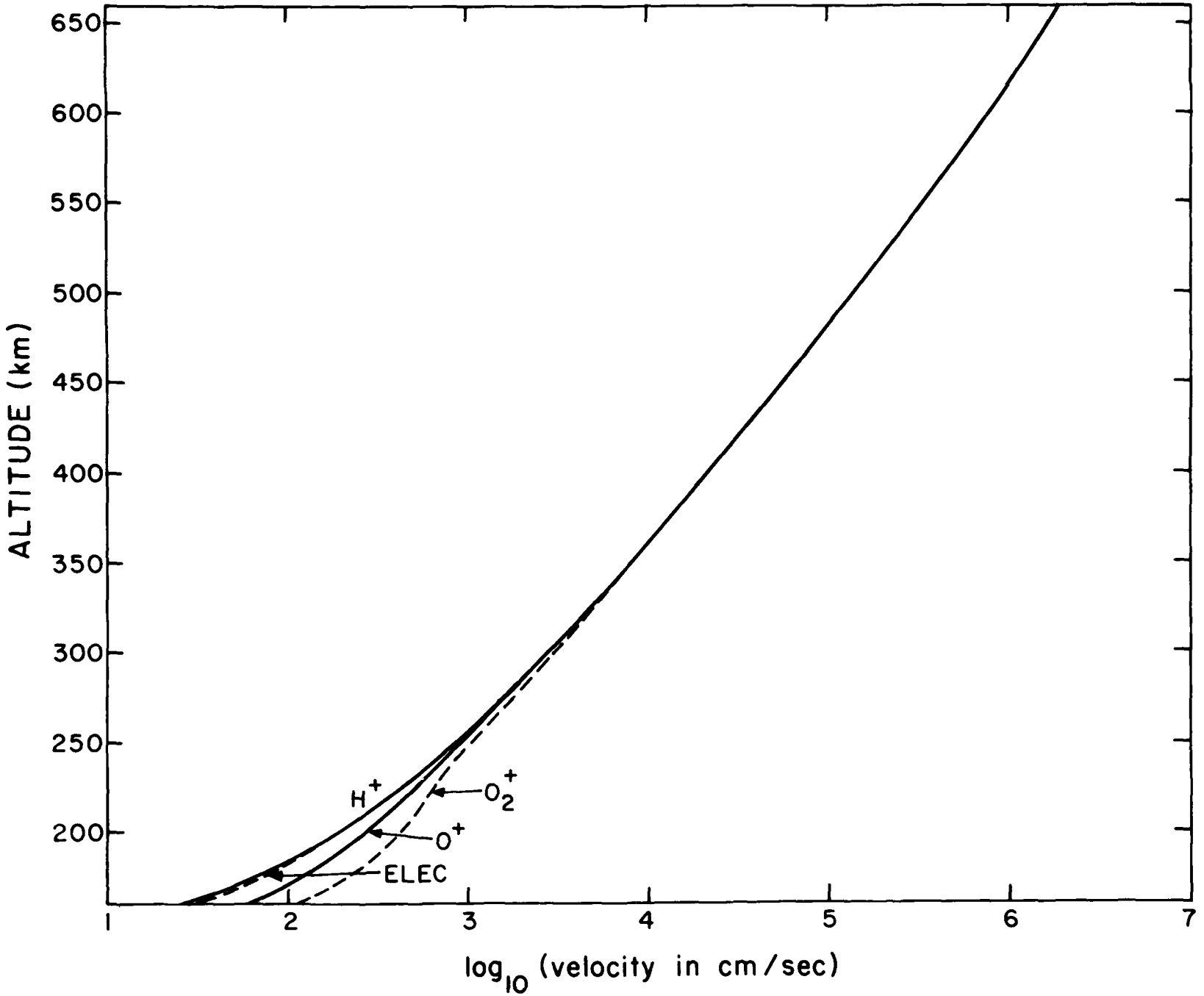

Fig. 7. Contribution to the drift velocity of ions and electrons from the gravitational force plotted against altitude

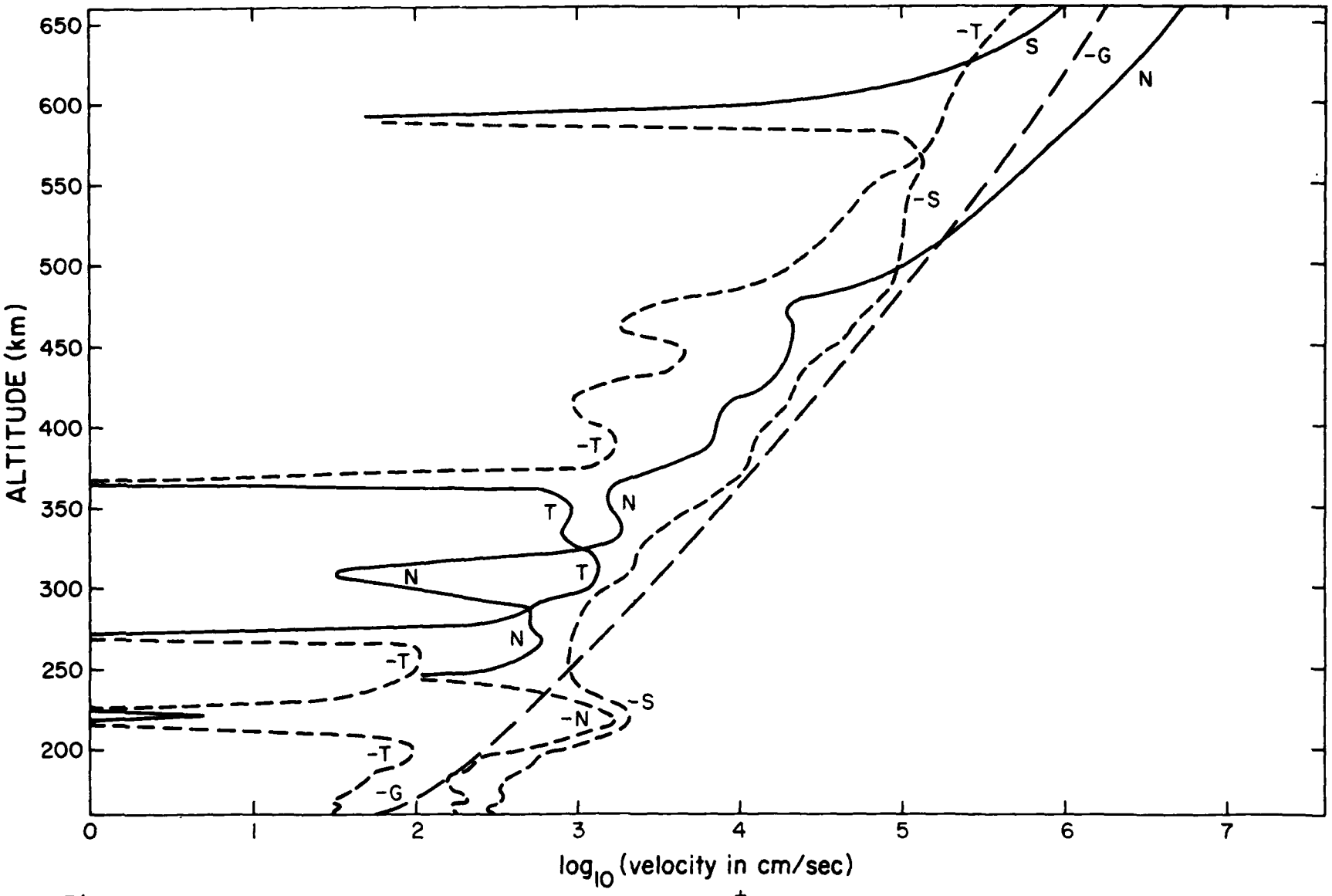

Fig. 8. Contributions to the drift velocity of O^+ ions from gravitational forces (curve labeled G), concentration gradients (curve labled N), temperature gradients (curve labeled T), as well as the sum of these contributions (labled S) plotted against altitude. Dashed lines are used to indicate negative contributions.

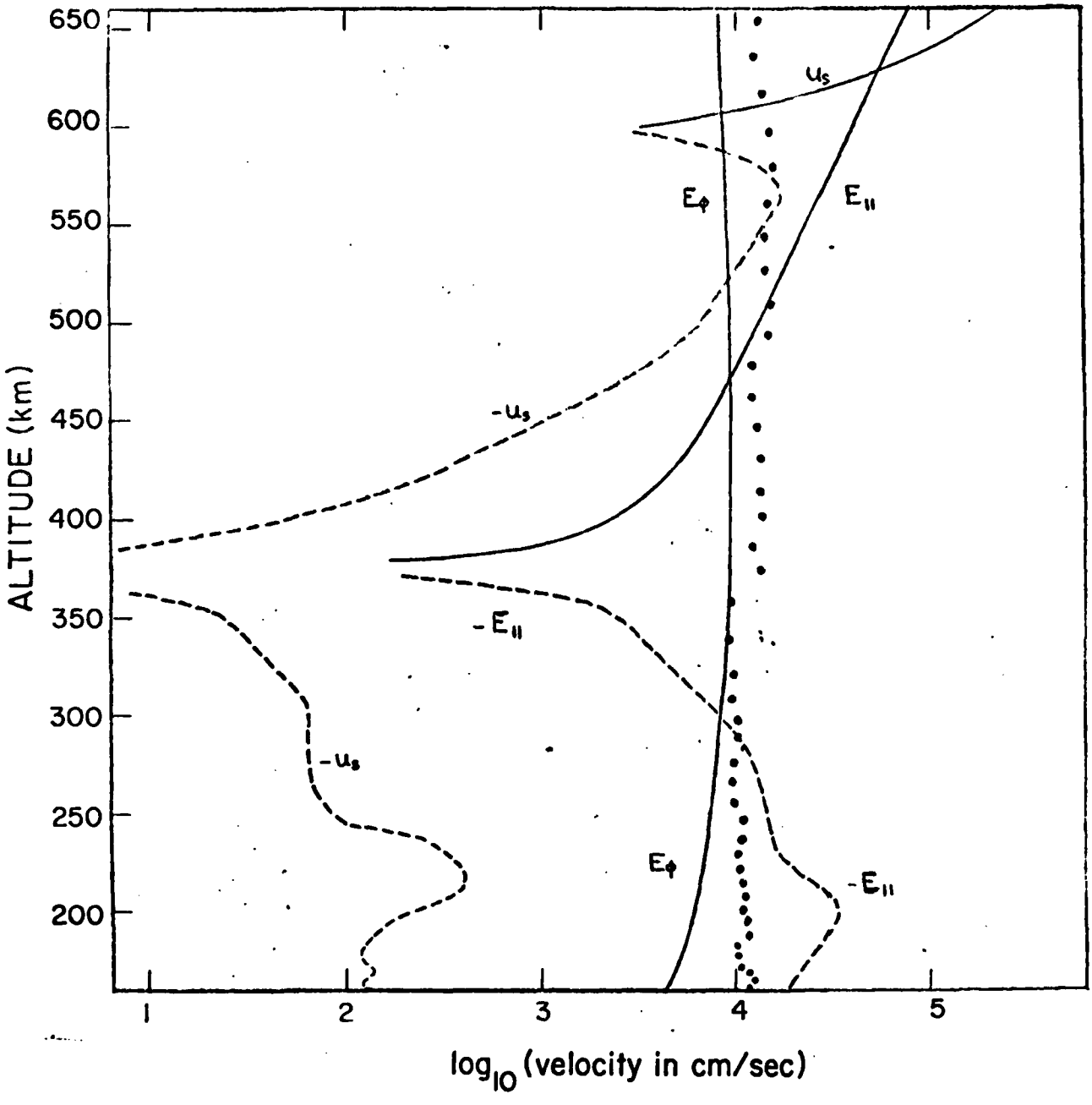

Fig. 9. The vertical component of the O^+ drift velocity. u_s represents contributions from the gravitational force and gradients of partial pressures. E_{11} and E_ϕ represent contributions from a parallel and eastward electric field of 1 and 3 mV/meter, respectively. The filled circles represent the observed vertical component of plasma drifts.

APPENDIX A

DATA

APPENDIX A

DATA

The data utilized in this report pertain to the upleg of orbit 594 of the Atmosphere Explorer C satellite (Dalgarno et al., 1973). The measurements made on this occasion (February 8, 1974) are representative of an undisturbed daytime atmosphere in the mid-latitude and equatorial region. The data are summarized in three tables.

Table A-1 lists ion concentrations as a function of altitude Z (in km) as measured by the MIMS instrument (Johnson, 1973). Concentrations are in units of cm^{-3} and listed in logarithmic (base 10) form. The electron concentration is the sum of the ion concentrations. An entry of -5 signifies that no measurement of the concentration was made at that altitude.

Table A-2 lists neutral concentrations (in cm^{-3}) in logarithmic form. For N_2, He, O, and $N(^4S)$ the measurements by the OSS instrument (Nier, 1973) were used to establish a Bates-Walker (Walker, 1965) profile from which values were obtained at all altitudes. The photochemical model of Oppenheimer et al. (1977) was used in conjunction with a Bates-Walker profile to establish the O_2 concentration. The H concentration represents a model calculation (Hedin et al., 1977). The NO concentration was measured by the UVNO experiment (Barth et al., 1973) and was extrapolated to altitudes above 260 km. The $N(^2D)$ concentration was measured by the VAE experiment (Hayes et al., 1973) and was extrapolated above 300 km.

Table A-3 lists the electron temperature (TE) measured by the CEP experiment (Hanson et al., 1973); the ion temperature (TI) measured by the RPA experiment (Brace et al., 1973), the neutral temperature (TBW) inferred from the O and N_2 concentration profiles, the zenith angle (SZA), magnetic latitude (MLAT), latitude (LAT), and local solar time (LST). No measurement of the neutral temperature (TN) was available on this occation. Temperatures are given in degrees Kelvin, angles in degrees, and time in hours.

TABLE A-1. Logarithmic Concentrations of Ions and Electrons (cm^{-3})

Z	O+	O2+	NO+	N+	N2+	H+	HO+	ELEC
656.7	5.09[illegible]	-5.000	-5.000	3.545	-5.000	4.383	2.880	5.137
637.6	5.174	-5.000	-5.000	3.580	-5.000	4.395	2.892	5.252
618.6	5.244	-5.000	-5.000	3.664	-5.000	4.374	2.913	5.311
600.4	5.314	-5.000	-5.000	3.722	-5.000	4.355	2.883	5.371
582.3	5.376	-5.000	-5.000	3.753	-5.000	4.303	2.862	5.422
564.0	5.432	-5.000	-5.000	3.800	-5.000	4.266	2.847	5.471
546.4	5.483	-5.000	-5.000	3.859	-5.000	4.196	2.795	5.515
529.0	5.524	-5.000	-5.000	3.879	-5.000	4.139	2.701	5.551
512.0	5.559	-5.000	-5.000	3.915	-5.000	4.054	2.649	5.582
495.3	5.594	-5.000	-5.000	3.959	-5.000	3.967	2.544	5.614
478.9	5.608	-5.000	-5.000	3.984	1.427	3.864	2.454	5.626
462.9	5.622	-5.000	-5.000	3.965	-5.000	3.757	2.331	5.637
447.2	5.642	-5.000	-5.000	3.963	-5.000	3.656	2.253	5.656
431.8	5.671	-5.000	-5.000	4.008	1.579	3.567	2.116	5.684
416.8	5.685	-5.000	-5.000	4.013	1.689	3.460	2.015	5.697
402.2	5.705	-5.000	-5.000	4.029	1.825	3.354	1.847	5.716
388.0	5.713	1.493	1.396	4.009	1.813	3.256	1.725	5.723
374.1	5.747	1.729	1.657	4.016	1.926	3.141	1.588	5.756
360.6	5.747	1.829	1.659	3.981	2.058	3.049	1.414	5.755
347.5	5.747	2.004	2.045	3.966	2.228	2.957	1.235	5.755
334.7	5.770	2.182	2.159	3.974	2.287	2.885	1.150	5.778
322.4	5.795	2.380	2.440	3.954	2.444	2.814	.903	5.796
310.5	5.777	2.544	2.600	3.923	2.594	2.728	.833	5.780
299.0	5.789	2.814	2.806	3.877	2.685	2.668	-5.000	5.796
287.9	5.789	2.936	3.030	3.848	2.867	2.575	-5.000	5.796
277.2	5.798	3.138	3.176	3.817	2.923	2.489	-5.000	5.805
267.0	5.810	3.313	3.339	3.762	2.993	2.409	-5.000	5.818
257.2	5.826	3.475	3.496	3.742	3.097	2.342	-5.000	5.834
247.9	5.832	3.621	3.636	3.691	3.181	2.276	-5.000	5.842
239.0	5.833	3.743	3.743	3.677	3.240	2.209	-5.000	5.844
230.5	5.808	3.835	3.905	3.588	3.256	2.118	-5.000	5.822
222.5	5.718	4.033	4.091	3.520	3.300	1.972	-5.000	5.741
215.0	5.595	4.183	4.313	3.374	3.336	1.811	-5.000	5.637
207.9	5.435	4.330	4.520	3.297	3.387	1.586	-5.000	5.520
201.2	5.352	4.421	4.633	3.242	3.402	1.470	-5.000	5.475
195.0	5.281	4.492	4.725	3.207	3.403	1.303	-5.000	5.446
189.3	5.211	4.561	4.795	3.138	3.409	1.149	-5.000	5.424
184.0	5.149	4.597	4.830	3.105	3.374	1.086	-5.000	5.401
179.2	5.093	4.653	4.865	3.025	3.353	1.037	-5.000	5.390
174.9	5.043	4.687	4.900	2.977	3.322	.966	-5.000	5.383
171.1	4.951	4.673	4.921	2.928	3.286	.799	-5.000	5.347
167.0	4.881	4.708	4.929	2.867	3.247	.712	-5.000	5.331
164.5	4.796	4.709	4.921	2.790	3.189	.582	-5.000	5.299
162.6	4.754	4.715	4.921	2.767	3.138	.561	-5.000	5.288
160.7	4.711	4.708	4.921	2.699	3.125	.510	-5.000	5.277
159.3	4.636	4.709	4.900	2.709	3.010	.432	-5.000	5.248
158.4	4.635	4.729	4.900	2.688	3.023	.398	-5.000	5.250
158.0	4.560	4.716	4.893	2.630	2.995	-5.000	-5.000	5.227

TABLE A-2. Logarithmic Concentrations of Neutrals (cm^{-3})

Z	O	N2	O2	HE	H	N(4S)	N(2D)	NO
656.7	5.635	2.542	.700	5.670	5.189	4.207	1.838	-5.549
637.6	5.786	2.806	.987	5.710	5.200	4.348	2.000	-5.114
618.6	5.935	3.067	1.271	5.760	5.210	4.438	2.161	-4.656
600.2	6.083	3.326	1.553	5.810	5.220	4.627	2.321	-4.199
582.0	6.229	3.582	1.830	5.850	5.230	4.767	2.475	-3.731
564.0	6.374	3.836	2.106	5.900	5.240	4.899	2.634	-3.274
546.4	6.517	4.085	2.377	5.940	5.250	5.037	2.789	-2.746
529.0	6.659	4.333	2.647	5.980	5.260	5.165	2.941	-2.253
512.0	6.798	4.576	2.912	6.030	5.269	5.296	3.091	-1.764
495.2	6.935	4.817	3.173	6.070	5.279	5.424	3.235	-1.280
478.6	7.070	5.054	3.431	6.110	5.288	5.551	3.385	-.801
462.2	7.203	5.286	3.683	6.150	5.297	5.675	3.528	-.334
447.2	7.334	5.515	3.932	6.190	5.306	5.798	3.669	.123
431.6	7.463	5.741	4.178	6.230	5.315	5.919	3.808	.569
416.2	7.590	5.962	4.418	6.267	5.324	6.037	3.944	1.000
402.2	7.713	6.178	4.653	6.304	5.333	6.153	4.077	1.413
388.0	7.834	6.389	4.882	6.339	5.341	6.266	4.207	1.809
374.1	7.952	6.597	5.108	6.377	5.350	6.377	4.335	2.189
360.6	8.068	6.799	5.328	6.407	5.358	6.485	4.460	2.550
347.5	8.181	6.997	5.542	6.433	5.366	6.591	4.581	2.892
334.7	8.293	7.190	5.753	6.458	5.375	6.694	4.700	3.217
322.4	8.403	7.377	5.956	6.490	5.383	6.795	4.816	3.529
310.5	8.511	7.559	6.154	6.527	5.391	6.892	4.928	3.830
299.0	8.618	7.736	6.346	6.558	5.399	6.987	5.036	4.069
287.9	8.723	7.907	6.532	6.585	5.408	7.079	5.142	4.314
277.2	8.827	8.074	6.713	6.612	5.416	7.168	5.245	4.549
267.0	8.929	8.233	6.887	6.640	5.424	7.254	5.347	4.754
257.2	9.029	8.388	7.055	6.667	5.432	7.337	5.439	5.079
247.9	9.128	8.536	7.215	6.693	5.441	7.417	5.530	5.266
239.0	9.225	8.679	7.371	6.730	5.449	7.494	5.618	5.421
230.5	9.320	8.817	7.521	6.757	5.458	7.569	5.680	5.542
222.5	9.413	8.949	7.665	6.785	5.467	7.641	5.760	5.699
214.8	9.504	9.076	7.801	6.822	5.476	7.709	5.820	5.730
207.5	9.594	9.196	7.932	6.842	5.485	7.775	5.860	5.904
200.6	9.682	9.312	8.059	6.879	5.495	7.839	5.890	6.000
194.0	9.768	9.422	8.178	6.907	5.505	7.900	5.920	6.030
187.8	9.852	9.528	8.291	6.945	5.514	7.958	5.910	6.171
181.9	9.934	9.628	8.398	6.975	5.524	8.013	5.900	6.270
176.4	10.014	9.715	8.498	7.007	5.530	8.064	5.875	6.370
171.2	10.092	9.800	8.589	7.043	5.544	8.112	5.840	6.381
166.3	10.168	9.876	8.673	7.070	5.553	8.155	5.800	6.433
161.8	10.242	9.945	8.747	7.107	5.563	8.195	5.732	6.492
157.6	10.314	10.006	8.814	7.125	5.571	8.230	5.670	6.516
153.7	10.385	10.056	8.868	7.170	5.579	8.259	5.620	6.541
150.1	10.454	10.098	8.914	7.188	5.587	8.283	5.579	6.545
146.8	10.521	10.130	8.949	7.192	5.593	8.301	5.550	6.564
143.8	10.587	10.150	8.971	7.210	5.599	8.313	5.528	6.563
141.0	10.650	10.159	8.981	7.232	5.603	8.319	5.519	6.584

TABLE A-3. Temperatures and Orbital Parameters

[illegible]	TI	TI	TN	TBW	SZA	MLAT	LAT	LST
[illegible]	1347.0	1455.0	.0	856.0	35.10	-15.78	-4.85	14.27
[illegible]	1342.0	1393.0	.0	856.0	35.07	-14.68	-3.93	14.25
[illegible]	1342.0	1314.0	.0	856.0	35.06	-13.98	-3.00	14.23
[illegible]	1342.0	1332.0	.0	856.0	35.08	-13.07	-2.07	14.21
[illegible]	1338.0	1342.0	.0	856.0	35.13	-12.16	-1.14	14.18
[illegible]	1356.0	1337.0	.0	856.0	35.19	-11.25	-.20	14.15
[illegible]	1375.0	1160.0	.0	856.0	35.29	-10.32	.75	14.13
[illegible]	1210.0	1135.0	.0	856.0	35.41	-9.40	1.70	14.10
[illegible]	1275.0	1104.0	.0	856.0	35.56	-8.47	2.65	14.08
[illegible]	1156.0	1080.0	.0	856.0	35.73	-7.53	3.61	14.05
[illegible]	1168.0	1062.0	.0	856.0	35.93	-6.59	4.58	14.02
[illegible]	1176.0	1047.0	.0	855.9	36.15	-5.64	5.54	14.00
[illegible]	1178.0	1035.0	.0	855.9	36.40	-4.69	6.50	13.97
[illegible]	1181.0	1021.0	.0	855.9	36.67	-3.73	7.49	13.95
[illegible]	1166.0	1003.0	.0	855.8	36.97	-2.78	8.47	13.92
[illegible]	1194.0	979.0	.0	855.8	37.30	-1.81	9.45	13.89
[illegible]	1195.0	965.6	.0	855.7	37.65	-.84	10.44	13.86
[illegible]	1169.0	948.2	.0	855.5	38.02	.13	11.43	13.84
[illegible]	1191.0	933.5	.0	855.3	38.42	1.10	12.43	13.81
[illegible]	1209.0	922.2	.0	855.0	38.84	2.08	13.43	13.78
[illegible]	1205.0	924.0	.0	854.6	39.28	3.06	14.43	13.75
[illegible]	1208.0	920.0	.0	854.0	39.75	4.05	15.43	13.72
[illegible]	1205.0	926.0	.0	853.3	40.23	5.03	16.44	13.70
[illegible]	1446.0	936.8	.0	852.3	40.74	6.03	17.45	13.67
[illegible]	1197.0	926.3	.0	851.1	41.27	7.02	18.47	13.64
[illegible]	1245.0	927.3	.0	849.4	41.82	8.02	19.47	13.61
[illegible]	1217.0	922.5	.0	847.4	42.38	9.01	20.48	13.57
[illegible]	1241.0	903.3	.0	844.7	42.97	10.01	21.50	13.54
[illegible]	1249.0	894.5	.0	841.5	43.57	11.02	22.52	13.51
[illegible]	1207.0	897.5	.0	837.6	44.19	12.02	23.54	13.48
[illegible]	1241.0	883.3	.0	832.7	44.83	13.03	24.56	13.45
[illegible]	1251.0	869.0	.0	827.0	45.48	14.03	25.58	13.41
[illegible]	1257.0	863.5	.0	820.4	46.15	15.04	26.60	13.38
[illegible]	1290.0	841.5	.0	812.8	46.84	16.05	27.63	13.34
[illegible]	1261.0	834.5	.0	804.0	47.54	17.06	28.65	13.31
[illegible]	1241.0	832.5	.0	794.3	48.25	18.07	29.67	13.27
[illegible]	1240.0	791.0	.0	783.8	48.97	19.08	30.69	13.23
[illegible]	1215.0	784.5	.0	772.4	49.71	20.08	31.71	13.19
[illegible]	1256.0	776.3	.0	760.5	50.46	21.09	32.73	13.15
[illegible]	1307.0	761.0	.0	748.4	51.22	22.10	33.75	13.11
[illegible]	1249.0	755.0	.0	736.4	52.00	23.11	34.76	13.07
[illegible]	1241.0	745.4	.0	724.9	52.78	24.11	35.78	13.03
[illegible]	1208.0	732.0	.0	713.9	53.57	25.11	36.79	12.99
[illegible]	1193.0	723.0	.0	704.5	54.37	26.11	37.80	12.94
[illegible]	1134.0	726.0	.0	696.2	55.18	27.11	38.80	12.90
[illegible]	1076.0	724.0	.0	689.8	56.00	28.11	39.80	12.85
[illegible]	1074.0	717.0	.0	685.6	56.82	29.10	40.80	12.80
[illegible]	1052.0	706.0	.0	683.7	57.66	30.09	41.79	12.75

APPENDIX B

COLLISION FREQUENCIES

APPENDIX B

COLLISION FREQUENCIES

This appendix contains expressions for the calculation of various types of momentum transfer collision frequencies. These are defined in such a way that

$$-n_s m_s \nu_{st} (\vec{u}_s - \vec{u}_t)$$

represents the force per unit volume exerted by species t on species s. n_s, m_s, and $\vec{u}_s$ are the concentration, mass, and velocity, respectively, for species s, and ν_{st} is the momentum transfer collision frequency of species s with species t. As defined, the collision frequencies satisfy the symmetry property

$$n_s m_s \nu_{st} = n_t m_t \nu_{ts} \cdot$$

The preceding definition is the most frequently used (cf. Schunk, 1977). It should be noted, however, that other definitions are in use as well. For example, Banks and Kockarts (1973), who have given a comprehensive review of collision frequencies, define them in such a way that

$$\nu_{st}\ (\text{Banks}) = (m_s/\mu_{st})\nu_{st}(\text{Schunk}).$$

where $\mu_{st} = m_s m_t/(m_s+m_t)$ is the reduced mass.

Electron-Neutral Momentum Transfer Collision Frequencies

$$\nu(e\text{-}O) = 8.2 \times 10^{-10}\ n(0)\ T_e^{1/2}$$

$$\nu(e\text{-}N_2) = 2.33 \times 10^{-11}\ n(N_2)(1-1.21\times10^{-4}T_e)\ T_e$$

$$\nu(e\text{-}O_2) = 1.82 \times 10^{-10}\, n(O_2)(1 + 3.6 \times 10^{-2}\, T_e^{1/2})\, T_e^{1/2}$$

$$\nu(e\text{-}He) = 4.6 \times 10^{-10}\, n(He)\, T_e^{1/2}$$

$$\nu(e\text{-}H) = 4.5 \times 10^{-9}\, n(H)\, (1\text{-}1.35 \times 10^{-4}\, T_e)\, T_e^{1/2}$$

$$\nu(e\text{-}N) = 6.0 \times 10^{-10}\, n(N)\, T_e^{1/2}$$

where T_e is the electron temperature, n(x) is the concentration of species x in units of cm^{-3}, and the collision frequencies are in sec^{-1}. Except for the collision frequency with N, which is an interpolation based on the values for He and O, these expressions are given by Banks and Kockarts (1973) and they pertain to elastic collisions. These authors estimate that the accuracy for N_2 and O_2 is about 20%, for H 25%, for He 10%, and state that the result for O is uncertain both as to magnitude and as to the dependence on T_e.

Ion-Neutral Momentum Transfer Collision Frequencies

At low temperatures the ion-neutral interaction arises from the induced dipole polarization of the neutral by the ion. The corresponding polarization collision frequency is

$$\nu_{in} = 2.6 \times 10^{-9}\, n(n)\, (A_{in}\alpha_n)^{1/2}/A_i$$

where n(n) is the neutral concentration in cm^{-3}, $A_{in} = A_i A_n/(A_i+A_n)$ is the reduced mass, A_i and A_n are the ion and neutral masses in atomic units, α_n is the neutral polarizability in units of 10^{-24} cm^3 and ν_{in} is in sec^{-1}. Except for the adjustment required by the different definitions, these expressions, as well as the polarizabilities listed below, are given by Banks and Kockarts (1973).

Polarizabilities of Neutral Gases

Neutral Gas	$\alpha(10^{-24}\ cm^3)$
H	0.667
He	0.82
N	1.1
O	0.79
O_2	1.59
NO	1.74
N_2	1.76

At higher temperatures, a repulsive force counters the polarization force. The resulting collision frequencies depend on the details of the particular ion-neutral pair, but there is no data for collisions at high temperatures. This lack of data is compensated to some extent by the fact that in the high-temperature regions of the atmosphere the most important collisions are resonant charge transfer collisions, i.e. collisions between an ion and its parent neutral. The values given by Banks and Kockarts (1973), adjusted by the factor μ_{in}/m_i, are

$$\nu(O^+-O) = 2.4 \times 10^{-13}\, T^{1/2}\, (10.6-0.67 \log_{10} T)^2\, n(O) \qquad T>470$$

$$\nu(O_2^+-O_2) = 1.7 \times 10^{-13}\, T^{1/2}\, (10.6-0.76 \log_{10} T)^2\, n(O_2) \qquad T>1600$$

$$\nu(N_2^+-H_2) = 1.85 \times 10^{-13}\, T^{1/2}\, (14.3-0.96 \log_{10} T)^2\, n(N_2) \qquad T>340$$

$$\nu(H^+-H) = 9.5 \times 10^{-13}\, T^{1/2}\, (14.4-1.17 \log_{10} T)^2\, n(H) \qquad T>100$$

$$\nu(N^+-N) = 2.6 \times 10^{-13}\, T^{1/2}\, (10.4-0.64 \log_{10} T)^2\, n(N) \qquad T>550$$

$$\nu(He^+-N) = 4.85 \times 10^{-13}\, T^{1/2}\, (11.6-1.05 \log_{10} T)^2\, n(He) \qquad T>100$$

where $T = T_i + T_n$ is the sum of the ion and neutral temperatures. These expressions are valid for temperatures above the limit indicated for each reaction.

Coulomb Collision Frequencies

For charged particles the collision frequency arising from the Coulomb interaction is

$$\nu_{st} = 8.47 \times 10^{-2} \ell n \Lambda \, z_s^2 z_t^2 A_{st}^{1/2} n_t / A_s T_{st}^{3/2}$$

$$= 1.27 \, z_s^2 Z_t^2 A_{st}^{1/2} n_t / A_s T_{st}^{3/2}$$

with $\ell n \Lambda = 15$ (cf. Banks & Kockarts, 1973). n_t is the concentration of species t, A_s, T_s, and z_s are the mass (in atomic units), temperature (in ^oK) and charge (in atomic units) of species s, and

$$A_{st} = A_s A_t / (A_s + A_t)$$

$$T_{st} = (A_s T_t + A_t T_s) / (A_s + A_T)$$

If electrons are one of the species, the expression simplifies to

$$\nu_{ei} = 54.5 \, n_i z_i^2 / T_e^{3/2}$$

$$\nu_{ie} = 2.98 \times 10^{-2} \, n_e z_i^2 / A_i T_e^{3/2}$$

Collision frequencies for electrons and for O^+ are shown in Figure B-1, and Figure B-2, respectively, based on the data given in Appendix A.

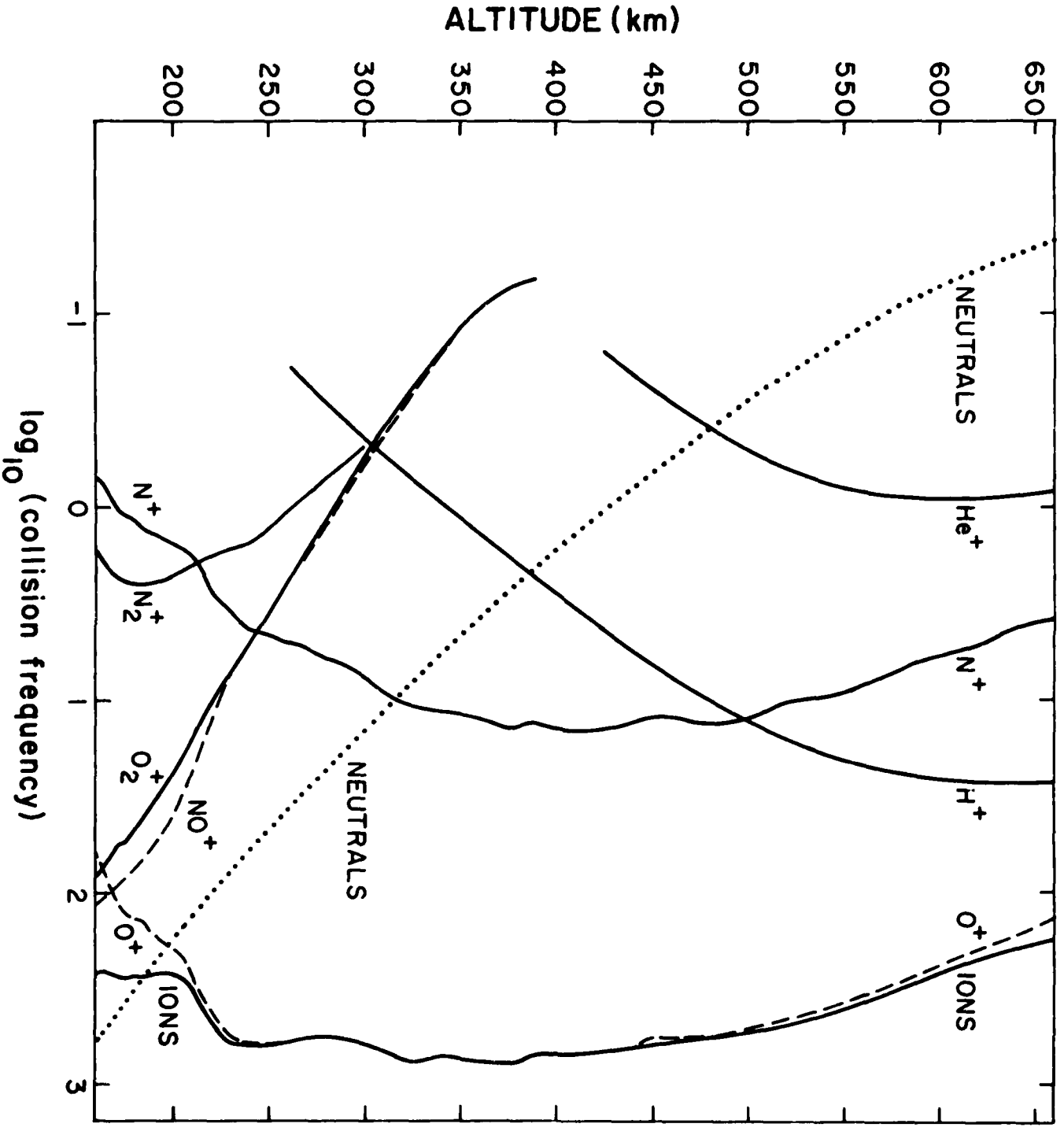

Fig. B-1. Collison frequencies of electrons with ions and neutrals (in sec^{-1}). Also shown is the sum of the collision frequency with all ions.

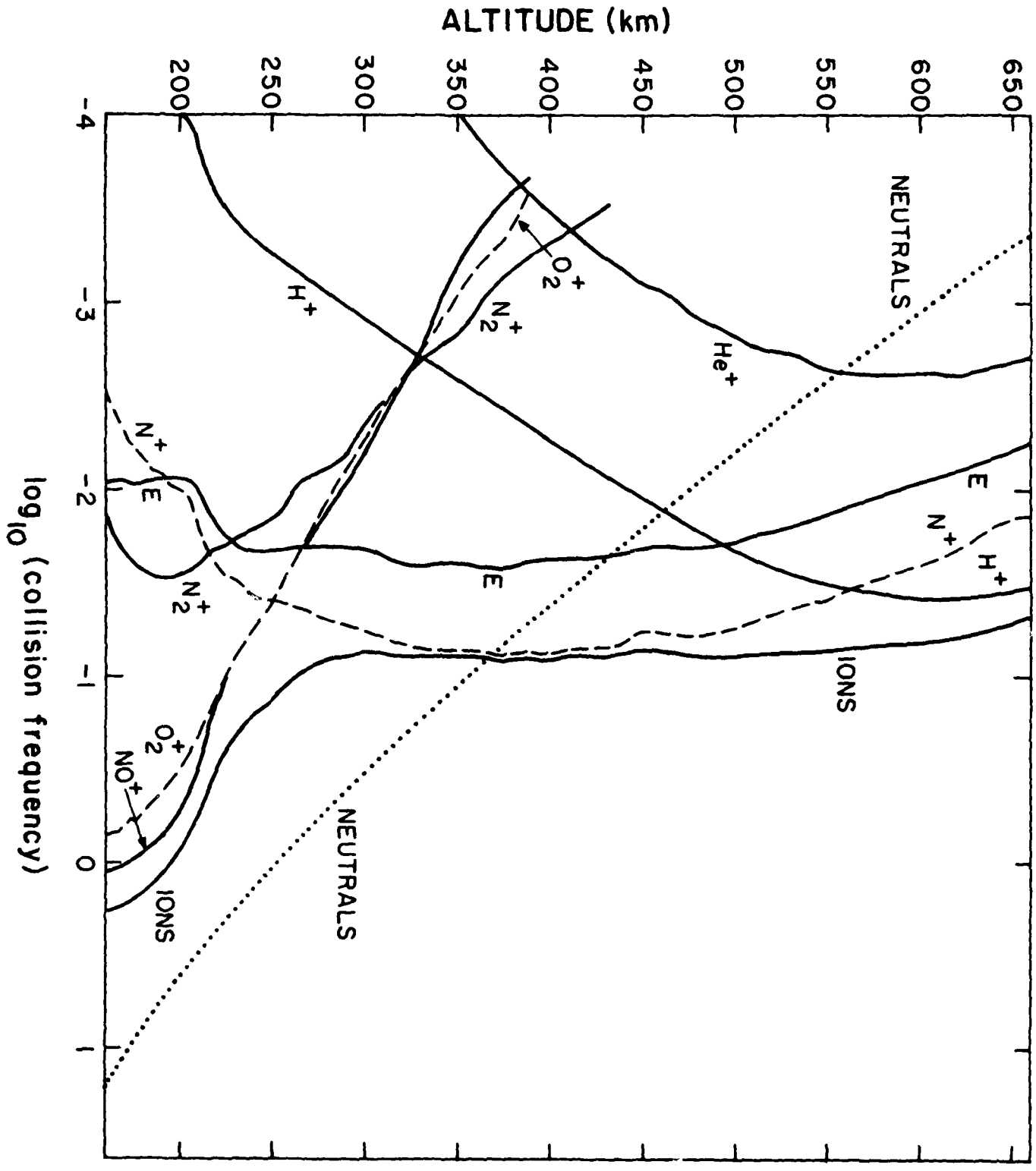

Fig. B-2. Collision frequences of O^+ with ions, electrons and neutrals in (sec^{-1}). The curved marked E pertains to electrons. Also shown is the sum of the collision frequencies with all other ions.

APPENDIX C

LISTING OF THE ELECTRON ENERGY DEPOSITION CODE AND THE CROSS SECTION DATA FILE

```
      PROGRAM RCTEMPR (INPUT,OUTPUT,TAPE1,TAPE2=OUTPUT,TAPE3=INPUT,
     1         TAPE4,TAPE5,TAPE6,TAPE7)
C      **** RCTEMPR ****       770912
C       THIS IS THE DRIVER THAT IS WRITTEN TO INTERFACE WITH THE
C       PRIMARY PRODUCTION FILES
       COMMON/XSXS/ NOSPEC, NOEXC(4),  NGRID(4,20),
     1EGRID(4,20,25),SPLC0(4,20,25),SPLC1(4,20,25),SPLC2(4,20,25),
     2SPLC3(4,20,25),THRESH(4,20),NIONFS(4),NIONGD(4),EIONGD(4,25),
     3DIFCON(4),TIXS0(4,25),TIXS1(4,25),TIXS2(4,25),TIXS3(4,25),DIXS0(4,
     425),DIXS1(4,25),DIXS2(4,25),DIXS3(4,25), THRICZ(4,6),
     5FRACT(4,6,25)
       COMMON/DENS/TE,NOALT,IALT(10),XDENS(4),XEDEN
       COMMON/GRID/INTGRID,XGRID(400),VGRID(400),PROGRID(400)
       COMMON /POINT/IPOINT(4,20),IIPONT(4),IDPONT(4)
       COMMON/ALPHA/NAME(4),STATE(4,20),ISTATE(4,6)
        COMMON IBGN,IOTEL,IAVGF,FLXMULT
C        BEWARE, THE ORDER OF SPECIES IN REDXSN MUST MATCH WITH
C        THOSE IN THE PRODUCTION FILE
       CALL SETGRID
C        SETGRID SETS UP THE INTEGRATION GRID
       WRITE(2,4)
     4 FORMAT(* ENTER NUMBER OF ALTITUDE VALUES(I2)*)
       READ(3,1) NOALT
C          NOALT IS THE NUMBER OF ALTITUDE VALUES TO BE DONE
     1 FORMAT(I2)
        WRITE(2,5)
     5 FORMAT(* ENTER NUMBERS FOR ALTITUDE RECORDS(20I4)*)
       READ(3,2) (IALT(I),I=1,NOALT)
       WRITE(2,6)
     6  FORMAT(* ENTER NUMBER OF INTERVALS FOR AVG.(I2)*)
        READ(3,1) IAVGF
C      N.B. IAVGF.LT.2 IMPLIES AVERAGED FLUX AND FLUX*4PI NOT COMPUTED
       WRITE(2,10)
    10 FORMAT(* ENTER FLUX MULTIPLICATION FACTOR(F3.1)*)
        READ(3,11) FLXMULT
    11 FORMAT(F3.1)
     2 FORMAT(2014)
        CALL REDXSN
       CALL SETPRC(-1)
       DO 3 I=1,NOALT
       CALL SETPRC(IALT(I))
       CALL WORK
     3 CONTINUE
       END
       SUBROUTINE SETPRC(KEY)
       COMMON IBGN,IOTEL,IAVGF,FLXMULT
       COMMON/GRID/INTGRID,XGRID(400),VGRID(400),PROGRID(400)
       DIMENSION XPRO(400),YPRO(400),C(400)
        DIMENSION WORDS(19)
       COMMON/DENS/TE,NOALT,IALT(10),XDENS(4),XEDEN
C         THIS ROUTINE SETS UP THE PRIMARY ELECTRON PRODUCTION DATA
C       KEY=-1 TO READ PRODUCTION GRID DATA,KEY&0 READS THE PRODUCTION
C       DATA FOR THE KEY*TH ALTITUDE ON THE FILE
       IF(KEY.NE.-1) GO TO 1
       READ (4,52) WORDS
    52 FORMAT (19A4)
       WRITE(2,2) WORDS
     2 FORMAT (1H1,19A4)
       READ (4,52) WORDS
       READ(4,3) NPTSPRC
       WRITE(2,23) NPTSPRC
```

```
   23 FORMAT(I4,* = NPTSPRO*)
    3 FORMAT(I5)
      READ(4,4) (XPRO(I),I=1,NPTSPRO)
      WRITE(2,21)
   21 FORMAT(*  ELECTRON PRODUCTION GRID *)
      WRITE(2,22) (XPRO(I),I=1,NPTSPRO)
   22 FORMAT (10E12.3)
      NMAX=NPTSPRO-1
      DO 17 I=1,NPTSPRO
   17 XGRID(I)=XPRO(I)
      DO 117 I=1,NMAX
  117 VGRID(I)=5.93E+7*SQRT(0.5*(XGRID(I)+XGRID(I+1)))
    4 FORMAT(5E15.5)
      REWIND 4
      RETURN
    1 CONTINUE
      I=NPTSPRO/5
      F=I
      F1=FLOAT(NPTSPRO)/5.0
      IF(F.EQ.F1) GO TO 5
      I=I+1
    5 CONTINUE
      I=I+3
      DO 6 J=1,I
      READ(4,3)
    6 CONTINUE
      IF(KEY.EQ.1) GO TO 7
      I=NPTSPRO/6
      F=I
      F1=FLOAT(NPTSPRO)/6.0
      IF(F.EQ.F1) GO TO 8
      I=I+1
    8 CONTINUE
C      STATEMENT I=I+10 REPLACED BY I=I+11 (RC,10/17/75)
      I=I+11
      IL=KEY-1
      DO 9 J=1,IL
      DO 9 K=1,I
      READ(4,3)
    9 CONTINUE
    7 CONTINUE
      READ(4,10)ZA
   10 FORMAT(25X,F12.6)
      READ(4,10) ALT
   13 FORMAT(* ALTITUDE IS*,F12.6)
      READ(4,10) T
      WRITE (5,13) ALT
      WRITE (2,11) ALT,ZA,T
   11 FORMAT (1X,119(1H-)/24H      ALT      SZA     TEMP/3F8.2)
      READ(4,14) XDENS(4)
      READ(4,14) XDENS(2)
      READ(4,14) XDENS(3)
      READ(4,14) XDENS(1)
   14 FORMAT(25X,E16.6)
      READ(4,15) TE
   15 FORMAT (26X,E16.6)
      READ(4,20) XEDEN
   20 FORMAT (22X,E16.6)
      READ(4,3)
C     ANOTHER DUMMY READ FOR "TOTAL ION DENSITY" (RC,10/17/75)
      READ (4,3)
```

```
      READ(4,16)(YPRO(K),K=1,NPTSPRO)
   16 FORMAT (6E12.4)
       TOTEL=0.0
      DO 32 K=1,NMAX
       YPRO(K)=YPRO(K)*FLXMULT
       TOTEL=TOTEL+YPRO(K)
      PROGRID(K)=YPRO(K)/(XGRID(K+1)-XGRID(K))
      C(K)=PROGRID(K)*VGRID(K)
      C(K)=C(K)/12.568
   32 CONTINUE
      WRITE(2,400)
  400 FORMAT(* INITIAL FLUX *)
      WRITE(2,22) (C(K),K=1,NMAX)
      REWIND 4
C      FIND END OF PRODUCTION SPECTRUM
      K=NPTSPRO-1
   18 IF(ABS(YPRO(K)-0.0).GT.1.0E-6) GO TO 19
      K=K-1
      GO TO 18
   19 CONTINUE
      IBGN=K
      WRITE(2,31) IBGN
   31 FORMAT(I4,* = IBGN*)
      WRITE(7,200) ALT,T,XDENS,TE,XEDEN
  200 FORMAT(8E10.4)
      WRITE (6,201) ALT
      RETURN
  201 FORMAT (F7.1)
      END
       SUBROUTINE WORK
      DIMENSION DFPROS(10),CFE(4,20),CFI(4,6),IIJ(4),PRDFA(400),PRDFAS(1
     10),FELS(10),FEL(400),PROBE(4,20),PROBI(4,6),EEF(400),FELWP(400),PR
     2O(400),DUMMY(6),Q(13),GE(20)
      COMMON IBGN,TOTEI,IAVGP
      COMMON/XSXS/ NOSPEC, NOEXC(4),  NGRID(4,20),
     1EGRID(4,20,25),SPLC0(4,20,25),SPLC1(4,20,25),SPLC2(4,20,25),
     2SPLC3(4,20,25),THRESH(4,20),NIONFS(4),NIONGD(4),EIONGD(4,25),
     3DIFCON(4),TIXS0(4,25),TIXS1(4,25),TIXS2(4,25),TIXS3(4,25),DIXS0(4,
     425),DIXS1(4,25),DIXS2(4,25),DIXS3(4,25), THRICZ(4,6),
     5FRACT(4,6,25)
      COMMON/DENS/TE,NOALT,IALT(10),XDENS(4),XEDEN
      COMMON/GRID/INTGRID,XGRID(400),VGRID(400),PROGRID(400)
      COMMON /POINT/IPCINT(4,20),IIPONT(4),IDPONT(4)
      COMMON/ALPHA/NAME(4),STATE(4,20),ISTATE(4,6)
      WRITE(2,70)
   70 FORMAT (/6H1*****,* THE PROBLEM CONDITIONS ARE_*/)
      WRITE(2,71) TE
   71 FORMAT(F10.2,* = ELECTRON TEMPERATURE *)
      WRITE(2,72) XEDEN
   72 FORMAT  (E10.2,* = ELECTRON DENSITY (CM-3)*)
      WRITE(2,62)(DIFCON(ICE),NAME(ICE),ICE=1,NOSPEC)
   62 FORMAT (F10.2,* = BEATY S IONIZATION EQUATION CONSTANT FOR *,A10)
      WRITE (2,73)
   73 FORMAT (/* THE HEAVY BODY NUMBER DENSITIES ARE_*)
      WRITE(2,74) (NAME(KK),KK=1,NOSPEC)
   74 FORMAT (10(2X,A10))
      WRITE(2,75)(XDENS(KK),KK=1,NOSPEC)
   75 FORMAT (10F12.3)
      NINT=INTGRID-1
      I=IBGN
      DO 371 J=1,I
```

```
        PRDFA(J)=PROGRID(J)
  371 CONTINUE
      IFLAG=0
      IONFG=0
      DFPRO=PRDFA(I)
      DES=(XGRID(I+1)-XGRID(I))/10.0
      ELESC=0.0
      DFPROS(1)=0.2*DFPRO
      DFPROS(10)=DFPROS(1)
      DFPROS(2)=0.4*DFPRO
      DFPROS(9)=DFPROS(2)
      DFPROS(3)=0.8*DFPRO
      DFPROS(8)=DFPROS(3)
      DFPROS(4)=1.6*DFPRO
      DFPROS(7)=DFPROS(4)
      DFPROS(5)=2.0*DFPRO
      DFPROS(6)=DFPROS(5)
      DO 15 J=1,NOSPEC
      KKMAX=NOEXC(J)
      DO 16 K=1,KKMAX
      PROBE(J,K)=0.0
   16 CONTINUE
      KKMAX=NIONFS(J)
      DO 17 K=1,KKMAX
      PROBI(J,K)=0.0
   17 CONTINUE
   15 CONTINUE
      DO 14 J=1,10
      PRDFAS(J)=0.0
   14 CONTINUE
      DO 2 J=1,10
C       CLEAR COLLISION FREQUENCY ARRAYS
      DO 3 K=1,NOSPEC
      KKMA=NIONFS(K)
      DO 4 KK=1,KKMA
      CFI(K,KK)=0.0
    4 CONTINUE
      KKMAX=NOEXC(K)
      DO 5   KK=1,KKMAX
      CFE(K,KK)=0.0
    5 CONTINUE
    3 CONTINUE
C   INITIALIZE POINTERS FOR EXCITATION AND IONIZATION GRIDS
      DO 1000 K=1,NOSPEC
      KKMAX=NOEXC(K)
      IIPONT(K)=1
      IDPONT(K)=1
      DO 1001 JJJ=1,KKMAX
      IPOINT(K,JJJ)=1
 1001 CONTINUE
 1000 CONTINUE
C       CALCULATE THE ENERGY FOR THE BIN, ALSO THE VELOCITY
      E=XGRID(I+1)+0.5*DES-FLOAT(J)*DES
      V=5.93E+7*SQRT(E)
      CALL DEDT(E,TE,XEDEN,DET,XL)
      ELCF=-DET/DES
      SUMEX=0.0
C       CALCULATE THE EXCITATION COLLISION FREQUENCIES
      DO 6 K=1,NOSPEC
      KKMAX=NOEXC(K)
      DO 7 KK=1,KKMAX
```

```
      IF(E.LT.THRESH(K,KK)) GO TO 7
      IF(J.NE.1) GO TO 26
   25 LI=-1
      GO TO 27
   26 LI=0
   27 CFE(K,KK)=QEX(K,KK,E,LI)*V*XDENS(K)
      SUMEX=SUMEX+CFE(K,KK)
      IFLAG=1
    7 CONTINUE
    6 CONTINUE
C      CALCULATE THE IONIZATION COLLISION FREQUENCIES
C      LOCATE ENERGY INDICIES FOR FRACTION
      DO 8 K=1,NOSPEC
      IF(E.LE.EIONGD(K,1)) GO TO 8
      III=1
   10 IF(E.GT.EIONGD(K,III).AND.E.LE.EIONGD(K,III+1)) GO TO 9
      III=III+1
      GO TO 10
    9 IIJ(K)=III
    8 CONTINUE
      SUMION=0.0
      DO 11 K=1,NOSPEC
      QI=QION(K,E,LI)
      KKMAX=NIONFS(K)
      DO 12 KK=1,KKMAX
      IF(E.LT.THRICZ(K,KK)) GO TO 12
      IIJKK=IIJ(K)
      CFI(K,KK)=QION(K,E,LI)*V*XDENS(K)*FRACT(K,KK,IIJKK)
      SUMION=SUMION+CFI(K,KK)
      IONFG=1
   12 CONTINUE
   11 CONTINUE
      SCF=SUMION+SUMEX+ELCF
      PROBION=SUMION/SCF
      PROBEX=SUMEX/SCF
      PROBEL=ELCF/SCF
      PROD=DFPROS(J)+PROFAS(J)
      XNNX=PROD*DES/SCF
      XNEE=PROD/SCF
      FELS(J)=V*PROD/SCF
      IF(J.EQ.10) GO TO 107
      PROFAS(J+1)=ELCF*(PROD/SCF)
  107 CONTINUE
C      ACCUMILATE PROBABILITIES
C      ELESC IS THE ENERGY LOSS TO ELASTIC SCATTERING PER ELECTRON
      ELESC=ELESC+(ELCF*DES*XNNX)
      DO 18 K=1,NOSPEC
      KKMAX=NOEXC(K)
      DO 19 KK=1,KKMAX
      PROBE(K,KK)=PROBE(K,KK)+CFE(K,KK)*XNNX
   19 CONTINUE
      KKMAX=NIONFS(K)
      DO 20 KK=1,KKMAX
      PROBI(K,KK)=PROBI(K,KK)+CFI(K,KK)*XNNX
   20 CONTINUE
   18 CONTINUE
C      LOOK AFTER DEGRADED ELECTRONS FROM EXCITATION
      XX=XNEF
      DO 21 K=1,NOSPEC
      KKMAX=NOEXC(K)
      DO 22 KK=1,KKMAX
```

```
      IF(E.LT.THRESH(K,KK)) GO TO 22
      EE=E-THRESH(K,KK)
      KKK=1
   24 IF(EE.GT.XGRID(KKK).AND.EE.LT.XGRID(KKK+1)) GO TO 23
      KKK=KKK+1
      GO TO 24
   23 PRDFA(KKK)=PRDFA(KKK)+XX*CFF(K,KK)*(DES/(XGRID(KKK+1)-XGRID(KKK)))
   22 CONTINUE
   21 CONTINUE
C       LOOK AFTER DEGRADED ELECTRONS FROM IONIZATION
      DO127 K=1,NOSPEC
      KKMAX=NIONES(K)
      DO 28 KK=1,KKMAX
      IF(E.LT.THRICZ(K,KK)) GO TO 28
      IIJKK=IIJ(K)
      TEMP=XX*XDENS(K)*FRACT(K,KK,IIJKK)*V
      ESMAX=E-THRICZ(K,KK)
      KKK=1
   30 IF(ESMAX.GE.XGRID(KKK).AND.ESMAX.LT.XGRID(KKK+1)) GO TO 29
      KKK=KKK+1
      GO TO 30
   29 ESMAX=0.5*ESMAX
      KKG=1
   32 IF(ESMAX.GE.XGRID(KKG).AND.ESMAX.LT.XGRID(KKG+1)) GO TO 31
      KKG=KKG+1
      GO TO 32
   31 IF(KKK.GT.1) GO TO 33
      EUL=2.0*ESMAX
      PRDFA(1)=PRDFA(1)+2.0*TEMP*DIFION(K,E,II,0,0,EUL,DUMMY)     *(DES/(
     1XGRID(2)-XGRID(1)))
      GO TO 28
   33 KQM1=KKG-1
      DO 34 KK1=1,KQM1
      IF(KKG .EQ.1) GO TO 34
      PRDFA(KK1)=PRDFA(KK1)+TEMP*DIFION(K,E,II,XGRID(KK1),XGRID(KK1+1),D
     1UMMY)     *(DES/(XGRID(KK1+1)-XGRID(KK1)))
   34 CONTINUE
      IF(KKG.EQ.1) GO TO 103
      PRDFA(KKG  )=PRDFA(KKG  )+TEMP*DIFION(K,E,II,XGRID(KKG  ),ESMAX,DU
     1MMY)     *(DES/(XGRID(KKG+1)-XGRID(KKG)))
  103 CONTINUE
      ESMAX=2.0*ESMAX
      UPPL=ESMAX-XGRID(KKK)
      PRDFA(KKK)=PRDFA(KKK)+TEMP*DIFION(K,E,II,0.0,UPPL
     1,DUMMY)*(DES/(XGRID(KKK+1)-XGRID(KKK)))
      IF(KKG.EQ.1)   GO TO  104
      ULL=ESMAX-XGRID(KKG+1)
      UPPL=0.5*ESMAX
      PRDFA(KKG)=PRDFA(KKG)+TEMP*DIFION(K,E,II,ULL,UPPL
     1                  ,DUMMY)     *(DES/(XGRID(KKG+1)-XGRID(KKG)))
  104 CONTINUE
      KKGMX=KKK-1
      KKGMN=KKG+1
      DO 35 KK1=KKGMN,KKGMX
      IF(KKGMN.GE.KKGMX) GO TO 35
      ULL=ESMAX-XGRID(KK1+1)
      UPPL=ESMAX-XGRID(KK1)
      PRDFA(KK1)=PRDFA(KK1)+TEMP*DIFION(K,E,II,ULL,UPPL                  ,D
     1UMMY)     *(DES/(XGRID(KK1+1)-XGRID(KK1)))
   35 CONTINUE
   28 CONTINUE
```

```
  127 CONTINUE
    2 CONTINUE
      SUM=0.0
      DO 36 J=1,10
      SUM=SUM+FELS(J)
   36 CONTINUE
      FEL(I)=SUM/10.
      IF(I.EQ.1) GO TO 37
      PRDFA(I-1)=PRDFA(I-1)+ELCF*(PROD/SCF)*(DES/(XGRID(I)-XGRID(I-1)))
      INN=I-1
      DO 38 IP=1,INN
      IRV=I-IP
C      IRV= BIN NUMBER
C      CLEAR COLLISION FREQUENCY ARRAYS
      DO 39 K=1,NOSPEC
      DO 40 KK=1,6
      CFI(K,KK)=0.0
   40 CONTINUE
      KKMAX=NOEXC(K)
      DO 41  KK=1,KKMAX
      CFE(K,KK)=0.0
   41 CONTINUE
   39 CONTINUE
      DE=XGRID(IRV+1)-XGRID(IRV)
      E=XGRID(IRV)+0.5*DE
      V=5.93E+7*SQRT(E)
      CALL DEDT(E,TE,XEDEN,DET,XL)
      ELCF=-DET/DE
C      CALCULATE THE EXCITATION COLLISION FREQUENCIES
      SUMEX=0.0
      DO 42 K=1,NOSPEC
      KKMAX=NOEXC(K)
      DO 43 KK=1,KKMAX
      IF(E.LT.THRESH(K,KK)) GO TO 43
      CFE(K,KK)=GEX(K,KK,E,LI)*V*XDENS(K)
      SUMEX=SUMEX+CFE(K,KK)
   43 CONTINUE
   42 CONTINUE
C      CALCULATE THE IONIZATION COLLISION FREQUENCIES
C      LOCATE THE ENERGY INDICIES FOR FRACTION
      DO 44 K=1,NOSPEC
      IF(E.LE.EIONGD(K,1)) GO TO 44
      III=1
   45 IF(E.GT.EIONGD(K,III).AND.E.LE.EIONGD(K,III+1)) GO TO 46
      III=III+1
      GO TO 45
   46 IIJ(K)=III
   44 CONTINUE
      SUMION=0.0
      DO 47 K=1,NOSPEC
      KKMAX=NIONPS(K)
      DO 48 KK=1,KKMAX
      IF(E.LT.THRICZ(K,KK)) GO TO 48
      IIJKK=IIJ(K)
      CFI(K,KK)=GION(K,E,LI)*V*XDENS(K)*FRACT(K,KK,IIJKK)
      SUMION=SUMION+CFI(K,KK)
   48 CONTINUE
   47 CONTINUE
      SCF=ELCF+SUMEX+SUMION
      PROBION=SUMION/SCF
      PROBEX=SUMEX/SCF
```

```
      PROBEL=ELCF/SCF
      GRO=PRDFA(IRV)
      XNNX=GRO*DE/SCF
      FEL(IRV)=V*GRO/SCF
      XNEE=GRO/SCF
      IF(IRV.EQ.1) GO TO 38
      PRDFA(IRV-1)=PRDFA(IRV-1)+ELCF*(GRO/SCF)    *(DE/(XGRID(IRV)-XGRID(
     1IRV-1)))
C       ACCUMILATE PROBABILITIES
      ELESC=ELESC+(ELCF*DE*XNNX)
      DO 49 K=1,NOSPEC
      KKMAX=NOEXC(K)
      DO 50 KK=1,KKMAX
      PROBE(K,KK)=PROBE(K,KK)+CFE(K,KK)*XNNX
   50 CONTINUE
      KKMAX=NIONFS(K)
      DO 51 KK=1,KKMAX
      PROBI(K,KK)=PROBI(K,KK)+CFI(K,KK)*XNNX
   51 CONTINUE
   49 CONTINUE
C       LOOK AFTER DEGRADED ELECTRONS FROM EXCITATION
       XX=XNEE
      DO 52 K=1,NOSPEC
      KKMAX=NOEXC(K)
      DO 53 KK=1,KKMAX
      IF(E.LT.THRESH(K,KK))  GO TO 53
      EE=E-THRESH(K,KK)
      KKK=1
   55 IF(EE.GE.XGRID(KKK).AND.EE.LT.XGRID(KKK+1)) GO TO 54
      KKK=KKK+1
      GO TO 55
   54 PRDFA(KKK)=PRDFA(KKK)+XX*CFE(K,KK)*(DE/(XGRID(KKK+1)-XGRID(KKK)))
   53 CONTINUE
   52 CONTINUE
C       LOOK AFTER DEGRADED ELECTRONS FROM IONIZATION
      DO 56 K=1,NOSPEC
      KKMAX=NIONFS(K)
      DO 57 KK=1,KKMAX
      IF(E.LT.THRIOZ(K,KK)) GO TO 57
      ESMAX=E-THRIOZ(K,KK)
      IIJKK=IIJ(K)
      TEMP=XX*XDENS(K)*V*FRACT(K,KK,IIJKK)
      KKK=1
   59 IF(ESMAX.GE.XGRID(KKK).AND.ESMAX.LT.XGRID(KKK+1)) GO TO 58
      KKK=KKK+1
      GO TO 59
   58 ESMAX=0.5*ESMAX
      KKO=1
   60 IF(ESMAX.GE.XGRID(KKO).AND.ESMAX.LT.XGRID(KKO+1)) GO TO 61
      KKO=KKO+1
      GO TO 60
   61 IF(KKK.GT.1)  GO TO 66
      EUL=2.0*ESMAX
      PRDFA(1)=PRDFA(1)+2.0*TEMP*DIFION(K,E,II,0.0,EUL,DUMMY)    *(DE/(XG
     1RID(2)-XGRID(1)))
      GO TO 57
   66 KOM1=KKO-1
      DO 67 KK1=1,KOM1
      IF(KKO .EQ.1) GO TO 67
      PRDFA(KK1)=PRDFA(KK1)+TEMP*DIFION(K,E,II,XGRID(KK1),XGRID(KK1+1),D
     1UMMY)    *(DE/(XGRID(KK1+1)-XGRID(KK1)))
```

```
 67 CONTINUE
    IF(KKQ.EQ.1)   GO TO  105
    PRDFA(KKQ  )=PRDFA(KKQ  )+TEMP*DIFION(K,E,LI,XGRID(KKQ  ),ESMAX,DU
   1MMY)     *(DE /(XGRID(KKQ+1)-XGRID(KKQ)))
105 CONTINUE
    ESMAX=2.0*ESMAX
    UPPL=ESMAX-XGRID(KKK)
    PRDFA(KKK)=PRDFA(KKK)+TEMP*DIFION(K,E,LI,0.0,UPPL
   1,DUMMY)*(DE /(XGRID(KKK+1)-XGRID(KKK)))
    IF(KKQ.EQ.1)   GO TO  106
    ULL=ESMAX-XGRID(KKQ+1)
    UPPL=0.5*ESMAX
    PRDFA(KKQ)=PRDFA(KKQ)+TEMP*DIFION(K,E,LI,ULL,UPPL
   1                ,DUMMY)     *(DE /(XGRID(KKQ+1)-XGRID(KKQ)))
106 CONTINUE
    KKQMX=KKK-1
    KKQMN=KKQ+1
    DO 68 KK1=KKQMN,KKQMX
    IF(KKQMN.GE.KKQMX) GO TO 68
    ULL=ESMAX-XGRID(KK1+1)
    UPPL=ESMAX-XGRID(KK1)
    PRDFA(KK1)=PRDFA(KK1)+TEMP*DIFION(K,E,LI,ULL,UPPL                ,D
   1UMMY)   *(DE/(XGRID(KK1+1)-XGRID(KK1)))
 68 CONTINUE
 57 CONTINUE
 56 CONTINUE
 38 CONTINUE
 37 CONTINUE
    E=(XGRID(I+1)+XGRID(I))*0.5
    V=5.93E+7*SQRT(E)
    WRITE(2,76)
 76 FORMAT (/6H *****,* SUMMARY OF EXCITATIONS PRODUCED_*)
    IF(IFLAG.EG.0) GO TO 77
    SUM1=0.0
    DO 78 K=1,NOSPEC
    WRITE (2,75)
    WRITE(2,74) NAME(K)
    WRITE(2,75)
    KKMAX=NOEXC(K)
    WRITE(2,74)(STATE(K,KK),KK=1,KKMAX)
    WRITE(2,75) (PROBE(K,KK),KK=1,KKMAX)
    SUM=0.0
    DO 86 KK=1,KKMAX
    SUM=SUM+PROBF(K,KK)
 86 CONTINUE
    WRITE(2,87) SUM,NAME(K)
    SUM1=SUM1+SUM
 78 CONTINUE
    WRITE(2,88) SUM1
    GO TO 79
 77 WRITE(2,80)
 80 FORMAT(//,69H   ENERGY IS BELOW ALL EXCITATION THRESHOLDS, LOSS TO
   1 ELECTRONS ONLY ,//)
 79 CONTINUE
    WRITE(2,81)
 81 FORMAT (/6H *****,* SUMMARY OF IONIZATIONS PRODUCED_*)
    IF(ICNFG.EG.0) GO TO 82
    SUM1=0.0
    DO 83 K=1,NOSPEC
    WRITE(2,75)
    WRITE(2,74) NAME(K)
```

```
      WRITE(2,75)
      KKMAX=NIONFS(K)
      WRITE(2,74) (ISTATE(K,KK),KK=1,KKMAX)
      WRITE(2,75) (PROBI(K,KK),KK=1,KKMAX)
      SUM=0.0
      DO 89 KK=1,KKMAX
      SUM=SUM+PROBI(K,KK)
   89 CONTINUE
      WRITE(2,90) SUM,NAME(K)
      SUM1=SUM1+SUM
   83 CONTINUE
      SPACE=0.0
      AC2O2=PROBI(1,1)+PROBI(1,3)+PROBI(1,5)
      AC4O2=PROBI(1,2)+PROBI(1,4)
      ACN2=PROBI(2,1)+PROBI(2,2)+PROBI(2,3)+PROBI(2,4)
      ACNP=PROBI(2,5)
      WRITE(6,926) ACN2,AC2O2,AC4O2,SPACE,PROBI(3,1),PROBI(3,2),
     1PROBI(3,3),ACNP
  926 FORMAT (7X,8E10.3)
       ELESC=ELESC+(SUM1+TOTEL)*(XGRID(2)-XGRID(1))
      WRITE(7,927) ELESC
  927 FORMAT (8E10.4)
      WRITE(2,91) SUM1
      WRITE(2,110) ELESC
  110 FORMAT (//F10.2,* = ENERGY LOST TO THERMAL ELECTRONS (EV CM-3*
     1          ,* SEC-1)*)
   87 FORMAT (/  E10.3,* = TOTAL EXCITATIONS OF *,A10)
   88 FORMAT(//  E10.3,* = TOTAL EXCITATIONS*)
   90 FORMAT (/  E10.3,* = TOTAL IONIZATIONS OF *,A10)
   91 FORMAT(//  E10.3,* = TOTAL IONIZATIONS*)
      GO TO 84
   82 WRITE(2,85)
   85 FORMAT(//,81H   ENERGY IS BELOW ALL IONIZATION THRESHOLDS, LOSS TO
     1 EXCITATIONS ( IF POSSIBLE )//,17H     AND ELECTRONS )
   84 CONTINUE
      WRITE(2,93)
   93 FORMAT(//* EQUILIBRIUM FLUX DISTRIBUTION (CM3 SEC STER EV)-1*)
      DO 94 KK=1,I
      EEE(KK)=(XGRID(KK)+XGRID(KK+1))*0.5
   94 CONTINUE
      WRITE(2,96)
   96 FORMAT (/6(9X,1HE,9X,1HF)/)
  653 FORMAT(8E10.3)
      DO 945 KK=1,I
      FEL(KK)=FEL(KK)/12.566
  945 CONTINUE
      WRITE(2,97) ((EEE(KK),FEL(KK)),KK=1,I)
      WRITE (2,2234) IAVGF,IAVGF
      IF (IAVGF.LT.2) GO TO 6314
       DO 2227 KK=1,I
       PRDFA(KK)=0.0
2227   CONTINUE
       IAVBB=IAVGF/2+1
       DO 2228 KK=1,IAVGF
       PRDFA(1)=PRDFA(1)+FEL(KK)
2228   CONTINUE
       PRDFA(1)=PRDFA(1)/FLOAT(IAVGF)
       DO 2229 KK=2,IAVBB
       PRDFA(KK)=PRDFA(1)
2229   CONTINUE
       IAVCC=I-IAVBB
```

```
      IAVAA=IAVBB+1
      DO 2230 KK=IAVAA,IAVCC
      ILLT=KK-IAVGF/2
      IVLT=KK+IAVGF/2
      DO 2231 IJAV=ILLT,IVLT
      PRDFA(KK)=PRDFA(KK)+FEL(IJAV)
2231  CONTINUE
      PRDFA(KK)=PRDFA(KK)/FLOAT(IAVGF)
2230  CONTINUE
      IAVCC=IAVCC+1
      DO 2232 KK=IAVCC,I
      PRDFA(IAVCC)=PRDFA(IAVCC)+FEL(KK)
2232  CONTINUE
      PRDFA(IAVCC)=PRDFA(IAVCC)/FLOAT(IAVGF)
      IAVCC=IAVCC+1
      DO 2233 KK=IAVCC,I
      PRDFA(KK)=PRDFA(IAVCC+1)
2233  CONTINUE
 2234 FORMAT (//13,* FLUX PER STERADIAN AVERAGED OVER*,I3,* INTERVALS*)
      WRITE(2,96)
      WRITE(2,97)((EEE(KK),PRDFA(KK)),KK=1,I)
 6314 WRITE(5,946)  I
  946 FORMAT(I5)
      WRITE(5,947) (FEL(KK),KK=1,I)
      WRITE(5,947) (EEE(KK),KK=1,I)
  947 FORMAT(6E12.4)
   97 FORMAT(6(F10.3,E10.3))
      IF (IAVGF.LT.2) GO TO 6315
      DO 900 KK=1,I
      FEL(KK)=12.568*FEL(KK)
  900 CONTINUE
      WRITE(2,300)
  300 FORMAT (// *EQUILIBRIUM FLUX, NOT PER STERADIAN*)
      WRITE(2,97)((EEE(KK),FEL(KK)),KK=1,I)
 6315 RETURN
      END
      SUBROUTINE REDXSN
C       THIS ROUTINE READS THE CROSS SECTION DATA
      COMMON/XSXS/ NOSPEC, NOEXC(4), NGRID(4,20),
     1EGRID(4,20,25),SPLC0(4,20,25),SPLC1(4,20,25),SPLC2(4,20,25),
     2SPLC3(4,20,25),THRESH(4,20),NIONFS(4),NIONGD(4),EIONGD(4,25),
     3DIFCON(4),TIXS0(4,25),TIXS1(4,25),TIXS2(4,25),TIXS3(4,25),DIXS0(4,
     425),DIXS1(4,25),DIXS2(4,25),DIXS3(4,25), THRICZ(4,6),
     5FRACT(4,6,25)
      COMMON/ALPHA/NAME(4),STATE(4,20),ISTATE(4,6)
      DIMENSION IFORM(8)
      READ(1,20)(IFORM(I),I=1,8)
   20 FORMAT(10A8)
      READ(1,1) NOSPEC
    1 FORMAT(2014)
C       NOSPEC IS THE NUMBER OF SPECIES PRESENT, LIMIT 4
      DO 2 I=1,NOSPEC
      READ(1,3) NAME(I),NOEXC(I)
    3 FORMAT(A10,I5,F6.2)
C       NAME(I) IS THE NAME OF THE SPECIE I
C       NOEXC(I) IS THE NUMBER OF EXCITATION CROSS SECTIONS FOR SPECI I
      N=NOEXC(I)
      DO 4 J=1,N
      READ(1,3) STATE(I,J),NGRID(I,J),THRESH(I,J)
C       STATE (I,J) IS THE STATE DESIGNATION
C       NGRID (I,J) IS THE NUMBER OF POINTS IN THE GRID
```

```
C       THRESH(I,J)  IS THE THRESHOLD ENERGY
        N1=NGRID(I,J)
        READ(1,1) LFORM
        IF(LFORM.EQ.0) GO TO 21
        READ(1,IFORM)(EGRID(I,J,K),K=1,N1)
        GO TO 22
   21   READ(1,5)(EGRID(I,J,K),K=1,N1)
   22   N1=N1-1
        READ(1,6)(SPLC0(I,J,K),K=1,N1)
        READ(1,6)(SPLC1(I,J,K),K=1,N1)
        READ(1,6)(SPLC2(I,J,K),K=1,N1)
        READ(1,6)(SPLC3(I,J,K),K=1,N1)
        READ(1,1) KYY
        IF(KYY.EQ.0) GO TO 4
        READ(1,6) CORCT
        DO 9 K=1,N1
        SPLC0(I,J,K)=SPLC0(I,J,K)*CORCT
        SPLC1(I,J,K)=SPLC1(I,J,K)*CORCT
        SPLC2(I,J,K)=SPLC2(I,J,K)*CORCT
        SPLC3(I,J,K)=SPLC3(I,J,K)*CORCT
    9   CONTINUE
    5   FORMAT(10(1X,F6.2))
    6   FORMAT(7(1X,E10.3))
C       EGRID IS THE ENERGY GRID FOR THE SPLINE FITS
C       SPLC0,SPLC1,SPLC2,SPLC3   ARE THE SPLINE COEFFICIENTS
    4   CONTINUE
        READ(1,1) NIONFS(I),NIONGD(I)
        READ(1,5) DIFCON(I)
C       NIONFS(I) IS THE NUMBER OF ION FINAL STATES,LIMIT 6 FOR EACH SPECIE
C       NIONGD(I) IS THE NUMBER OF GRID POINTS FOR IONIZATION CROSS
C         SECTION DATA
C        DIFCON(I)  IS THE CONSTANT IN BEATYJS IONIZATION EQUATION
        N2=NIONFS(I)
        N3=NIONGD(I)
        READ(1,1) LEFORM
        IF (LEFORM.EQ.0) GO TO 23
        READ(1,IFORM)(EIONGD(I,J),J=1,N3)
        GO TO 24
   23   READ(1,5)(EIONGD(I,J),J=1,N3)
   24   N3=N3-1
        READ(1,6)(TIXS0(I,J),J=1,N3)
        READ(1,6)(TIXS1(I,J),J=1,N3)
        READ(1,6)(TIXS2(I,J),J=1,N3)
        READ(1,6)(TIXS3(I,J),J=1,N3)
        READ(1,6)(DIXS0(I,J),J=1,N3)
        READ(1,6)(DIXS1(I,J),J=1,N3)
        READ(1,6)(DIXS2(I,J),J=1,N3)
        READ(1,6)(DIXS3(I,J),J=1,N3)
        READ(1,1) KYY
        IF(KYY.EQ.0) GO TO 10
        READ(1,6) CORCT
        DO 11 J=1,N3
        TIXS0(I,J)=TIXS0(I,J)*CORCT
        TIXS1(I,J)=TIXS1(I,J)*CORCT
        TIXS2(I,J)=TIXS2(I,J)*CORCT
        TIXS3(I,J)=TIXS3(I,J)*CORCT
        DIXS0(I,J)=DIXS0(I,J)*CORCT
        DIXS1(I,J)=DIXS1(I,J)*CORCT
        DIXS2(I,J)=DIXS2(I,J)*CORCT
        DIXS3(I,J)=DIXS3(I,J)*CORCT
   11   CONTINUE
```

```
   10 CONTINUE
C        EIONGD IS THE IONIZATION CROSS SECTION ENERGY GRID
C        TIXS0 TO TIXS3  ARE THE TOTAL IONIZATION CSOSS SECTICN SPLINE
C         COEFFICIENTS
C       DIXS0 TO DIXS3 ARE THE DIFFERENTIAL CROSS SECTICN SPLINE COEFFICIENTS
C       FOR THE NUMERATOR IN BEATY(S EQUATION
        DO 7  J=1,N2
        READ(1,8) ISTATE(I,J),THRIOZ(I,J)
    8 FORMAT(A8,F6.2)
C        ISTATE IS THE FINAL ION STATE DESIGNATICN
C        THRIOZ IS THE THRESHOLD
        READ(1,5)(FRACT(I,J,K),K=1,N3)
    7 CONTINUE
    2 CONTINUE
C        FRACT ARE THE BRANCHING RATIOS
        RETURN
        END
        FUNCTION QION(I,E,KEY)
        COMMON/XSXS/ NOSPEC, NCEXC(4), NGRID(4,20),
       1EGRID(4,20,25),SPLC0(4,20,25),SPLC1(4,20,25),SPLC2(4,20,25),
       2SPLC3(4,20,25),THRESH(4,20),NIONFS(4),NIONGD(4),EIONGD(4,25),
       3DIFCON(4),TIXS0(4,25),TIXS1(4,25),TIXS2(4,25),TIXS3(4,25),DIXS0(4,
       425),DIXS1(4,25),DIXS2(4,25),DIXS3(4,25), THRIOZ(4,6),
       5FRACT(4,6,25)
        COMMCN /POINT/IPCINT(4,20),IIPONT(4),IDPONT(4)
        COMMON/ALPHA/NAME(4),STATE(4,20),ISTATE(4,6)
C        THIS FUNCTICN CALCULATES THE TOTAL ELECTRCN INPACT IONIZATION
C        CROSS SECTICN FCR THE SPECIE I AT ENERGY E,  KEY ANC IIPCNT ARE
C       USED TO SAVE TIME IN THE ENERGY GRD SEARCH,  IF KEY=-1, WE START
C        AT THE BEGINNING OF THE ARRAY IN THE SEARCH AND SET IIPCNT BEFORE
C        EXIT,   IF KEY = 0, WE START AT IIPCNT ANC RESET IIPONT IF NECESSARY.
C        IF KEY IS POSITIVE, WE STARI AT KEY AND RESET IIPONT IF NECESSARY
  120 FORMAT(4H I =,I4,6H KEY =,I4)
  110 FORMAT(4H E =,  E9.2,14H EIONGD(I,1) =,  E9.2)
        IF(E.GE.EICNGD(I,1)) GO TO 2
    1 QION=0.0
        RETURN
    2 NN=NIONGD(I)
        IF(E.GT.FICNGD(I,NN))   GO TO 1
  100 FORMAT(5H NN =,I4,4H I =,I4,4H E =,E9.2,
       16H KEY =,I4)
    3 CONTINUE
        IF(KEY) 4,5,6
    4 IP=1
    9 IF(E.GE.FICNGD(I,IP).AND.E.LT.EIONGD(I,IP+1))   GO TC 7
    8 IP=IP+1
        GO TO 9
    7 IIPONT(I)=IP
   10 X=E-EIONGD(I,IP)
        Y=EICNGD(I,IP+1)-E
        QICN=X*(TIXS3(I,IP)+TIXS1(I,IP)*X**2)+Y*(TIXS2(I,IP)+TIXS0(I,IP)*Y
       1**2)
        RETURN
    5 IP=IIPCNT(I)
   12 CONTINUE
        IF(E.GE.EICNGD(I,IP).AND.E.LT.EIONGD(I,IP+1))  GO TO 10
   11 IF(E.GE.FICNGD(I,IP))  GO TO 8
   13 IP=IP-1
        IF(E.GE.EICNGD(I,IP).AND.E.LT.EIONGD(I,IP+1))  GO TO 7
        GO TO 13
    6 IP=KEY
```

```
      IIPONT(I)=IP
      GO TO 12
      END
      FUNCTION DIFION(I,E,KEY,E0,E1,F)
      COMMON/XSXS/ NOSPEC, NOEXC(4), NGRID(4,20),
     1EGRID(4,20,25),SPLC0(4,20,25),SPLC1(4,20,25),SPLC2(4,20,25),
     2SPLC3(4,20,25),THRESH(4,20),NIONFS(4),NIONGD(4),EIONGD(4,25),
     3DIFCON(4),TIXS0(4,25),TIXS1(4,25),TIXS2(4,25),TIXS3(4,25),DIXS0(4,
     425),DIXS1(4,25),DIXS2(4,25),DIXS3(4,25), THRIOZ(4,6),
     5FRACT(4,6,25)
      COMMON /POINT/IPOINT(4,20),IIPONT(4),IDPONT(4)
      COMMON/ALPHA/NAME(4),STATE(4,20),ISTATE(4,6)
      DIMENSION F(6)
C    THIS FUNCTION CALCULATES THE ELECTRON IMPACT IONIZATION DIFFERENTIAL
C       CROSS SECTION FOR THE SPECIE I AT ENERGY E.  KEY AND IIPONT ARE
C      USED TO SAVE TIME IN THE ENERGY GRD SEARCH.  IF KEY=-1, WE START
C       AT THE BEGINNING OF THE ARRAY IN THE SEARCH AND SET IDPONT BEFORE
C       EXIT.   IF KEY = 0, WE START AT IDPONT AND RESET IDPONT IF NECESSARY.
C       IF KEY IS POSITIVE, WE START AT KEY AND RESET IDPONT IF NECESSARY
C       WE INTEGRATE BEATY'S EQUATION FROM E0 TO E1 USING A CUBIC FIT
C       WHICH  IMPLIES  SMALL STEP SIZES.  THE FRACTIONAL YEALD TO
C       DIFFERENT ION STATES ARE RETURNED IN THE ARRAY F.
      IF(E.GE.EIONGD(1,1)) GO TO 2
    1 QION=0.0
      RETURN
    2 NN=NIONGD(I)
      IF(E.GT.EIONGD(I,NN))   GO TO 1
    3 CONTINUE
      IF(KEY) 4,5,6
    4 IP=1
    9 IF(E.GE.EIONGD(I,IP).AND.E.LT.EIONGD(I,IP+1))    GO TO 7
    8 IP=IP+1
      GO TO 9
    7 IDPONT(I)=IP
   10 X=E-EIONGD(I,IP)
      Y=EIONGD(I,IP+1)-E
      CONC=X*(DIXS3(I,IP)+DIXS1(I,IP)*X**2)+Y*(DIXS2(I,IP)+DIXS0(I,IP)*Y
     1**2)
      ND=NIONFS(I)
      DO 14 J=1,ND
      F(J)=FRACT(I,J,IP)
   14 CONTINUE
      EMID=0.5*(E1+E0)
      DE=0.5*(E1-E0)
      EXX=1.0/(1.0+(E0/DIFCON(I))**2.1)+4.0/(1.0+(EMID/DIFCON(I))**2.1)
     1+1.0/(1.0+(E1/DIFCON(I))**2.1)
      DIFION=CONC*EXX*DE/3.0
      RETURN
    5 IP=IDPONT(I)
   12 CONTINUE
      IF(E.GE.EIONGD(I,IP).AND.E.LT.EIONGD(I,IP+1))   GO TO 10
   11 IF(E.GE.EIONGD(I,IP))  GO TO 8
   13 IP=IP-1
      IF(E.GE.EIONGD(I,IP).AND.E.LT.EIONGD(I,IP+1))   GO TO 7
       GO TO 13
    6 IP=KEY
      IDPONT(I)=IP
      GO TO 12
      END
      FUNCTION QEX(I,J,E,KEY)
      COMMON/XSXS/ NOSPEC, NOEXC(4), NGRID(4,20),
```

```
     1EGRID(4,20,25),SPLC0(4,20,25),SPLC1(4,20,25),SPLC2(4,20,25),
     2SPLC3(4,20,25),THRESH(4,20),NIONFS(4),NIONGD(4),EIONGD(4,25),
     3DIFCON(4),TIXS0(4,25),TIXS1(4,25),TIXS2(4,25),TIXS3(4,25),DIXS0(4,
     425),DIXS1(4,25),DIXS2(4,25),DIXS3(4,25), THRIOZ(4,6),
     5FRACT(4,6,25)
      COMMON /POINT/IPOINT(4,20),IIPONT(4),IDPONT(4)
      COMMON/ALPHA/NAME(4),STATE(4,20),ISTATE(4,6)
C      THIS FUNCTION CALCULATES THE ELECTRON IMPACT EXCITATION CROSS
C       SECTION FOR THE PROCESS J IN SPECIE I AT THE ENERGY E.  KEY
C      AND IPOINT ARE USED TO SAVE TIME IN THE ENERGY GRID SEARCH) IF
C    KEY =-1, WE START AT THE BEGINNING OF THE ARRAY IN THE SEARCH AND
C      SET IPOINT BEFORE EXIT.  IF KEY =0,WE START AT IPOINT AND RESET IPOINT
C     IF NECESSARY(  IF KEY IS POSITIVE, WE START AT KEY AND RESET IPOINT
C      IF NECESSARY)
      IF(E.GT.EGRID(I,J,1))  GO TO 2
    1 QEX=0.0
      RETURN
    2 J1=NGRID(I,J)
      IF(E.GE.EGRID(I,J,J1))   GO TO 1
    3 CONTINUE
      IF(KEY) 4,5,6
    4 IP=1
    9 IF(E.GE.EGRID(I,J,IP).AND.E.LT.EGRID(I,J,IP+1))   GO TO 7
    8 IP=IP+1
      GO TO 9
    7 IPOINT(I,J)=IP
   10 X=E-EGRID(I,J,IP)
      Y=EGRID(I,J,IP+1)-E
      QEX=X*(SPLC3(I,J,IP)+SPLC1(I,J,IP)*X**2)+Y*(SPLC2(I,J,IP)+SPLC0(I,
     1J,IP)*Y**2)
      RETURN
    5 IP=IPOINT(I,J)
   12 CONTINUE
      IF(E.GE.EGRID(I,J,IP).AND.E.LT.EGRID(I,J,IP+1))  GO TO 10
   11 IF(E.GE.EGRID(I,J,IP))   GO TO 8
   13 IP=IP-1
      IF(IP.EQ.0) GO TO 1
      IF(E.GE.EGRID(I,J,IP).AND.E.LT.EGRID(I,J,IP+1))  GO TO 7
      GO TO 13
    6 IP=KEY
      IPOINT(I,J)=IP
      GO TO 12
      END
      SUBROUTINE SETGRID
C      SETGRID SETS UP THE GRID FOR INTEGRATION
      COMMON/GRID/INTGRID,XGRID(400),VGRID(400),PROGRID(400)
      DIMENSION ED(10),EF(10),NPTS(10),DEE(10)
      READ(1,1) ITYPE
C      ITYPE SPECIFIES THE TYPE OF GRID DATA .  IF ITYPE =1, READS
C      INTGRID POINTS FOR XGRID)  IF ITYPE =2, READS NRANGE SETS OF
C      INITIAL VALUES(FINAL VALUES( AND NUMBER OF POINTS
C      IF ITYPE =3, READS INITIAL VALUE AND NRANGE SETS OF INTERVALS
C      AND NUMBER OF POINTS
C      ITYPE=4, XGRID IS SET IN PRODUCTION SUBROUTINE
    1 FORMAT(I4)
      GO TO (2,3,4,341),ITYPE
  341 RETURN
    2 READ(1,1) INTGRID
      READ(1,5) (XGRID(I),I=1,INTGRID)
    5 FORMAT(10(1X,F6.2))
      DO 12  K=1,INTGRID
```

```
      VGRID(K)=5.93E+7*SQRT(XGRID(K))
   12 CONTINUE
      RETURN
    3 READ(1,1) NRANGE
      DO 6 I=1,NRANGE
      READ(1,7) EO(I),NPTS(I),EF(I)
    7 FORMAT(1X,F6.2,2X,I4,2X,F6.2)
    6 CONTINUE
      INDEX=1
      DO 8 I=1,NRANGE
      XGRID(INDEX)=EO(I)
      DE=(EF(1)-EO(I))/FLOAT(NPTS(I)-1)
      NMAX=NPTS(I)
      DO 9 J=2,NMAX
      INDEX=INDEX+1
      XGRID(INDEX)=XGRID(INDEX-1)+DE
    9 CONTINUE
    8 CONTINUE
      INTGRID=INDEX
      DO 13  K=1,INTGRID
      VGRID(K)=5.93E+7*SQRT(XGRID(K))
   13 CONTINUE
      RETURN
    4 READ(1,5) FOO
      READ(1,1) NRANGE
      DO 10 I=1,NRANGE
      READ(1,7) DEF(I),NPTS(I)
   10 CONTINUE
      INDEX=1
      XGRID(1)=ECO
      DO 11 I=1,NRANGE
      NMAX=NPTS(I)
      DO 11 J=1,NMAX
      INDEX=INDEX+1
      XGRID(INDEX)=XGRID(INDEX-1)+DEE(I)
   11 CONTINUE
      INTGRID=INDEX
      DO 14  K=1,INTGRID
      VGRID(K)=5.93E+7*SQRT(XGRID(K))
   14 CONTINUE
      RETURN
      END
      SUBROUTINE DEDT(E,TE,RHOE,DET,XL)
C      THIS ROUTINE CALCULATES ENERGY LOSS TO THE THERMAL ELECTRONS
C      USING FITS BY SCHWARTZ, NISBET, AND GREEN JGR 76,8425 (1971)
C      WHERE E IS THE PHOTOELECTRON ENERGY, TE THE THERMAL ELECTRON
C      TEMPERATURE, RHOE IS THE ELECTRON DENSITY, DE/DT IS  RETURNED
C      VIA DET, L VIA XL.
      EE=8.618E-5*TE
      X=(E-EE)/(E-0.53*EF)
      DET=0.0
      XL=0.0
      IF (X.LE.0.0) GO TO 1
      X=X**2.36
      DET=-2.E-4*(RHOE**0.97)*X/(E**0.44)
      XL=3.37E-12*X/((RHOE**.03)*(E**0.94))
    1 RETURN
      END
0004
(8(1X,F9.2))
   4
```

```
MOL, O        14
A 3SIG+U      12  4.50
1
      4.50       6.00       7.00       8.00       9.00      10.00      20.00      30.00
     40.00      50.00     100.00     200.00
 -2.183E-20  6.549E-20 -1.025E-18 -2.756E-19 -2.275E-20 -1.341E-21  1.079E-21
 -1.350E-23  1.053E-22  1.009E-23  6.648E-25
  4.366E-20 -1.025E-18 -2.756E-19 -2.275E-20 -1.341E-20  1.079E-21 -1.350E-23
  1.053E-22  5.044E-23  1.330E-24 -3.324E-25
  4.911E-20  1.074E-17  1.829E-17  1.970E-17  1.944E-17  2.038E-18  1.206E-18
  1.021E-18  8.285E-19  1.155E-19  3.332E-20
  7.108E-18  1.829E-17  1.970E-17  1.944E-17  1.905E-17  1.206E-18  1.021E-18
  8.285E-19  6.988E-19  7.662E-20  2.431E-20

B 1SIG+G      20  1.62
1
      1.62       2.94       5.00       6.47       7.94      10.00      12.06      15.00
     20.00      25.00      30.00      35.00      40.00      45.00      50.00      60.00
     70.00      80.00      90.00     100.00
  3.381E-20 -4.333E-20  1.494E-20 -4.107E-20  1.020E-20 -7.464E-21  2.393E-21
  1.626E-22  2.603E-22 -5.889E-23 -2.551E-23  1.617E-22 -5.104E-23  4.321E-23
  7.503E-24  4.588E-24  2.245E-24  1.331E-24  1.160E-24
 -6.762E-20  1.066E-20 -4.107E-20  1.429E-20 -7.464E-21  3.415E-21  2.765E-22
  2.603E-22 -5.889E-23 -2.551E-23  1.617E-22 -5.104E-23  4.321E-23  1.501E-23
  4.588E-24  2.245E-24  1.331E-24  1.160E-24 -5.798E-25
 -5.891E-20  7.038E-19  1.134E-18  1.449E-18  8.582E-19  8.637E-19  4.654E-19
  2.245E-19  1.649E-19  1.443E-19  1.149E-19  8.168E-20  7.270E-20  5.606E-20
  2.239E-20  1.561E-20  1.159E-20  8.907E-21  7.027E-21
  9.292E-19  7.868E-19  1.449E-18  1.232E-18  8.637E-19  6.792E-19  3.864E-19
  1.649E-19  1.443E-19  1.149E-19  8.168E-20  7.270E-20  5.606E-20  4.590E-20
  1.561E-20  1.159E-20  8.907E-21  7.027E-21  5.843E-21

A 1DELT G     20   .88
1
       .88       2.94       5.00       6.47       7.94      10.00      12.06      15.00
     20.00      25.00      30.00      35.00      40.00      45.00      50.00      60.00
     70.00      80.00      90.00     100.00
  1.043E-20 -2.085E-20  1.073E-20 -1.642E-19 -2.045E-20  3.454E-21  1.611E-20
 -1.188E-21  7.413E-22  4.948E-22  1.433E-22  7.596E-23  1.289E-22 -3.138E-23
  4.233E-23  1.264E-23  9.792E-24  4.887E-24  4.861E-24
 -2.065E-20  7.658E-21 -1.642E-19 -2.865E-20  3.454E-21  2.299E-20 -2.021E-21
  7.413E-22  4.948E-22  1.433E-22  7.596E-23  1.289E-22 -3.138E-23  8.467E-23
  1.264E-23  9.792E-24  4.887E-24  4.861E-24 -2.430E-24
 -4.424E-20  1.961E-18  4.836E-18  6.477E-18  4.317E-18  3.383E-18  1.707E-18
  9.439E-19  6.673E-19  5.018E-19  4.106E-19  3.409E-19  2.826E-19  2.436E-19
  9.677E-20  7.212E-20  5.505E-20  4.386E-20  3.560E-20
  1.961E-18  3.435E-18  6.477E-18  5.990E-18  3.383E-18  2.538E-18  1.572E-18
  6.673E-19  5.018E-19  4.106E-19  3.409E-19  2.826E-19  2.436E-19  1.999E-19
  7.212E-20  5.505E-20  4.386E-20  3.560E-20  3.026E-20

A4P1U RY3     20 12.70
1
      12.70      17.69      22.68      27.67      32.66      37.65      42.64      47.62
      52.61      57.60      59.25      60.30      62.03      64.87      69.54      77.20
      89.77     110.42     144.33     200.00
 -3.458E-21  6.915E-21 -4.637E-21 -1.902E-21 -1.781E-21 -1.066E-21 -7.396E-22
 -4.850E-22 -3.283E-22 -6.729E-22 -9.355E-22 -5.221E-22 -2.773E-22 -1.343E-22
 -5.541E-23 -1.691E-23 -1.708E-24  1.239E-24  1.668E-24
  6.915E-21 -4.637E-21 -1.902E-21 -1.781E-21 -1.066E-21 -7.396E-22 -4.850E-22
 -3.283E-22 -2.215E-22 -6.005E-22 -8.573E-22 -4.553E-22 -2.205E-22 -9.098E-23
 -2.777E-23 -2.804E-24  2.034E-24  2.738E-24 -8.338E-25
```

```
  8.607E-20  7.065E-19  2.360E-18  3.321E-18  3.997E-18  4.408E-18  4.659E-18
  4.800E-18  4.869E-18  1.484E-17  2.311E-17  1.407E-17  8.560E-18  5.198E-18
  3.142E-18  1.879E-18  1.102E-18  6.243E-19  3.355E-19
  7.065E-19  2.360E-18  3.321E-18  3.997E-18  4.408E-18  4.659E-18  4.800E-18
  4.869E-18  4.886E-18  1.484E-17  2.310E-17  1.405E-17  8.531E-18  5.155E-18
  3.083E-18  1.808E-18  1.026E-18  5.561E-19  2.922E-19

A4PIU RY4    20 14.60
1
     14.60      20.34      26.07      31.81      37.54      43.28      49.01      54.75
     60.49      66.22      67.85      68.88      70.57      73.31      77.79      85.09
     97.02     116.47     148.21     200.00
 -4.587E-22  9.174E-22 -6.151E-22 -2.523E-22 -2.363E-22 -1.414E-22 -9.810E-23
 -6.434E-23 -4.355E-23 -1.032E-22 -1.485E-22 -8.443E-23 -4.611E-23 -2.333E-23
 -1.038E-23 -3.678E-24 -7.129E-25  7.987E-26  2.923E-25
  9.174E-22 -6.151E-22 -2.523E-22 -2.363E-22 -1.414E-22 -9.810E-23 -6.434E-23
 -4.355E-23 -2.937E-23 -9.382E-23 -1.378E-22 -7.523E-23 -3.807E-23 -1.694E-23
 -6.001E-24 -1.163E-24  1.303E-25  4.769E-25 -1.461E-25
  1.509E-20  1.239E-19  4.137E-19  5.822E-19  7.008E-19  7.728E-19  8.169E-19
  8.416E-19  8.536E-19  3.009E-18  4.763E-18  2.918E-18  1.787E-18  1.093E-18
  6.661E-19  4.028E-19  2.398E-19  1.389E-19  7.679E-20
  1.239E-19  4.137E-19  5.822E-19  7.008E-19  7.728E-19  8.169E-19  8.416E-19
  8.536E-19  8.570E-19  3.009E-18  4.762E-18  2.916E-18  1.783E-18  1.086E-18
  6.568E-19  3.910E-19  2.267E-19  1.261E-19  6.783E-20

A4PIU SUM    20 15.60
1
     15.60      21.73      27.86      33.99      40.11      46.24      52.37      58.50
     64.63      70.76      72.38      73.40      75.06      77.75      82.13      89.24
    100.82     119.64     150.24     200.00
 -3.492E-22  6.984E-22 -4.683E-22 -1.921E-22 -1.799E-22 -1.076E-22 -7.469E-23
 -4.898E-23 -3.316E-23 -8.425E-23 -1.233E-22 -7.068E-23 -3.910E-23 -2.018E-23
 -9.269E-24 -3.487E-24 -8.067E-25 -2.511E-27  2.461E-25
  6.984E-22 -4.683E-22 -1.921E-22 -1.799E-22 -1.076E-22 -7.469E-23 -4.898E-23
 -3.316E-23 -2.235E-23 -7.717E-23 -1.149E-22 -6.357E-23 -3.281E-23 -1.507E-23
 -5.670E-24 -1.312E-24 -4.083E-27  4.002E-25 -1.230E-25
  1.312E-20  1.077E-19  3.596E-19  5.060E-19  6.091E-19  6.717E-19  7.100E-19
  7.315E-19  7.419E-19  2.804E-18  4.479E-18  2.754E-18  1.692E-18  1.039E-18
  6.358E-19  3.866E-19  2.316E-19  1.356E-19  7.605E-20
  1.077E-19  3.596E-19  5.060E-19  6.091E-19  6.717E-19  7.100E-19  7.315E-19
  7.419E-19  7.449E-19  2.804E-18  4.478E-18  2.752E-18  1.689E-18  1.033E-18
  6.282E-19  3.767E-19  2.205E-19  1.243E-19  6.767E-20

A2PIU RY3    20 13.20
1
     13.20      18.39      23.57      28.76      33.94      39.13      44.31      49.50
     54.69      59.87      61.51      62.56      64.28      67.09      71.71      79.28
     91.68     112.02     145.35     200.00
 -2.851E-21  5.701E-21 -3.823E-21 -1.568E-21 -1.469E-21 -8.787E-22 -6.097E-22
 -3.999E-22 -2.706E-22 -5.775E-22 -8.104E-22 -4.547E-22 -2.434E-22 -1.194E-22
 -5.034E-23 -1.607E-23 -2.076E-24  9.338E-25  1.496E-24
  5.701E-21 -3.823E-21 -1.568E-21 -1.469E-21 -8.787E-22 -6.097E-22 -3.999E-22
 -2.706E-22 -1.626E-22 -5.181E-22 -7.453E-22 -3.989E-22 -1.957E-22 -8.252E-23
 -2.635E-23 -3.404E-24  1.531E-24  2.452E-24 -7.478E-25
  7.666E-20  6.293E-19  2.102E-18  2.957E-18  3.560E-18  3.926E-18  4.150E-18
  4.275E-18  4.336E-18  1.376E-17  2.152E-17  1.312E-17  7.996E-18  4.864E-18
  2.947E-18  1.768E-18  1.041E-18  5.934E-19  3.214E-19
  6.293E-19  2.102E-18  2.957E-18  3.560E-18  3.926E-18  4.150E-18  4.275E-18
  4.336E-18  4.354E-18  1.376E-17  2.151E-17  1.311E-17  7.972E-18  4.828E-18
  2.896E-18  1.705E-18  9.738E-19  5.314E-19  2.810E-19
```

```
A2PIU RY4     20 15,30
1
     15,30       21,31       27,32       33,33       39,34       45,35       51,36       57,37
     63,39       69,40       71,02       72,05       73,71       76,42       80,82       88,00
     99,68      118,69      149,63      200,00
 -3,882E-22   7,763E-22  -5,205E-22  -2,135E-22  -2,000E-22  -1,197E-22  -8,302E-23
 -5,445E-23  -3,686E-23  -9,176E-23  -1,336E-22  -7,640E-23  -4,210E-23  -2,161E-23
 -9,835E-24  -3,638E-24  -8,027E-25   2,104E-26   2,663E-25
  7,763E-22  -5,205E-22  -2,135E-22  -2,000E-22  -1,197E-22  -8,302E-23  -5,445E-23
 -3,686E-23  -2,485E-23  -8,386E-23  -1,244E-22  -6,854E-23  -3,517E-23  -1,601E-23
 -5,921E-24  -1,307E-24   3,424E-26   4,335E-25  -1,332E-25
  1,402E-20   1,151E-19   3,845E-19   5,410E-19   6,513E-19   7,182E-19   7,591E-19
  7,821E-19   7,933E-19   2,938E-18   4,679E-18   2,874E-18   1,764E-18   1,082E-18
  6,613E-19   4,014E-19   2,402E-19   1,401E-19   7,824E-20
  1,151E-19   3,845E-19   5,410E-19   6,513E-19   7,182E-19   7,591E-19   7,821E-19
  7,933E-19   7,964E-19   2,938E-18   4,678E-18   2,872E-18   1,760E-18   1,076E-18
  6,529E-19   3,907E-19   2,280E-19   1,280E-19   6,947E-20

A2PIU SUM     20 16,20
1
     16,20       22,56       28,93       35,29       41,66       48,02       54,39       60,75
     67,11       73,48       75,10       76,11       77,75       80,41       84,73       91,73
    103,09      121,53      151,45      200,00
 -3,628E-22   7,255E-22  -4,865E-22  -1,996E-22  -1,869E-22  -1,118E-22  -7,759E-23
 -5,089E-23  -3,445E-23  -9,108E-23  -1,346E-22  -7,754E-23  -4,320E-23  -2,254E-23
 -1,054E-23  -4,092E-24  -1,029E-24  -5,420E-26   2,672E-25
  7,255E-22  -4,865E-22  -1,996E-22  -1,869E-22  -1,118E-22  -7,759E-23  -5,089E-23
 -3,445E-23  -2,322E-23  -8,378E-23  -1,258E-22  -7,010E-23  -3,657E-23  -1,710E-23
 -6,639E-24  -1,670E-24  -8,794E-26   4,336E-25  -1,336E-25
  1,469E-20   1,206E-19   4,029E-19   5,669E-19   6,824E-19   7,525E-19   7,954E-19
  8,195E-19   8,312E-19   3,270E-18   5,251E-18   3,235E-18   1,993E-18   1,226E-18
  7,523E-19   4,588E-19   2,763E-19   1,625E-19   9,189E-20
  1,206E-19   4,029E-19   5,669E-19   6,824E-19   7,525E-19   7,954E-19   8,195E-19
  8,312E-19   8,345E-19   3,269E-18   5,250E-18   3,233E-18   1,989E-18   1,220E-18
  7,440E-19   4,480E-19   2,637E-19   1,497E-19   8,213E-20

B4S-G RY3     20 15,70
1
     15,70       21,87       28,04       34,20       40,37       46,54       52,71       58,87
     65,04       71,21       72,84       73,85       75,51       78,19       82,56       89,66
    101,20      119,95      150,44      200,00
 -5,352E-22   1,070E-21  -7,177E-22  -2,945E-22  -2,757E-22  -1,650E-22  -1,145E-22
 -7,508E-23  -5,082E-23  -1,300E-22  -1,905E-22  -1,093E-22  -6,055E-23  -3,131E-23
 -1,443E-23  -5,457E-24  -1,281E-24  -1,555E-26   3,803E-25
  1,070E-21  -7,177E-22  -2,945E-22  -2,757E-22  -1,650E-22  -1,145E-22  -7,508E-23
 -5,082E-23  -3,426E-23  -1,192E-22  -1,777E-22  -9,843E-23  -5,089E-23  -2,345E-23
 -8,870E-24  -2,083E-24  -2,528E-26   6,182E-25  -1,902E-25
  2,036E-20   1,671E-19   5,562E-19   7,855E-19   9,456E-19   1,043E-18   1,102E-18
  1,136E-18   1,152E-18   4,383E-18   7,007E-18   4,309E-18   2,649E-18   1,627E-18
  9,962E-19   6,060E-19   3,636E-19   2,129E-19   1,196E-19
  1,671E-19   5,562E-19   7,855E-19   9,456E-19   1,043E-18   1,102E-18   1,136E-18
  1,152E-18   1,156E-18   4,383E-18   7,005E-18   4,306E-18   2,644E-18   1,619E-18
  9,844E-19   5,907E-19   3,461E-19   1,953E-19   1,065E-19

B COM RY3     20 19,60
1
     19,60       27,30       35,00       42,70       50,40       58,10       65,80       73,50
     81,20       88,90       90,50       91,47       93,01       95,48       99,44      105,78
    115,94      132,21      158,27      200,00
 -1,180E-22   2,360E-22  -1,582E-22  -6,491E-23  -6,078E-23  -3,637E-23  -2,524E-23
 -1,655E-23  -1,120E-23  -3,630E-23  -5,657E-23  -3,345E-23  -1,932E-23  -1,062E-23
```

```
 -5.390E-24 -2.406E-24 -8.284E-25 -1.836E-25  7.973E-26
  2.360E-22 -1.582E-22 -6.491E-23 -6.078E-23 -3.637E-23 -2.524E-23 -1.655E-23
 -1.120E-23 -7.550E-24 -3.403E-23 -5.358E-23 -3.094E-23 -1.701E-23 -8.634E-24
 -3.853E-24 -1.327E-24 -2.940E-25  1.277E-25 -3.986E-26
  6.996E-21  5.743E-20  1.918E-19  2.699E-19  3.249E-19  3.583E-19  3.787E-19
  3.902E-19  3.957E-19  1.908E-18  3.171E-18  1.980E-18  1.236E-18  7.706E-19
  4.799E-19  2.977E-19  1.832E-19  1.110E-19  6.535E-20
  5.743E-20  1.918E-19  2.699E-19  3.249E-19  3.583E-19  3.787E-19  3.902E-19
  3.957E-19  3.973E-19  1.908E-18  3.171E-18  1.979E-18  1.234E-18  7.684E-19
  4.766E-19  2.932E-19  1.776E-19  1.048E-19  5.985E-20

SCH. RUN.     13  8.40
1
      8.40      10.00      15.09      20.00      30.00      40.00      50.00      60.00
     70.00      80.00      90.00     100.00     200.00
  2.652E-19 -1.668E-19  1.733E-19 -4.417E-20  9.057E-21 -3.297E-21  1.102E-22
  3.160E-22  5.587E-23 -4.395E-22  7.020E-22 -8.859E-24
 -5.305E-19  1.671E-19 -8.996E-20  9.057E-21 -3.297E-21  1.102E-22  3.160E-22
  5.587E-23 -4.395E-22  7.020E-22 -8.859E-23  4.429E-24
 -6.790E-19  5.987E-18 -3.533E-18  9.388E-18  5.456E-18  6.959E-18  6.483E-18
  6.073E-18  5.853E-18  5.667E-18  5.217E-18  6.065E-19
  6.660E-18 -3.709E-18  1.229E-17  5.456E-18  6.959E-18  6.483E-18  6.073E-18
  5.853E-18  5.667E-18  5.217E-18  5.188E-18  2.852E-19

CF ALL 9.9    12  9.90
1
      9.90      15.09      20.00      30.00      40.00      50.00      60.00      70.00
     80.00      90.00     100.00     200.00
  3.200E-22 -6.765E-22 -6.766E-22 -2.133E-22 -4.850E-23 -1.130E-23 -3.731E-23
  4.352E-23  6.212E-24 -5.837E-23  1.928E-24
 -6.400E-22 -1.378E-21 -2.137E-22 -4.850E-23 -1.130E-23 -3.731E-23  4.352E-23
  6.212E-24 -5.837E-23  1.928E-23 -9.640E-25
 -8.620E-21  5.627E-19  5.448E-19  6.843E-19  6.955E-19  6.777E-19  6.531E-19
  6.061E-19  5.853E-19  5.681E-19  3.251E-20
  5.342E-19  1.005E-18  6.843E-19  6.955E-19  6.777E-19  6.531E-19  6.061E-19
  5.853E-19  5.681E-19  5.160E-19  4.397E-20

LUMP VIB      11   .19
1
       .19        .38        .50        .66        .94       1.00       1.25       1.50
      2.00       2.50       2.81
 -1.240E-17  3.711E-17 -8.554E-17 -1.300E-17 -1.647E-17 -1.165E-17 -2.015E-17
  1.141E-18  1.609E-18 -1.287E-19
  2.481E-17 -1.068E-16 -2.349E-17 -3.620E-16 -4.697E-17 -2.015E-17  2.281E-18
  1.609E-18 -7.981E-20  6.436E-20
  4.337E-19  2.442E-17  1.614E-17  2.541E-17  1.311E-16  3.385E-17  3.376E-17
  1.284E-17  6.474E-18  4.045E-18
  1.564E-17  4.417E-17  4.464E-17  2.910E-17  1.337E-16  3.376E-17  2.611E-17
  6.474E-18  2.520E-16 -6.185E-21

   5  20
  17.40
1
      12.20      13.00      15.00      17.00      22.00      24.00      30.00      40.00
     50.00      60.00      70.00      80.00      90.00     100.00     110.00     120.00
    125.00     140.00     150.00     200.00
 -2.714E-04  2.171E-04  1.855E-04  2.163E-04  1.217E-04  7.023E-06  9.275E-08
 -3.949E-05 -2.213E-05 -1.200E-05 -1.986E-05  1.431E-06 -1.587E-05  2.041E-06
 -8.294E-06 -1.728E-06 -1.486E-06 -8.797E-07 -3.183E-07
  5.427E-04  1.855E-04  5.407E-04  4.869E-05  2.107E-05  1.546E-07 -3.949E-05
 -2.213E-05 -1.200E-05 -1.986E-05  1.431E-06 -1.587E-05  2.041E-06 -8.294E-06
```

```
 -8.638E-07 -4.458E-06 -5.865E-07 -1.592E-06  1.592E-07
  1.737E-04  1.213E-02  4.776E-02  3.059E-02  2.360E-01  1.011E-01  1.020E-01
  1.709E-01  2.162E-01  2.482E-01  2.730E-01  2.859E-01  2.996E-01  3.038E-01
  3.092E-01  6.192E-01  2.067E-01  3.081E-01  6.200E-02
  3.215E-02  4.776E-02  8.764E-02  9.338E-02  3.039E-01  1.700E-01  1.709E-01
  2.162E-01  2.482E-01  2.730E-01  2.859E-01  2.996E-01  3.038E-01  3.092E-01
  3.097E-01  6.193E-01  2.055E-01  3.062E-01  5.720E-02
  1.058E-02 -8.463E-03  2.238E-03 -1.156E-04  8.083E-05 -1.417E-05 -6.435E-07
 -2.647E-06 -3.476E-07 -9.252E-08 -6.024E-07  4.120E-07 -5.656E-07  2.805E-07
 -2.662E-07  1.290E-07 -9.669E-09  1.718E-08 -8.248E-10
 -2.116E-02  2.238E-03 -2.889E-04  3.233E-05 -4.250E-05 -1.073E-06 -2.647E-06
 -3.476E-07 -9.252E-08 -6.024E-07  4.120E-07 -5.656E-07  2.805E-07 -2.662E-07
  6.450E-08 -2.901E-06  1.145E-08 -4.124E-09  4.124E-10
 -6.770E-03  6.636E-02  2.575E-02  1.796E-02  4.901E-02  1.824E-02  1.238E-02
  1.438E-02  1.480E-02  1.501E-02  1.516E-02  1.496E-02  1.500E-02  1.470E-02
  1.456E-02  2.856E-02  9.434E-03  1.375E-02  2.700E-03
  9.480E-02  2.575E-02  3.884E-02  1.892E-02  5.337E-02  2.056E-02  1.438E-02
  1.480E-02  1.501E-02  1.516E-02  1.496E-02  1.500E-02  1.470E-02  1.456E-02
  1.427E-02  2.829E-02  9.163E-03  1.349E-02  2.434E-03
)
 8.7970E-17
X2PI G   12.20
   1.00   1.00   0.50   0.27   0.26   0.17   0.17   0.17   0.17   0.17   0.17
   0.17   0.17   0.17   0.17   0.17   0.17   0.17   0.17   0.17   0.17   0.17
A4PI U   16.10
   0.00   0.00   0.50   0.41   0.40   0.37   0.37   0.37   0.37   0.37
   0.37   0.37   0.37   0.37   0.37   0.37   0.37   0.37   0.37   0.37
A2PI U   16.90
   0.00   0.00   0.00   0.24   0.23   0.22   0.22   0.22   0.22   0.22
   0.22   0.22   0.22   0.22   0.22   0.22   0.22   0.22   0.22   0.22
B4SIG -G 18.20
   0.00   0.00   0.00   0.08   0.07   0.15   0.15   0.15   0.15   0.15   0.15
   0.15   0.15   0.15   0.15   0.15   0.15   0.15   0.15   0.15
  B       23.00
   0.00   0.00   0.00   0.00   0.04   0.09   0.09   0.09   0.09   0.09
   0.09   0.09   0.09   0.09   0.09   0.09   0.09   0.09   0.09
MOL. N          9
A1PI           15  8.40

   8.40   8.50   9.00  10.00  11.00  12.00  13.00  16.00  20.50  25.00
  35.00  50.00  70.00 100.00 200.00
  4.619E-19 -1.848E-19  2.125E-19  4.088E-19  1.152E-18 -2.019E-18 -2.593E-20
 -2.660E-20 -4.062E-21 -4.714E-22  7.931E-22  6.327E-23  2.717E-23  3.280E-24
 -9.238E-19  4.250E-19  4.088E-19  1.152E-18 -2.019E-18 -7.778E-20 -3.990E-20
 -4.062E-21 -1.048E-21  1.190E-21  8.436E-23  4.076E-23  1.093E-23 -1.640E-24
 -4.619E-21  1.046E-18  2.788E-18  8.591E-18  1.685E-17  3.202E-17  1.190E-17
  9.650E-18  9.082E-18  3.647E-18  1.488E-18  8.247E-19  3.755E-19  4.720E-20
  5.009E-18  5.894E-18  8.591E-18  1.685E-17  3.202E-17  3.508E-17  1.403E-17
  9.082E-18  8.021E-18  2.381E-18  1.114E-18  5.837E-19  2.568E-19  5.640E-20
   0
W3DEL           10  7.20

   7.20   7.50   8.00  15.00  20.00  25.00  30.00  40.00  75.00  90.00
  2.162E-20 -2.594E-20  5.373E-21 -6.505E-21 -1.705E-21 -1.074E-21 -2.002E-22
  7.687E-23 -6.770E-23
 -4.323E-20  7.522E-20 -4.647E-21 -1.705E-21 -1.074E-21 -4.004E-22  2.690E-22
 -2.901E-23  3.385E-23
 -1.945E-21  3.365E-19 -2.004E-19  1.483E-18  1.683E-18  1.627E-18  7.200E-19
  3.155E-20  1.372E-19
  5.539E-19  8.612E-19  1.171E-18  1.683E-18  1.627E-18  1.410E-18  4.131E-19
  8.783E-20  4.118E-20
```

```
   0
A3SIG          14  6.14

   6.14   6.50   7.00   7.50   8.00   9.00  10.00  12.00  13.00  20.00
  35.00  50.00  70.00  90.00
 -1.441E-18  2.076E-18 -4.746E-19 -1.374E-19  4.760E-19 -1.274E-18 -6.904E-19
  7.794E-19  1.219E-20 -1.593E-23  1.662E-23  1.176E-22 -8.614E-24
  2.883E-18 -4.746E-19 -1.374E-19  9.521E-19 -1.274E-18 -1.381E-18  3.897E-19
  8.532E-20 -3.413E-23  1.662E-23  1.569E-22 -8.614E-24  4.307E-24
  1.868E-19  4.815E-18  1.434E-17  2.315E-17  1.552E-17  2.627E-17  1.676E-17
  1.722E-17  1.546E-18  6.036E-19  3.296E-19  3.794E-20  3.345E-20
  7.035E-18  1.434E-17  2.315E-17  3.176E-17  2.627E-17  2.938E-17  7.441E-18
  1.491E-17  1.287E-18  3.296E-19  7.804E-20  3.345E-20  8.277E-21
   0
B3PI           14  7.40

   7.40   7.50   9.00  10.50  11.50  12.00  13.00  16.00  20.00  25.00
  35.00  50.00  70.00  90.00
 -6.842E-18  9.122E-19 -1.916E-18 -4.541E-18  3.221E-20  2.986E-18  3.449E-19
 -4.973E-20  1.320E-20 -8.447E-22  1.562E-22  9.099E-23  6.145E-24 -4.503+115
  1.368E-17 -1.916E-18 -3.027E-18  1.610E-20  5.971E-18  1.035E-18 -6.630E-20
  1.650E-20 -1.689E-21  2.343E-22  1.213E-22  6.145E-24 -3.072E-24  4.940-223
  6.842E-20 -5.246E-20  3.631E-17  6.454E-17  8.199E-17  2.701E-17  2.896E-18
  4.296E-18  1.870E-18  9.845E-19  3.648E-19  8.360E-20  4.254E-20  4.940-223
  2.986E-17  3.631E-17  4.681E-17  4.098E-17  5.851E-17  1.697E-17  5.263E-18
  2.486E-18  1.842E-18  5.766E-19  1.327E-19  4.254E-20  1.623E-20  3.730E-23
   0
C3P1           15 10.80

  10.80  11.50  12.00  12.50  13.00  14.00  15.00  16.00  18.00  20.00
  25.00  35.00  50.00  70.00  90.00
 -2.090E-19  5.851E-19  1.189E-17 -5.132E-18  4.321E-18 -8.680E-18  2.400E-18
  3.949E-20  3.145E-20  3.388E-20 -1.948E-21  2.498E-22  9.146E-23  1.434E-23
  4.179E-19  1.189E-17 -5.132E-18  8.642E-18 -8.680E-18  2.400E-18  7.897E-20
  3.145E-20  8.470E-20 -3.897E-21  3.748E-22  1.219E-22  1.434E-23 -7.172E-24
  1.024E-19  3.604E-18  7.028E-18  2.828E-17  1.768E-17  5.068E-17  3.160E-17
  1.334E-17  9.374E-18  1.753E-18  1.195E-18  4.105E-19  1.034E-19  4.426E-20
  2.474E-18  7.028E-18  2.828E-17  4.184E-17  5.068E-17  3.160E-17  2.692E-17
  9.374E-18  6.161E-18  2.097E-18  6.625E-19  1.592E-19  4.426E-20  1.953E-20
   0
T12.4           9 12.40

  12.40  12.50  15.00  20.00  30.00  50.00  70.00 110.00 200.00
  3.004E-19 -2.404E-20  2.476E-20 -2.130E-21 -3.996E-22 -1.019E-21 -1.377E-22
  1.699E-24
 -6.009E-19  4.951E-20 -4.260E-21 -7.992E-22 -1.019E-21 -2.755E-22  3.823E-24
 -8.495E-25
 -3.004E-21  2.502F-19  6.811E-19  2.913E-18  3.510E-18  6.657E-18  3.845E-18
  1.570E-18
  2.506E-18  2.291E-18  5.506E-18  6.780E-18  6.657E-18  7.360E-18  3.556E-18
  1.340E-18
   1
    .33
T16.4           8 13.50

  13.50  14.00  17.00  22.00  30.00  50.00 100.00 200.00
 -2.332E-19  7.774E-20  2.496E-20 -1.520E-21 -8.307E-22 -4.473E-22  1.273E-23
  4.664E-19  4.160E-20 -2.432E-21 -2.077E-21 -1.118E-21  2.547E-23 -6.367E-24
  5.831E-20 -5.971E-19  9.759E-19  4.347E-18  4.182E-18  4.218E-18  1.673E-18
  4.988E-19  2.292E-18  6.861E-18  9.758E-18  8.197E-18  3.536E-18  1.564E-18
   1
```

```
    .33
N2(VIB)       12   .43

   0.00    .50   1.00   1.25   1.50   1.75   2.00   2.50   3.00   3.50
   4.50   5.00
-1.156E-19  2.311E-19 -3.218E-18  1.320E-16 -4.591E-16  7.570E-15 -1.937E-15
-1.682E-15  1.197E-15  5.343E-17 -3.886E-17
 2.311E-19 -1.609E-18  1.320E-16 -4.591E-16  7.570E-15 -3.874E-15 -1.682E-15
 1.197E-15  1.069E-16 -1.943E-17  1.943E-17
 2.889E-20  6.422E-19  2.601E-18  1.751E-18  5.039E-17 -7.313E-17  1.684E-15
 2.220E-15  2.342E-16 -1.843E-17  3.306E-17
 6.422E-19  1.602E-18  1.751E-18  5.039E-17 -7.313E-17  2.642E-15  2.220E-15
 2.342E-16  4.329E-17  3.110E-17 -4.858E-18
  1
    .33
N2(DIS)       12 12.00

  12.00  16.00  20.00  25.00  30.00  35.00  55.00  80.00  90.00 120.00
 150.00 200.00
-8.237E-20  1.647E-19 -8.624E-20 -2.495E-20 -1.397E-20  2.078E-22 -3.170E-22
 4.080E-23 -3.681E-22  2.362E-22 -1.273E-23
 1.647E-19 -1.078E-19 -2.495E-20 -1.397E-20  8.312E-22 -3.963E-22  1.632E-23
-1.104E-21  2.362E-22 -2.121E-23  6.364E-24
 1.318E-18  3.614E-18  1.816E-17  2.462E-17  2.735E-17  6.917E-18  6.358E-18
 1.560E-17  5.465E-18  4.054E-18  2.372E-18
 3.614E-18  2.172E-17  2.462E-17  2.735E-17  2.798E-17  7.859E-18  6.230E-18
 1.551E-17  4.054E-18  3.919E-18  2.084E-18
  1
    .33
   5  17
  12.70

  15.50  16.00  19.00  21.00  25.00  35.00  40.00  45.00  50.00  55.00
  60.00  70.00  80.00  90.00 100.00 140.00 200.00
-1.945E-19  6.484E-20 -6.342E-21  7.283E-21  4.894E-21 -2.974E-20  6.859E-21
 2.305E-21 -1.608E-20  3.609E-21  1.221E-21 -4.665E-21  1.240E-21 -1.946E-22
-1.404E-22 -2.047E-23
 3.891E-19 -4.228E-21  1.457E-20  1.224E-20 -1.487E-20  6.859E-21  2.305E-21
-1.608E-20  3.609E-21  2.442E-21 -4.665E-21  1.240E-21 -1.946E-22 -5.614E-22
-3.070E-23  1.023E-23
 4.863E-20  2.648E-19  1.085E-17  8.733E-18  6.011E-18  2.854E-17  3.123E-17
 3.494E-17  3.900E-17  4.065E-17  2.133E-17  2.407E-17  2.401E-17  2.469E-17
 6.525E-18  4.207E-18
 4.993E-18  7.251E-18  1.764E-17  1.605E-17  1.539E-17  3.123E-17  3.494E-17
 3.900E-17  4.065E-17  4.284E-17  2.407E-17  2.401E-17  2.469E-17  2.526E-17
 6.249E-18  3.563E-18
 2.538E-20 -8.460E-21  1.522E-20 -1.032E-21  4.045E-22 -2.885E-21  1.690E-21
 4.431E-22 -9.827E-22  5.277E-22  1.560E-22 -2.698E-22  1.232E-22  6.845E-24
-5.155E-24 -1.309E-25
-5.076E-20  1.015E-20 -2.065E-21  1.011E-21 -1.442E-21  1.690E-21  4.431E-22
-9.827E-22  5.277E-22  3.119E-22 -2.098E-22  1.232E-22  6.845E-24 -2.062E-23
-1.963E-25  6.545E-26
 2.535E-17  4.319E-18  6.334E-18  3.334E-18  1.394E-18  3.380E-18  3.136E-18
 3.145E-18  3.221E-18  3.149E-18  1.566E-18  1.644E-18  1.560E-18  1.549E-18
 3.935E-19  2.378E-19
 2.547E-17  4.172E-18  6.643E-18  3.569E-18  1.798E-18  3.136E-18  3.145E-18
 3.221E-18  3.149E-18  3.156E-18  1.644E-18  1.560E-18  1.549E-18  1.543E-18
 3.563E-19  1.983E-19
  0
X2SIG+G  15.58
   1.00    .89    .80    .75    .63    .54    .54    .54    .54    .54
```

```
    .54     .54     .54     .54     .54     .54
A2PI U    16.73
   0.00     .10     .15     .15     .13     .12     .12     .12     .12     .12
    .12     .12     .12     .12     .12     .12
B2SIG+G   18.75
   0.00     .01     .05     .05     .05     .04     .04     .04     .04     .04
    .04     .04     .04     .04     .04     .04
LUMPED    22.80
   0.00    0.00    0.00     .05     .09     .07     .07     .07     .07     .07
    .07     .07     .07     .07     .07     .07
DISC. I.  25.0
    .00     .00     .00     .00     .10     .23     .23     .23     .23     .23
    .23     .23     .23     .23     .23     .23
ATOM O        18
2P4 1D        11  1.96

   1.96    2.96    3.96    5.96    9.46   16.96   31.96   51.96  100.00  150.00
 200.00
  5.315E-19 -1.063E-18 -6.396E-19 -1.593E-21  3.208E-21  1.409E-22  1.036E-22
  1.724E-23  4.640E-24 -4.660E-25
 -1.063E-18 -1.279E-18 -2.788E-21  6.875E-21  2.818E-22  1.382E-22  4.141E-23
  4.830E-24 -4.660E-25  4.558E-25
 -5.315E-19  1.606E-17  1.506E-17  7.877E-18  2.886E-18  1.122E-18  4.836E-19
  7.054E-20  3.399E-21  5.565E-21
  1.606E-17  2.628E-17  1.376E-17  6.487E-18  2.291E-18  6.689E-19  2.484E-19
  4.466E-21  5.565E-21  7.406E-22
   0
2P4 1S        13  4.18

   4.18    6.68    9.18   11.68   14.18   19.18   24.18   34.18   44.18   54.18
 100.00  150.00  200.00
  1.297E-20 -2.594E-20 -5.195E-21  1.925E-21  2.763E-23  7.587E-23 -5.552E-24
 -2.311E-24  1.480E-23  3.956E-24  8.712E-26  7.389E-26
 -2.594E-20 -5.195E-21  1.925E-21  5.526E-23  7.587E-23 -1.110E-23 -2.311E-24
  1.480E-23  1.813E-23  9.507E-26  7.389E-26 -6.696E-27
 -6.108E-20  9.622E-19  1.032E-18  9.080E-19  4.273E-19  3.781E-19  1.706E-19
  1.302E-19  8.852E-20  4.244E-21  1.582E-21  3.553E-22
  9.622E-19  1.032E-18  9.080E-19  8.557E-19  3.781E-19  3.403E-19  1.302E-19
  8.852E-20  5.569E-20  1.765E-21  3.553E-22  2.367E-22
   0
3S5S(ZS)      10  9.15

   9.15    9.60   11.62   14.06   17.01   20.59   24.91   33.15   48.54   53.39
 -6.642E-19  2.959E-19 -8.502E-21 -2.054E-19  4.269E-20  4.266E-21  2.478E-21
 -1.104E-22  6.253E-22
  1.328E-18 -1.027E-20 -2.464E-19  5.180E-20  5.147E-21  4.726E-21 -2.061E-22
  1.971E-22 -3.127E-22
  1.345E-19 -8.115E-19  4.149E-18  8.567E-18  3.364E-18  1.703E-18  3.293E-19
  1.561E-19  1.622E-20
  1.509E-18  4.992E-18  9.675E-18  4.295E-18  2.085E-18  8.609E-19  2.567E-19
 -3.693E-20  7.355E-21
   0
O 4S3S3S      19  9.50

   9.50   12.00   14.50   17.00   19.50   22.00   24.50   29.50   37.00   44.50
  54.50   62.00   74.50   82.00  102.00  127.00  152.00  172.00  199.50
  1.232E-20  1.225E-20 -3.036E-21 -3.348E-21 -3.603E-21 -2.846E-21 -1.114E-21
 -4.177E-22 -1.806E-22 -6.180E-23 -2.623E-23 -6.754E-24  2.269E-24  1.431E-24
  1.797E-24  1.448E-24  1.396E-24  7.672E-25
  1.225E-20 -3.036E-21 -3.348E-21 -3.603E-21 -2.846E-21 -2.228E-21 -6.265E-22
 -1.808E-22 -6.241E-23 -1.968E-23 -1.126E-23  1.361E-24  3.816E-24  2.246E-24
```

```
  1.448E-24  1.117E-24  1.055E-24  8.185E-25
 -7.699E-20  2.584E-19  1.053E-18  1.734E-18  2.289E-18  2.709E-18  1.532E-18
  1.160E-18  1.230E-18  9.326E-19  1.212E-18  7.078E-19  1.116E-18  4.040E-19
  2.949E-19  2.660E-19  3.035E-19  2.062E-19
  2.584E-19  1.053E-18  1.734E-18  2.289E-18  2.709E-18  3.022E-18  1.720E-18
  1.230E-18  1.240E-18  9.097E-19  1.178E-18  6.695E-19  1.079E-18  3.691E-19
  2.660E-19  2.426E-19  2.839E-19  1.895E-19

O 4S3P5P      24 10.70

  10.70  13.20  15.70  18.20  20.70  23.20  25.70  28.20  30.70  33.20
  35.70  38.20  40.70  43.20  48.20  53.20  63.20  73.20  85.70 100.70
 125.70 150.70 175.70 198.20
 -1.616E-20 -1.433E-20 -1.523E-21 -1.081E-21  2.244E-23  1.590E-22  1.734E-22
  2.355E-22  1.647E-22  1.616E-22  1.297E-22  1.069E-22  9.564E-23  3.689E-23
  2.781E-23  9.533E-24  5.347E-24  2.542E-24  1.192E-24  3.866E-25  1.620E-25
  8.669E-26  5.057E-26
 -1.433E-20 -1.523E-21 -1.081E-21  2.244E-23  1.590E-22  1.734E-22  2.355E-22
  1.647E-22  1.616E-22  1.297E-22  1.069E-22  9.564E-23  7.379E-23  2.781E-23
  1.907E-23  5.347E-24  3.177E-24  1.430E-24  6.444E-25  1.620E-25  8.669E-26
  4.551E-26  4.012E-26
  1.010E-19  6.672E-19  6.959E-19  6.676E-19  5.987E-19  5.306E-19  4.685E-19
  4.129E-19  3.662E-19  3.256E-19  2.911E-19  2.614E-19  2.358E-19  1.062E-19
  8.824E-20  3.654E-20  2.709E-20  1.653E-20  1.028E-20  4.438E-21  2.975E-21
  2.119E-21  1.770E-21
  6.672E-19  6.959E-19  6.676E-19  5.987E-19  5.306E-19  4.685E-19  4.129E-19
  3.662E-19  3.256E-19  2.911E-19  2.614E-19  2.358E-19  2.137E-19  8.824E-20
  7.450E-20  2.709E-20  2.084E-20  1.243E-20  7.655E-21  2.975E-21  2.119E-21
  1.588E-21  1.401E-21

C 4S3P3P      22 11.00

  11.00  13.50  16.00  18.50  21.00  23.50  26.00  28.50  31.00  33.50
  36.00  38.50  43.50  53.50  66.00  78.50  88.50 101.00 126.00 151.00
 176.00 198.50
 -2.291E-20 -4.488E-21 -2.226E-22 -4.459E-22 -8.661E-23 -5.888E-23 -1.069E-23
 -7.703E-25  1.377E-23  9.692E-24  1.786E-23  7.430E-24  3.422E-24  2.062E-24
  1.307E-24  1.193E-24  6.781E-25  2.599E-25  1.451E-25  9.425E-26  7.417E-26
 -4.488E-21 -2.226E-22 -4.459E-22 -8.661E-23 -5.888E-23 -1.069E-23 -7.703E-25
  1.377E-23  9.692E-24  1.786E-23  1.486E-23  6.844E-24  2.577E-24  1.307E-24
  9.548E-25  8.476E-25  5.199E-25  1.451E-25  9.425E-26  6.675E-26  5.071E-26
  1.432E-19  3.314E-19  3.512E-19  3.627E-19  3.575E-19  3.491E-19  3.384E-19
  3.274E-19  3.163E-19  3.057E-19  2.955E-19  1.428E-19  6.681E-20  4.760E-20
  4.217E-20  4.753E-20  3.527E-20  1.610E-20  1.401E-20  1.246E-20  1.253E-20
  3.314E-19  3.512E-19  3.627E-19  3.575E-19  3.491E-19  3.384E-19  3.274E-19
  3.163E-19  3.057E-19  2.955E-19  2.859E-19  1.341E-19  5.964E-20  4.217E-20
  3.797E-20  4.414E-20  3.245E-20  1.401E-20  1.246E-20  1.127E-20  1.157E-20

C 3D3D        19 12.10

  12.10  14.60  17.10  19.60  22.10  24.60  27.10  29.60  32.10  39.60
  47.10  54.60  64.60  74.60 102.10 127.10 149.60 174.60 199.60
```

APPENDIX D

PARTIAL LISTING OF A TYPICAL PHOTOELECTRON PRODUCTION INPUT FILE FROM ATMOSPHERIC EXPLORER C SATELLITE ORBIT 284 UPLEG

```
 1.00 /  1.00   *  HINTEREGGER FLUX,FITTED ATMOSPHERE   KE 0284U . 7
 PHOTOELECTRON ENERGY GRID IN EV - 5E15.5
 100=NPTSPRO
    .00000E 00     .10000E 01     .20000E 01     .30000E 01     .40000E 01
    .50000E 01     .60000E 01     .70000E 01     .80000E 01     .90000E 01
    .10000E 02     .11000E 02     .12000E 02     .13000E 02     .14000E 02
    .15000E 02     .16000E 02     .17000E 02     .18000E 02     .19000E 02
    .20000E 02     .21000E 02     .22000E 02     .23000E 02     .24000E 02
    .25000E 02     .26000E 02     .27000E 02     .28000E 02     .29000E 02
    .30000E 02     .31000E 02     .32000E 02     .33000E 02     .34000E 02
    .35000E 02     .36000E 02     .37000E 02     .38000E 02     .39000E 02
    .40000E 02     .41000E 02     .42000E 02     .43000E 02     .44000E 02
    .45000E 02     .46000E 02     .47000E 02     .48000E 02     .49000E 02
    .50000E 02     .51000E 02     .52000E 02     .53000E 02     .54000E 02
    .55000E 02     .56000E 02     .57000E 02     .58000E 02     .59000E 02
    .60000E 02     .61000E 02     .62000E 02     .63000E 02     .64000E 02
    .65000E 02     .66000E 02     .67000E 02     .68000E 02     .69000E 02
    .70000E 02     .71000E 02     .72000E 02     .73000E 02     .74000E 02
    .75000E 02     .76000E 02     .77000E 02     .78000E 02     .79000E 02
    .80000E 02     .81000E 02     .82000E 02     .83000E 02     .84000E 02
    .85000E 02     .86000E 02     .87000E 02     .88000E 02     .89000E 02
    .90000E 02     .91000E 02     .92000E 02     .93000E 02     .94000E 02
    .95000E 02     .96000E 02     .97000E 02     .98000E 02     .99000E 02
SOLAR ZENITH                  53.649994
ALTITUDE                     409.000000
TEMPERATURE                  714.856934
DENSITIES       HE              .523700E 07
                N2              .380200E 06
                O               .213252E 08
                O2              .241455E 04    25X,E16.6
 ELECTRON TEMPERATURE            .122000E 04
 ELECTRON DENSITY             .241300E 06
 TOTAL ION DENSITY            .000000E 00
 PHOTOELECTRON SPECTRUM       6E12.4
  .9140E 00   .6662E 00   .4917E 00   .1650E 00   .2497E 00   .1481E 00
  .2921E 00   .1839E 00   .1088E 00   .1130E 00   .3006E-01   .4289E-01
  .1734E 00   .3197E-01   .9165E-02   .7310E-01   .2082E 00   .5949E-01
  .2379E-01   .2114E-01   .9690E-01   .9782E-02   .3993E 00   .6301E 00
  .3443E-01   .2723E-01   .5330E-01   .4286E 00   .7199E-01   .6878E-01
  .4311E-01   .9951E-01   .4250E-01   .3647E-01   .7218E-01   .3098E-01
  .2046E-01   .3069E-01   .1934E-01   .1667E-01   .2093E-01   .1444E-01
  .1621E-01   .2078E-01   .1959E-01   .1778E-01   .1607E-01   .3110E-01
  .2164E-01   .1697E-01   .2887E-01   .2848E-01   .2541E-01   .2936E-01
  .2724E-01   .3358E-01   .1205E-01   .1673E-01   .1699E-01   .2632E-02
  .2394E-02   .2966E-02   .1234E-02   .1767E-02   .4726E-02   .6976E-03
  .3637E-02   .1844E-02   .9774E-03   .2444E-02   .4343E-04   .3562E-03
  .3276E-03   .2844E-04   .6999E-05   .1620E-03   .7693E-04   .2860E-03
  .2177E-03   .2343E-04   .2250E-03   .2571E-03   .1059E-03   .1757E-03
  .1317E-03   .5568E-04   .9834E-04   .1798E-03   .1458E-03   .1219E-03
  .1549E-03   .1146E-03   .2227E-03   .9297E-04   .1897E-03   .1560E-03
  .7661E-04   .2068E-03   .9358E-04   .1153E-01
SOLAR ZENITH                  54.809993
ALTITUDE                     394.300049
TEMPERATURE                  714.728271
DENSITIES       HE              .556800E 07
                N2              .102300E 07
                O               .358147E 08
                O2              .767109E 04    25X,E16.6
 ELECTRON TEMPERATURE            .122700E 04
 ELECTRON DENSITY             .306300E 06
 TOTAL ION DENSITY            .000000E 00
 PHOTOELECTRON SPECTRUM       6E12.4
  .1382E 01   .1118E 01   .9205E 00   .2987E 00   .4309E 00   .2570E 00
  .4936E 00   .3119E 00   .1853E 00   .1757E 00   .5211E-01   .7611E-01
  .2895E 00   .5414E-01   .1577E-01   .1232E 00   .2607E 00   .1001E 00
```

PRECEDING PAGE BLANK - NOT FILMED

```
 .4043E-01  .3376E-01  .1589E 00  .1591E-01  .6687E 00  .1051E 01
 .6266E-01  .4777E-01  .8796E-01  .7192E 00  .1210E 00  .1156E 00
 .7184E-01  .1678E 00  .7152E-01  .6136E-01  .1211E 00  .5212E-01
 .3396E-01  .5118E-01  .3179E-01  .2733E-01  .3509E-01  .2348E-01
 .2680E-01  .3473E-01  .3192E-01  .2935E-01  .2594E-01  .5090E-01
 .3643E-01  .2852E-01  .4851E-01  .4790E-01  .4281E-01  .4945E-01
 .3914E-01  .5651E-01  .2021E-01  .2808E-01  .2837E-01  .4445E-02
 .3996E-02  .4970E-02  .2085E-02  .2978E-02  .7954E-02  .1184E-02
 .6123E-02  .3109E-02  .1644E-02  .4130E-02  .6107E-04  .6002E-03
 .5451E-03  .4825E-04  .1243E-04  .2690E-03  .1255E-03  .4802E-03
 .3675E-03  .4207E-04  .3791E-03  .4261E-03  .1767E-03  .2962E-03
 .2171E-03  .9440E-04  .1453E-03  .3018E-03  .2439E-03  .2052E-03
 .2604E-03  .1914E-03  .3735E-03  .1506E-03  .3142E-03  .2528E-03
 .1264E-03  .3465E-03  .1507E-03  .1915E-01
SOLAR ZENITH                    55.990005
ALTITUDE                       360.699951
TEMPERATURE                    714.496094
DENSITIES          HE           .695800E 07
                   N2           .269100E 07
                   O            .594733E 08
                   O2           .233425E 05   25X,E16.6
 ELECTRON TEMPERATURE            .130000E 04
 ELECTRON DENSITY              .380900E 06
 TOTAL ION DENSITY             .000000E 00
 PHOTOELECTRON SPECTRUM        6E12.4
  .2274E 01  .1847E 01  .1358E 01  .5112E 00  .7461E 00  .4510E 00
  .8293E 00  .5254E 00  .3143E 00  .2842E 00  .9141E-01  .1375E 00
  .4795E 00  .9106E-01  .2795E-01  .2056E 00  .4299E 00  .1702E 00
  .7011E-01  .5598E-01  .2620E 00  .2713E-01  .1111E 01  .1739E 01
  .1197E 00  .8741E-01  .1462E 00  .1193E 01  .2028E 00  .1928E 00
  .1200E 00  .2810E 00  .1205E 00  .1026E 00  .2017E 00  .8704E-01
  .5654E-01  .8498E-01  .5269E-01  .4554E-01  .5856E-01  .3896E-01
  .4450E-01  .5787E-01  .5280E-01  .4874E-01  .4287E-01  .8387E-01
  .6102E-01  .4773E-01  .9074E-01  .7972E-01  .7150E-01  .8251E-01
  .6541E-01  .9428E-01  .3373E-01  .4665E-01  .4699E-01  .7442E-02
  .6621E-02  .8262E-02  .3493E-02  .4975E-02  .1325E-01  .1998E-02
  .1020E-01  .5191E-02  .2735E-02  .6807E-02  .9814E-04  .1002E-02
  .9025E-03  .8139E-04  .2238E-04  .4452E-03  .2096E-03  .8001E-03
  .6152E-03  .7687E-04  .6331E-03  .7063E-03  .2954E-03  .4947E-03
  .3610E-03  .1590E-03  .2424E-03  .5039E-03  .4063E-03  .3457E-03
  .4366E-03  .3199E-03  .6226E-03  .2485E-03  .5222E-03  .4177E-03
  .2104E-03  .5781E-03  .2484E-03  .3182E-01
SOLAR ZENITH                    57.229996
ALTITUDE                       338.100098
TEMPERATURE                    714.085693
DENSITIES          HE           .713200E 07
                   N2           .647500E 07
                   O            .954134E 08
                   O2           .683061E 05   25X,E16.6
 ELECTRON TEMPERATURE            .136500E 04
 ELECTRON DENSITY              .434900E 06
 TOTAL ION DENSITY             .000000E 00
 PHOTOELECTRON SPECTRUM        6E12.4
  .3889E 01  .2589E 01  .2185E 01  .9900E 00  .1263E 01  .7755E 00
  .1350E 01  .8580E 00  .5182E 00  .4439E 00  .1573E 00  .2448E 00
  .7680E 00  .1485E 00  .4878E-01  .3319E 00  .6326E 00  .2823E 00
  .1191E 00  .9027E-01  .4175E 00  .4538E-01  .1784E 01  .2775E 01
  .2263E 00  .1581E 00  .2353E 00  .1910E 01  .3295E 00  .3111E 00
  .1944E 00  .4556E 00  .1974E 00  .1660E 00  .3246E 00  .1407E 00
  .9119E-01  .1364E 00  .8454E-01  .7366E-01  .9442E-01  .6271E-01
  .7152E-01  .9331E-01  .8461E-01  .7836E-01  .5871E-01  .1335E 00
  .9902E-01  .7740E-01  .1299E 00  .1282E 00  .1156E 00  .1332E 00
  .1058E 00  .1522E 00  .5450E-01  .7488E-01  .7516E-01  .1207E-01
  .1060E-01  .1328E-01  .5670E-02  .8044E-02  .2134E-01  .3275E-02
  .1644E-01  .3389E-02  .4400E-02  .1092E-01  .1547E-03  .1617E-02
  .1444E-02  .1334E-15  .3569E-04  .7118E-03  .3408E-03  .1289E-12
```

```
 .9975E-03  .1386E-03  .1023E-02  .1133E-02  .4791E-03  .7998E-03
 .5817E-03  .2602E-03  .3927E-03  .8150E-03  .6553E-03  .5658E-03
 .7098E-03  .5185E-03  .1004E-02  .3971E-03  .8405E-03  .6686E-03
 .3396E-03  .9341E-03  .3966E-03  .5117E-01
SOLAR ZENITH                      57.869995
ALTITUDE                          327.300049
TEMPERATURE                       713.782959
DENSITIES      HE                   .781900E 07
               N2                   .944800E 07
               O                    .126071E 09
               O2                   .114444E 06    25X,E16.6
 ELECTRON TEMPERATURE               .140000E 04
 ELECTRON DENSITY                  .471900E 06
 TOTAL ION DENSITY                 .000000E 00
 PHOTOELECTRON SPECTRUM            6E12.4
 .5182E 01  .3947E 01  .2884E 01  .1203E 01  .1694E 01  .1045E 01
 .1785E 01  .1138E 01  .6893E 00  .5813E 00  .2119E 00  .3329E 00
 .1013E 01  .1969E 00  .6605E-01  .4387E 00  .8127E 00  .3763E 00
 .1600E 00  .1194E 00  .5497E 00  .6070E-01  .2355E 01  .3656E 01
 .3129E 00  .2161E 00  .3109E 00  .2518E 01  .4367E 00  .4113E 00
 .2573E 00  .6034E 00  .2622E 00  .2197E 00  .4289E 00  .1861E 00
 .1206E 00  .1801E 00  .1116E 00  .9750E-01  .1252E 00  .8289E-01
 .9449E-01  .1234E 00  .1117E 00  .1035E 00  .9071E-01  .1759E 00
 .1312E 00  .1025E 00  .1716E 00  .1695E 00  .1530E 00  .1762E 00
 .1401E 00  .2013E 00  .7212E-01  .9888E-01  .9915E-01  .1599E-01
 .1399E-01  .1755E-01  .7516E-02  .1065E-01  .2822E-01  .4354E-02
 .2175E-01  .1110E-01  .5815E-02  .1442E-01  .2036E-03  .2141E-02
 .1905E-02  .1776E-03  .5401E-04  .9393E-03  .4521E-03  .1705E-02
 .1322E-02  .1894E-03  .1354E-02  .1496E-02  .6351E-03  .1059E-02
 .7694E-03  .3458E-03  .5203E-03  .1079E-02  .8672E-03  .7521E-03
 .9416E-03  .6871E-03  .1329E-02  .5242E-03  .1112E-02  .8829E-03
 .4496E-03  .1237E-02  .5233E-03  .6760E-01
SOLAR ZENITH                      58.509995
ALTITUDE                          316.699951
TEMPERATURE                       713.386963
DENSITIES      HE                   .836000E 07
               N2                   .143300E 08
               O                    .160019E 09
               O2                   .190304E 06    25X,E16.6
 ELECTRON TEMPERATURE               .143000E 04
 ELECTRON DENSITY                  .520300E 06
 TOTAL ION DENSITY                 .000000E 00
 PHOTOELECTRON SPECTRUM            6E12.4
 .6295E 01  .4942E 01  .3641E 01  .1597E 01  .2218E 01  .1382E 01
 .2290E 01  .1458E 01  .8888E 00  .7379E 00  .2804E 00  .4483E 00
 .1284E 01  .2523E 00  .8840E-01  .5585E 00  .1034E 01  .4887E 00
 .2108E 00  .1539E 00  .6977E 00  .7995E-01  .2991E 01  .4627E 01
 .4352E 00  .2945E 00  .3971E 00  .3189E 01  .5590E 00  .5238E 00
 .3294E 00  .7708E 00  .3375E 00  .2803E 00  .5454E 00  .2373E 00
 .1540E 00  .2289E 00  .1424E 00  .1252E 00  .1597E 00  .1063E 00
 .1205E 00  .1573E 00  .1426E 00  .1321E 00  .1162E 00  .2234E 00
 .1676E 00  .1311E 00  .2182E 00  .2153E 00  .1950E 00  .2244E 00
 .1787E 00 *
```

APPENDIX E

LISTING AND SAMPLE OUTPUT OF A CODE WHICH CALCULATES THE PRODUCTION OF SECONDARY AURORAL ELECTRONS

```
C      ****  SCS16  ****
C      CALCULATES PRODUCTION SPECTRUM OF SECONDARY ELECTRONS
       DIMENSION NAMES(4),AEP(4),SIG(4),WP(4),RHO(4),P(4),AR(4)
       DIMENSION NORBIT(5),PES(200)
       DATA NAMES/16H  HE  N2  01  02/
       DATA AEP/1.443E-18, 1.134E-17, 4.750E-18, 9.692E-18/
       DATA SIG/3.480E-17, 2.160E-16, 1.240E-16, 2.530E-16/
       DATA RHO/5.370E+06, 3.199E+08, 6.486E+08, 1.698E+07/
       DATA  WP/15.80    , 12.70    , 17.40    , 17.40    /
C
       PRINT 100
  100  FORMAT (' ENTER PFLUX,NORBIT (E10.3,5X,5A4)')
       READ (1,110) PFLUX,NORBIT
  110  FORMAT (E10.3,5X,5A4)
       DO 120 K=1,4
       P(K)=RHO(K)*SIG(K)*PFLUX
  120  AR(K)=RHO(K)*AEP(K)*PFLUX
C
       DO 210 N=1,200
       ES=N-0.5
       CC=0.0
       DO 200 K=1,4
  200  CC=CC+AR(K)/(1.0+(ES/WP(K))**2.1)
  210  PES(N)=CC
C
       WRITE (2,300) NORBIT,PFLUX
  300  FORMAT (5A4,5X,E10.3,'=ASSUMED PRIMARY FLUX'/)
       WRITE (2,310) NAMES
  310  FORMAT (4(8X,A4),2X,'CONSTITUENT')
       WRITE (2,320) WP
  320  FORMAT (4F12.2,2X,'W(EP)=BEATY IONIZATION PARAMETER')
       WRITE (2,330) AEP
  330  FORMAT (4(1PE12.3),2X,'A(EP)=DIFFERENTIAL CROSS SECTION')
       WRITE (2,340) SIG
  340  FORMAT (4(1PE12.3),2X,'TOTAL IONIZATION CROSS SECTION')
       WRITE (2,350) RHO
  350  FORMAT (4(1PE12.3),2X,'NUMBER DENSITY')
       WRITE (2,360) P
  360  FORMAT (4(1PE12.3),2X,'TOTAL ION PRODUCTION RATE')
       WRITE (2,370) PES
  370  FORMAT (5E12.4)
       END
```

C-1165UA RC 4-23-76 .150E 08=ASSUMED PRIMARY FLUX

HE	N2	01	02	CONSTITUENT	
15.80	12.70	17.40	17.40	W(EP)=BEATY IONIZATION PARAMETER	
1.443E-18	1.134E-17	4.750E-18	5.692E-18	A(EP)=DIFFERENTIAL CROSS SECTION	
3.480E-17	2.160E-16	1.240E-16	2.530E-16	TOTAL IONIZATION CROSS SECTION	
5.370E 06	3.199E 08	6.486E 08	1.698E 07	NUMBER DENSITY	
2.803E-03	1.036E 00	1.206E 00	6.444E-02	TOTAL ION PRODUCTION RATE	
.1031E 00	.1023E 00	.1007E 00	.9818E-01	.9499E-01	.9122E-01
.8702E-01	.8256E-01	.7797E-01	.7335E-01	.6881E-01	.6441E-01
.6020E-01	.5621E-01	.5245E-01	.4894E-01	.4566E-01	.4263E-01
.3981E-01	.3721E-01	.3481E-01	.3259E-01	.3055E-01	.2866E-01
.2692E-01	.2532E-01	.2384E-01	.2247E-01	.2120E-01	.2002E-01
.1894E-01	.1793E-01	.1699E-01	.1612E-01	.1531E-01	.1455E-01
.1385E-01	.1319E-01	.1257E-01	.1200E-01	.1146E-01	.1095E-01
.1047E-01	.1003E-01	.9607E-02	.9212E-02	.8839E-02	.8487E-02
.8155E-02	.7842E-02	.7545E-02	.7264E-02	.6998E-02	.6745E-02
.6506E-02	.6278E-02	.6062E-02	.5856E-02	.5660E-02	.5474E-02
.5296E-02	.5127E-02	.4965E-02	.4811E-02	.4663E-02	.4522E-02
.4387E-02	.4258E-02	.4134E-02	.4015E-02	.3901E-02	.3792E-02
.3688E-02	.3587E-02	.3490E-02	.3397E-02	.3308E-02	.3222E-02
.3139E-02	.3060E-02	.2983E-02	.2909E-02	.2838E-02	.2769E-02
.2703E-02	.2638E-02	.2577E-02	.2517E-02	.2459E-02	.2403E-02
.2349E-02	.2297E-02	.2246E-02	.2197E-02	.2150E-02	.2104E-02
.2059E-02	.2016E-02	.1974E-02	.1934E-02	.1894E-02	.1856E-02
.1819E-02	.1783E-02	.1748E-02	.1714E-02	.1681E-02	.1649E-02
.1618E-02	.1587E-02	.1558E-02	.1529E-02	.1501E-02	.1474E-02
.1448E-02	.1422E-02	.1397E-02	.1372E-02	.1348E-02	.1325E-02
.1302E-02	.1280E-02	.1259E-02	.1238E-02	.1217E-02	.1197E-02
.1178E-02	.1159E-02	.1140E-02	.1122E-02	.1104E-02	.1087E-02
.1070E-02	.1053E-02	.1037E-02	.1021E-02	.1006E-02	.9904E-03
.9756E-03	.9612E-03	.9470E-03	.9331E-03	.9196E-03	.9063E-03
.8933E-03	.8806E-03	.8681E-03	.8559E-03	.8440E-03	.8323E-03
.8208E-03	.8096E-03	.7985E-03	.7877E-03	.7772E-03	.7668E-03
.7566E-03	.7466E-03	.7369E-03	.7273E-03	.7179E-03	.7086E-03
.6996E-03	.6907E-03	.6820E-03	.6734E-03	.6650E-03	.6567E-03
.6486E-03	.6407E-03	.6329E-03	.6252E-03	.6177E-03	.6103E-03
.6030E-03	.5958E-03	.5888E-03	.5819E-03	.5751E-03	.5685E-03
.5619E-03	.5555E-03	.5491E-03	.5429E-03	.5368E-03	.5308E-03
.5248E-03	.5190E-03	.5132E-03	.5076E-03	.5021E-03	.4966E-03
.4912E-03	.4860E-03	.4807E-03	.4756E-03	.4706E-03	.4656E-03
.4607E-03	.4559E-03				

APPENDIX F

PHOTOIONIZATION AND PHOTOABSORPTION CROSS SECTIONS OF He, O, N_2 AND O_2 FOR AERONOMIC CALCULATIONS

K. KIRBY, E.R. CONSTANTINIDES, S. BABEU,

M. OPPENHEIMER, AND G.A. VICTOR

Harvard-Smithsonian Center for Astrophysics
60 Garden Street
Cambridge, Mass. 02138

AD-A083 010 SMITHSONIAN ASTROPHYSICAL OBSERVATORY CAMBRIDGE MASS F/G 4/1
CALCULATIONS PERTAINING TO THE ENERGY BALANCE AND PLASMA MOTION--ETC(U)
NOV 79 A DALGARNO, E CONSTANTINIDES F19628-78-C-0047
UNCLASSIFIED AFGL-TR-79-0270 NL

2 OF 2
AD A083010

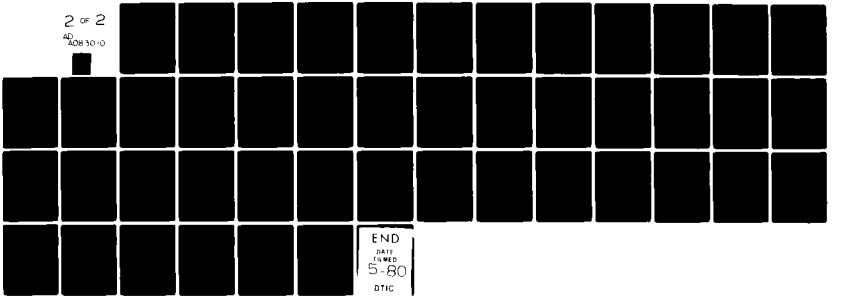

END
DATE FILMED
5-80
DTIC

Photoionization and Photoabsorption Cross Sections of He, O, N_2 and O_2 for Aeronomic Calculations

K. Kirby, E.R. Constantinides, S. Babeu,
M. Oppenheimer*, and G.A. Victor

Harvard-Smithsonian Center for Astrophysics
60 Garden Street
Cambridge, Mass. 02138

Abstract

A compilation of photoionization and photoabsorption cross sections is presented for He, O, N_2, and O_2 for use in studies of ion and photoelectron production in the terrestrial ionosphere. In wavelength regions where rapid variations occur in the cross sections, averaged cross sections are calculated. When necessary the cross sections have been extrapolated to shorter wavelengths. The cross sections are tabulated at the wavelengths of the solar lines and continua given in the solar reference spectrum of Hinteregger from $\sim$1030 Å to $\sim$34 Å. For molecules, N_2 and O_2, branching ratios are given for ionization into the ground and electronic states of the molecular ions and for dissociative ionization.

*John Simon Guggenheim Memorial Foundation Fellow '78-'79.

I. Introduction

Any detailed theoretical study of the earth's upper atmosphere must begin with a calculation of the production rates for major ions and photoelectrons due to solar radiation. We have constructed a program to compute these rates using a model atmosphere or measured neutral particle densities[1,2], the solar flux tabulated on a 1 Å grid and observed by Hinteregger[3], and Heroux and Hinteregger[4], and a compilation of experimental and theoretical photoionization and photoabsorption cross sections which we report here. This program was undertaken in conjunction with the series of Atmosphere Explorer satellites (AE-C,D,E) which carried instruments to measure simultaneously many geophysical parameters of the terrestrial ionosphere. These experiments have been described in volume 8 of Radio Science (1973). The neutral species of interest in the altitude range above 120 km are He, O, N_2, and O_2, with photoionization thresholds at 504 Å, 910 Å, 796 Å and 1027 Å, respectively. The minor constituents, N and NO, are not included in this compilation.

We have been guided in our tabulation by the intended atmospheric applications of the cross sections, for which a detailed presentation of the variation of the cross sections is neither necessary nor desirable. In wavelength regions in which the cross sections are highly structured we have

frequently computed and tabulated averaged values. The accuracy of the atmosphere calculations is limited here by uncertainties in the intensities of the incident solar radiation and in the densities of the neutral constituents. Many of the measured cross sections have been obtained at low spectral resolution and at room temperature. We adopt these nevertheless but the possibility of important errors should be noted[5].

Total photoabsorption cross sections for the atomic constituents He and O refer only to photoionization. For the molecular constituents N_2 and O_2 they include photoionization, photodissociation and discrete band absorption to excited electronic states. In photoionization events, different final electronic atomic and molecular states of the ionic products may be populated and dissociative ionization of the molecular species may occur.

All the photoionization and photoabsorption cross sections presented here have been tabulated, using interpolation and extrapolation where necessary, at the solar line and continuum wavelengths of the Hinteregger reference solar flux[3] which is based on measurements by the Extreme Ultraviolet Spectrophotometer (EUVS) on board AE-C[6] and on rocket data [7,8]. We restrict the tabulation to the wavelength region from the photoionization threshold of O_2 at 1027 $\mathring{A}$

to 33.74 Å which is the shortest wavelength in Hinteregger's compilation before the nitrogen K-shell ionization edge at 31 Å. The intensity of the solar flux decreases rapidly for wavelengths below about 170 Å, so that the solar flux and the cross section data at short wavelengths are not required with high accuracy for most aeronomy applications.

Specific cross sections for multiple ionization, are not included in our tabulation except that the total photoabsorption cross sections include them. At 260 Å double ionization of N_2 contributes only about 2% of the total oscillator strength[9], and although the multiple ionization fraction becomes slightly larger at shorter wavelengths, the solar flux is decreasing rapidly in this region and the overall effect on the ion abundance is negligible.

Because the cross section data have been obtained from many different experimental and theoretical sources and have involved interpolation and extrapolation, the accuracy is not uniform. Although we are concerned primarily with valence shell rather than inner shell processes, the total cross sections of the molecular species at short wavelengths (<150 Å) where extrapolation has been carried out include the cross sections for inner-shell processes. The branching ratios for production of excited electronic states of N_2^+ and O_2^+ are unknown in the wavelength region below 304 Å,

and lacking any data we have used the 304 Å values down to 34 Å. In practice the branching ratios for inner shell absorption presumably increase compared to the valence shell cross sections as the wavelength decreases. At wavelengths longer than ∿650 Å there are several regions in the molecular cross sections which are densely structured. Because the solar flux used in the calculations is not tabulated on as fine a wavelength scale as the oscillations in the cross sections, we fitted a straight line through the peaks at half height. In other regions, in which the structure was less dense we replaced the peaks by square waves such that in integrating over the full width of the lines, using the grid of solar wavelengths given by Hinteregger, the effective cross section is equivalent to the integrated cross section at finer resolution. Thus we have distorted the shapes and magnitudes of the cross section data in order to obtain equivalent integrated cross sections using our solar wavelength scale. At particular wavelengths then, individual cross sections may be incorrect. In addition, there is some ambiguity in the cross sections adopted at the solar lines due to the limited spacecraft spectrometer resolution, to the pressure dependence of the laboratory data, and to the uncertain widths of the solar lines compared to the laboratory line sources. Thus, errors in the production rates could occur

if there exists a coincidence, not properly included, between a resonance for an absorbing species and a solar line. Where we have discovered inconsistencies between several sets of data we have generally favored the recent values. The following section discusses the details of and the various sources for the cross sections which are presented in Table 1. Because cross sections for each species are treated differently in the tables due to the diverse nature of the sources for the data, it is desirable to consult Section II before using any of the data in the tables.

We have incorporated the data presented here and the tabulation of the EUV flux given by Hinteregger[3] into a program which calculates the ionization rates for thermospheric constituents. Table A shows the production rate in s^{-1} for the various ion states in an atmosphere with zero opacity. These production rates are valid at altiutudes above 400 kilometers for daytime solar zenith angles.

II. Discussion of Cross Section Data

He: For He, with photoionization threshold at 504 Å, there are accurate theoretical[10,11] and experimental[12,13] cross sections available which generally agree with each other to within about 5%. The cross sections near threshold (504 Å $\geq \lambda \geq$ 454 Å) were taken from Doyle, Oppenheimer, and Dalgarno[14]. The close-coupling calculation of Jacobs[10] for

a simple system like He is probably accurate to about 2%, except in the neighborhood of narrow resonances. We converted Jacobs' values[10] of the continuum oscillator strength to cross sections and did a least squares fit to the values from 454 Å to 130 Å. As the cross section curve is entirely smooth in this region, little error should result from this procedure. For wavelengths shorter than 130 Å we used the fit to extrapolate the cross sections.

O: Photoionization of the 2p valence shell electron of atomic oxygen leads to $O^+(^4S^o)$, $O^+(^2D^o)$, and $O^+(^2P^o)$ with thresholds at 910.4 Å, 732 Å, and 665 Å, respectively. We used the empirical fits to the partial cross sections for these three channels given by Henry[15], normalized to the calculated total ionization cross sections of Taylor and Burke[16]. Recent measurements near threshold by Kohl et al.[17] tend to confirm the values of Taylor and Burke as well as those of Pradhan and Saraph[18], which are 15-20% higher overall than those of Henry[15]. Several resonances identified by Taylor and Burke[16] were included, from 706-608 Å, below the $^2D^o$ limit.

Removing the 2s inner shell electron of atomic oxygen gives rise to $O^+(^4P^e)$ and $O^+(^2P^e)$ with thresholds at 435 Å and 315 Å respectively. The partial cross sections for this process were obtained from calculations of Dalgarno, Henry and Stewart[19] as modified by Henry[20]. The branching ratios of Henry[20] at 304 Å have been confirmed by Dehmer and Dehmer[21].

Total ionization cross sections for wavelengths shorter than 435 Å were obtained by adding these partial cross sections for inner shell ionization to the total ionization cross sections of Taylor and Burke[16].

N_2: For wavelengths shorter than 660 Å, the ionization efficiency has been found to be unity[22], and the photoionization and photoabsorption cross sections are equal. In the region 180 Å-650 Å we interpolated the total absorption cross section data of Lee, Carlson, Judge and Ogawa[22] to obtain cross sections at each wavelength in the Hinteregger reference flux. These authors conservatively estimated the error in the cross sections to be ±20%, and as there is almost no structure in this region the interpolated cross sections should be of the same accuracy. We found good agreement of the cross sections with more recent data of Hamnet, Stoll and Brion[23] as well as those of Gurtler, Saile and Koch[24]. We have not included the peaks attributed to the Rydberg series leading to the $C^2\Sigma_u^+$ state of N_2^+ between 500 and 550 Å[24] and they are probably not significant for our studies. From 180 Å to 34 Å the data were extrapolated so that consistency was obtained with the absorption cross sections given at 100 Å, 68 Å, and 44.6 Å by Huffman[25]. From 650 to 668 Å a smooth curve was drawn joining the absorption data of Lee et al.[22] and the data of Huffman[25], passing through two points measured by Samson, Haddad and Gardner[26]. As the

ionization decreases from 100% starting at 660 Å, we will now discuss absorption and ionization cross sections separately.

Where considerable structure in the cross section is evident, from 668 Å to 734 Å, the total absorption cross sections were obtained from Huffman[25]. We estimated a background cross section σ_b by drawing in a base-line on the graphs of his data; superimposed on σ_b was the peak cross section, σp. Each peak area was approximated as a square wave over the same wavelength interval as the actual triangular line-shape. Any dips in the cross sections were approximated in similar fashion. The total cross section at each wavelength was therefore the sum (or difference) of σ_b and σ_p. From 734 Å to 986 Å Carter[27] has tabulated oscillator strengths for N_2 between adjacent pairs of wavelengths and again a square shape to the absorption cross section between these wavelengths was assumed. Longward of 986 Å, conflicting measurements for the N_2 cross section have been reported, and above 1000 Å no detectable absorption was observed by Huffman, Tanaka and Larrabee[28]. Thus from 986 Å to 1030 Å we have set the N_2 absorption cross sections to zero.

Photoionization cross sections in the region from 660 Å to threshold at 796 Å were explicitly calculated using a least squares fit to the ionization data of Cook and

Metzger[29] and the absorption cross sections previously described. Our values for both photoabsorption and photoionization cross sections in the wavelength range 100 Å to 796 Å appear to be reasonably consistent with the recent discrete line source measurements of Samson, Haddad and Gardner[26] and the work of Cole and Dexter[9] from 50 Å to 340 Å.

Photoionization and absorption cross sections of N_2 at a number of solar lines listed in Huffman's[25] Table I were included explicitly. The majority of these values are from earlier work of Samson and Cairns[30]. Not all the solar lines listed in Huffman[25] were identical with those given in the Hinteregger reference spectrum, and several lines were combined and the cross sections averaged.

The dissociative ionization of N_2, producing N^+ ions, was treated as arising from a single state with threshold at 509 Å. The partial cross sections for this process were obtained by multiplying the total ionization cross sections by the fractional yield for dissociative ionization obtained from Table B. Values for this yield were derived from the data of Wight, Van der Wiel and Brion[31] and of Fryar and Browning[32]. The dissociative ionization yield, Y, can be obtained from Table B by linear interpolation between the listed values, with the exception of the region from 387 Å to 477 Å where the following form should be:

$$Y=0.0329+8.13\times10^{-6}\times(\lambda-442)^2$$

The remaining part of the total ionization cross section, $\sigma_{ion}(1-Y)$, is apportioned among five electronic states of N_2^+ according to the branching ratios listed in Table C. At each wavelength, the branching ratios sum to 1 and at wavelengths not listed in Table C the ratios can be obtained by linear interpolation between adjacent values. Partial photoionization cross sections are obtained by multiplying the total cross section (minus the dissociative ionization cross section) by the relevant branching ratio. Branching ratios for N_2 photoionization have been given by a number of workers[26,23,33,34] and the agreement among the published results is generally within 10%. There appears to be some structure present in the published branching ratios between 670 Å and 720 Å, but this we have not included because the measurements differ the most here and no strong solar lines appear in this region. Since no measurements have been reported for wavelengths shorter than 210 Å, we assumed constant branching ratios from 210 Å to 34 Å. For most aeronomic calculations this assumption is of minor importance.

O_2: The photoabsorption and photoionization cross sections for O_2 in wavelength range 612-34 Å were obtained in an analogous fashion to the N_2 cross sections in this region, from the data

of Lee, Carlson, Judge and Ogawa[22] and from the short wavelength values of Huffman[25]. The ionization yield is equal to unity for wavelengths shorter than ~670 Å. For wavelengths longer than 670 Å, a great deal of structure is present in both the ionization and absorption cross sections.

From 612 Å to 742 Å absorption cross sections were obtained by graphically interpolating the points of Samson, Gardner and Haddad[35]. Such a fit passes roughly through the highly structured region of Cook and Metzger[29] and is in general agreement with the overall contour of their data. From 742 Å to 870 Å the cross sections are densely structured and we used a least squares fit to the absorption data, region by region, to give a smooth overall profile which joins Samson's[35] data at 742 Å. The absorption profile in the 870-1030 Å region is marked by wider, well-separated peaks and we used Huffman's[25] data to fit a superposition of background and peak cross sections, σ_b and σ_p as described for N_2. Our photoabsorption cross sections for O_2 from 50-350 Å are consistent with the recent measurements of Mehlman, Ederer and Saloman[36], Cole and Dexter[9], and of Samson et al.[35]

Photoionization cross sections from 670 Å to 745 Å were obtained by a smooth fit to the ionization measurements of Samson et al.[35] which gives a curve similar in shape to

the overall profile of the earlier Cook and Metzger[29] results. The Samson measurements are 50%-60% higher than the Cook and Metzger data over much of this region; from 745 Å longward the two sets of data are in harmony. From 745 Å to 870 Å we used a least squares fit to the highly structured data of Cook and Metzger and in the region 870-1030 Å we used Cook and Metzger[29] ionization data and total absorption cross sections to obtain ionization cross sections as described for N_2. At the solar lines listed in the reference spectrum we adopted the ionization and absorption cross sections listed in Huffman[25], as discussed for N_2.

From the photionization threshold at 1027 Å to the dissociative ionization threshold at 662 Å we have used the branching ratios for production of O_2^+ electronic states given by Samson, Gardner and Haddad[35] and listed in Table D. In the region 304 Å-662 Å, Fryar and Browning[32] have measured the total cross section for dissociative ionization and obtained values which exceed the sum of the partial cross sections of five predissociating O_2^+ states (labeled 4-8 in Table D) measured by Samson et al.[35] To reconcile this difference we include an additional predissociating branch (labeled 9 in Table D) with threshold at 662 Å. The addition of the branch made renormalization of the other branching ratios necessary. As no measurements have been reported for

wavelengths shorter than 304 Å we assumed constant branching ratios from 304 Å to 34 Å. Branching ratios at any wavelength from 34 Å to 1027 Å can be obtained by linear interpolation of the values in Table D. At each wavelength branching ratios sum to unity and the partial cross sections are obtained by multiplying the total cross section by the relevant branching ratio.

Acknowledgement

We thank Professor A. Dalgarno for a critical reading of the manuscript. This work was partly supported by NASA and partly by the Air Force Geophysics Laboratory.

REFERENCES

1. A.O. Nier, W.E. Potter, D.R. Hickman, and K. Mauersberger, Radio Sci. 8, 271 (1973).
2. D.T. Pelz, C.A. Reber, A.E. Hedin, and G.R. Carignan, Radio Sci. 8, 277 (1973).
3. H. Hinteregger, J. Atmos. Terr. Phys. 38, 791 (1976).
4. L. Heroux and H.E. Hinteregger, J. Geophys. Res. 83, 5305, (1978).
5. R.D. Hudson and V.L. Carter, Can. J. Chem. 47, 1840 (1969).
6. H.E. Hinteregger, D.E. Bedo, and J.E. Manson, Radio Sci. 8, 349 (1973).
7. L. Heroux and J.E. Higgins, J. Geophys. Res. 82, 3307 (1977).
8. J.E. Manson, J. Geophys. Res. 81, 1629 (1976).
9. B.E. Cole and R.N. Dexter, J. Phys. B. 11, 1011 (1978).
10. V. Jacobs, Phys. Rev. A3, 289 (1971).
11. A.L. Stewart, J. Phys. B 11, 2449 (1978).
12. J.A.R. Samson, Phys. Rep. 28C, 303 (1976).
13. J.B. West and G.V. Marr, Proc. Roy. Soc. A349, 397 (1976).
14. H. Doyle, M. Oppenheimer, and A. Dalgarno, Phys. Rev. A 11, 909 (1975).
15. R.J.W. Henry, Ap. J. 161, 1153 (1970).
16. K.T. Taylor and P.G. Burke, J. Phys. B. 9, L353 (1976).
17. J.L. Kohl, G.P. Lafyatis, H.P. Palenius, and W.H. Parkinson, Phys. Rev. A18, 571, 1978.
18. A.K. Pradhan and H.E. Saraph, J. Phys. B 10, 3365 (1977).
19. A. Dalgarno, R.J.W. Henry, and A.L. Stewart, Plan. Sp. Sci. 12, 235 (1964).

20. R.J.W. Henry, Plan. Sp. Sci. 15, 1747 (1967).

21. J.L. Dehmer and P.M. Dehmer, J. Chem. Phys. 67, 1782 (1977).

22. L.C. Lee, R.W. Carlson, D.L. Judge, and M. Ogawa, J. Quant. Spectr. Rad. Tran. 13, 1023 (1973).

23. A. Hamnet, W. Stoll and C.E. Brion, J. El. Spectr. and Rel. Phen. 8, 367 (1976).

24. P. Gurtler, V. Saile, and E.E. Koch, Chem. Phys. Lett. 48, 245 (1977).

25. R.E. Huffman, Can. J. Chem. 47, 1823 (1969).

26. J.A.R. Samson, G.N. Haddad, and J.L. Gardner, J. Phys. B. 10, 1749 (1977).

27. V. Carter, J. Chem. Phys. 56, 4195 (1972).

28. R.E. Huffman, Y. Tanaka, and J.C. Larrabee, J. Chem. Phys. 39, 910 (1963).

29. G.R. Cook and P.H. Metzger, J. Chem. Phys. 41, 321 (1964).

30. J.A.R. Samson and R.B. Cairns, F. Geophys. Res. 69, 4583 (1964).

31. G.R. Wight, M.J. Van der Wiel, and C.E. Brion, J. Phys. B. 9, 675 (1976).

32. J. Fryar and R. Browning, Plan. Sp. Sci. 21, 709 (1973).

33. E.W. Plummer, T. Gustafson, W. Gudat and D.E. Eastman, Phys. Rev. A 15, 2339 (1977).

34. L.C. Lee, J. Phys. B. 10, 3033 (1977).

35. J.A.R. Samson, J.L. Gardner and G.N. Haddad, J. El. Spectr. and Rel. Phen. 12, 281 (1977).

36. G. Mehlman, D.L. Ederer, and E.B. Saloman, J. Chem. Phys. 68, 1862 (1978).

37. M. Cohen and A. Dalgarno, Proc. Roy. Soc. A 280, 258 (1964).

Explanation of Table 1.

Photoionization and Photoabsorption Cross Sections for O, He, N_2 and O_2

All cross sections are in units of 10^{-18} cm^2.

Before using the table, it is advisable to read Section II.

LAMBDA — Wavelength in angstroms for which the solar flux is given by Hinteregger[3].

O+(4S), O+(2D), O+(2P) — Cross sections for photoionization of a 2p valence electron of atomic oxygen giving the ground state $O^+(^4S^o)$ or excited states $O^+(^2D^o)$ or $O^+(^2P^o)$.

O+(4P), O+(2P*) — Cross sections for photoionization of a 2s electron to give $O^+(^4P^e)$ or $O^+(^2P^e)$. The * indicates $^2P^e$ rather than $^2P^o$.

TOT.O+ — Oxygen <u>total</u> <u>photoionization</u> cross section.

N2(ABS), O2(ABS) — Total <u>photoabsorption</u> cross sections for N_2 and O_2 respectively. These are cross sections for ionization, dissociation, and transitions to excited vibrational and rotational levels.

N2(ION), O2(ION) — Total <u>photoionization</u> cross sections of N_2 and O_2 respectively.

Table A

Ion production rates in s^{-1} calculated using the tabulated cross sections and the Hinteregger solar flux from 1030 Å to 32 Å in an optically thin atmosphere

Ion	Rate
He^+	4.84×10^{-8}
$O^+(^4S^o)$	1.23×10^{-7}
$O^+(^2D^o)$	9.29×10^{-8}
$O^+(^2P^o)$	5.42×10^{-8}
$N_2^+(X^2\Sigma_g^+)$	3.08×10^{-7}
N^+ [a]	3.98×10^{-8}
$O_2^+(X^2\Pi_g)$	2.64×10^{-7}
$O_2^+(a^4\Pi_u)$	1.54×10^{-7}
O^+ [b]	8.70×10^{-8}

a) N^+ produced by dissociative ionization of N_2.

b) O^+ produced by dissociative ionization of O_2.

Table A: In constructing the table it has been assumed that any excited atomic and bound molecular states produced radiate to the lowest state to which they are corrected by a dipole transition. For example, the production rates for all the doublet excited states of O_2^+ are included in the production rate of $O_2^+(X^2\Pi_g)$. The excited $O^+(^4P^e)$ state decays to $O^+(^4S)$, while the $O^+(^2P^e)$ state radiates to $O^+(^2D^o)$ and $O^+(^2P^o)$ according to the branching ratio 2.59:1[37]. The ionization caused by absorption of these "secondary photons" has been neglected.

Table B

Fractional Yield for Dissociative Ionization of N_2*

λ (Å)	Yield
210	0.360
240	0.346
302	0.202
387*	0.033
477*	0.041
496	0.024
509	0.000

*See text

Table B: The cross section for dissociative ionization of N_2 at any wavelength from 32 Å to 509 Å is obtained by linear interpolation of the values for the yield, except from 387 Å to 477 Å where the formula in Section II should be used, and multiplying by the total ionization cross section.

Table C

Branching Ratios for the Photoionization of N_2
See text for sources

Branch	1	2	3	4	5
Designation	$X^2\Sigma_g^+$	$A^2\Pi_u$	$B^2\Sigma_u^+$	$F^2\Sigma_u$	$^2\Sigma_g^+$
λ(Å)	Branching Ratios				
210	0.271	0.275	0.110	0.064	0.278
240	0.271	0.345	0.110	0.064	0.210
280	0.271	0.470	0.095	0.040	0.124
300	0.271	0.470	0.110	0.074	0.075
332	0.300	0.520	0.120	0.060	0.000
428	0.460	0.460	0.080	0.000	
500	0.404	0.506	0.090		
600	0.308	0.589	0.103		
660	0.308	0.589	0.103		
660.01	0.308	0.692	0.000		
720	0.420	0.580			
747	1.000	0.000			
796	1.000				

Table C: From 796 Å to 509 Å, partial photoionization cross sections can be obtained by multiplying the total ionization cross section by the interpolated branching ratio. For wavelengths shorter than 509 Å, the cross section due to dissociative ionization must first be subtracted from the total ionization cross section.

Table D

Branching Ratios for the Photoionization of O_2
See text for sources

Branch	1	2	3	4	5	6	7	8	9
Designation	$X^2\Pi_g$	$a^4\Pi_u + A^2\Pi_u$	$b^4\Sigma_g^-$	$B^2\Sigma_g^-$	$^2\Pi_u$	$c^4\Sigma_u^-$	$^2\Sigma_u^-$	$^{2,4}\Sigma_g^-$	662 Å
λ (Å)	Branching Ratios								
304	0.365	0.205	0.125	0.055	0.060	0.035	0.030	0.125	0.000
323	0.374	0.210	0.124	0.055	0.060	0.035	0.030	0.000	0.112
454	0.432	0.243	0.120	0.055	0.060	0.035	0.000		0.055
461	0.435	0.245	0.120	0.055	0.060	0.035			0.050
504	0.384	0.270	0.126	0.079	0.026	0.000			0.115
537	0.345	0.290	0.130	0.098	0.000				0.137
556	0.356	0.230	0.225	0.109					0.080
573	0.365	0.270	0.216	0.119					0.030
584	0.306	0.330	0.210	0.125					0.030
598	0.230	0.295	0.375	0.058					0.045
610	0.235	0.385	0.305	0.000					0.075
637	0.245	0.350	0.370						0.036
645	0.340	0.305	0.330						0.025
662	0.270	0.385	0.345						0.000
684	0.482	0.518	0.000						
704	0.675	0.325							
720	0.565	0.435							
737	0.565	0.435							
774	1.000	0.000							
1026	1.000								

Table D: For molecular oxygen, the first three columns labeled $X^2\Pi_g$, $a^4\Pi_u + A^2\Pi_u$, and $b^4\Sigma_g^-$ give branching ratios to bound molecular ion states, while the last six columns represent dissociating ionic states. The sum of the branching ratios for the last six columns for wavelengths less than 662 Å multiplied by the total ionization cross section gives the total dissociative ionization cross section.

LAMBDA	O+(4S)	O+(2D)	O+(2P)	C+(4P)	C+(2P*)	C+(IC1)	HE	N2(ABS)	N2(ICN)	O2(ABS)	O2(ICN)
33.74	0.08	0.09	0.06	0.03	0.02	0.27	0.10	0.11	0.11	0.30	0.30
40.95	0.08	0.09	0.06	0.03	0.02	0.27	0.12	0.14	0.14	0.31	0.31
43.76	0.08	0.08	0.05	0.03	0.02	0.26	0.12	0.16	0.16	0.31	0.31
44.02	0.08	0.08	0.05	0.03	0.02	0.26	0.13	0.16	0.16	0.31	0.31
44.16	0.08	0.08	0.05	0.03	0.02	0.26	0.13	0.16	0.16	0.31	0.31
45.66	0.08	0.08	0.05	0.03	0.02	0.26	0.13	0.20	0.20	0.33	0.33
46.40	0.08	0.08	0.05	0.03	0.02	0.26	0.13	0.21	0.21	0.35	0.35
46.67	0.08	0.08	0.06	0.03	0.02	0.26	0.13	0.21	0.21	0.36	0.36
47.87	0.08	0.09	0.06	0.03	0.02	0.28	0.14	0.23	0.23	0.39	0.39
49.22	0.09	0.09	0.06	0.03	0.02	0.29	0.14	0.24	0.24	0.42	0.42
50.36	0.09	0.10	0.06	0.03	0.02	0.31	0.14	0.26	0.26	0.45	0.45
50.52	0.09	0.10	0.06	0.03	0.02	0.31	0.14	0.26	0.26	0.45	0.45
50.69	0.09	0.10	0.06	0.03	0.02	0.31	0.14	0.26	0.26	0.46	0.46
52.30	0.10	0.11	0.07	0.03	0.03	0.33	0.15	0.29	0.29	0.50	0.50
52.91	0.10	0.11	0.07	0.03	0.03	0.34	0.15	0.29	0.29	0.51	0.51
54.15	0.10	0.12	0.07	0.03	0.03	0.35	0.15	0.31	0.31	0.54	0.54
54.42	0.10	0.12	0.07	0.03	0.03	0.35	0.15	0.32	0.32	0.55	0.55
54.70	0.10	0.12	0.08	0.03	0.03	0.36	0.15	0.32	0.32	0.56	0.56
55.06	0.11	0.12	0.08	0.03	0.03	0.36	0.15	0.32	0.32	0.57	0.57
55.34	0.11	0.12	0.08	0.04	0.03	0.37	0.15	0.33	0.33	0.57	0.57
56.08	0.11	0.12	0.08	0.04	0.03	0.37	0.16	0.34	0.34	0.59	0.59
56.92	0.11	0.13	0.08	0.04	0.03	0.38	0.16	0.35	0.35	0.61	0.61
57.36	0.11	0.13	0.08	0.04	0.03	0.39	0.16	0.36	0.36	0.62	0.62
57.56	0.11	0.13	0.08	0.04	0.03	0.39	0.16	0.36	0.36	0.63	0.63
57.68	0.12	0.13	0.08	0.04	0.03	0.40	0.16	0.36	0.36	0.64	0.64
58.98	0.12	0.14	0.09	0.04	0.03	0.41	0.16	0.38	0.38	0.66	0.66
59.82	0.12	0.14	0.09	0.04	0.03	0.41	0.17	0.39	0.39	0.68	0.68
60.30	0.12	0.14	0.09	0.04	0.03	0.42	0.17	0.40	0.40	0.70	0.70
60.65	0.13	0.14	0.09	0.04	0.03	0.44	0.17	0.40	0.40	0.71	0.71
61.07	0.13	0.15	0.09	0.04	0.03	0.44	0.17	0.41	0.41	0.72	0.72
61.63	0.13	0.15	0.10	0.04	0.04	0.46	0.17	0.41	0.41	0.73	0.73
61.90	0.14	0.15	0.10	0.04	0.04	0.47	0.17	0.42	0.42	0.74	0.74
62.30	0.14	0.16	0.10	0.05	0.04	0.48	0.17	0.42	0.42	0.75	0.75
62.35	0.14	0.16	0.10	0.05	0.04	0.48	0.17	0.42	0.42	0.75	0.75
62.77	0.14	0.16	0.10	0.05	0.04	0.49	0.17	0.43	0.43	0.76	0.76
62.92	0.14	0.16	0.10	0.05	0.04	0.49	0.17	0.43	0.43	0.76	0.76
63.16	0.15	0.16	0.10	0.05	0.04	0.50	0.17	0.44	0.44	0.77	0.77
63.30	0.15	0.17	0.10	0.05	0.04	0.50	0.17	0.44	0.44	0.77	0.77
63.65	0.15	0.17	0.11	0.05	0.04	0.51	0.18	0.44	0.44	0.78	0.78
63.72	0.15	0.17	0.11	0.05	0.04	0.52	0.18	0.44	0.44	0.78	0.78

[illegible]	[illegible]	[illegible]	0.11	0.05	0.04	0.53	0.18	0.45	0.45	0.79	0.79
[illegible]	0.15	0.18	0.11	0.05	0.04	0.54	0.18	0.46	0.46	0.81	0.81
65.21	0.15	0.16	0.12	0.05	0.04	0.56	0.18	0.46	0.46	0.82	0.82
65.71	0.17	0.19	0.12	0.05	0.04	0.57	0.18	0.47	0.47	0.83	0.83
65.85	0.17	0.19	0.12	0.05	0.04	0.57	0.18	0.47	0.47	0.84	0.84
66.30	0.17	0.19	0.12	0.06	0.05	0.59	0.18	0.48	0.48	0.85	0.85
67.14	0.18	0.20	0.13	0.06	0.05	0.61	0.19	0.49	0.49	0.87	0.87
67.35	0.18	0.20	0.13	0.06	0.05	0.62	0.19	0.49	0.49	0.87	0.87
68.35	0.19	0.21	0.13	0.06	0.05	0.64	0.19	0.50	0.50	0.91	0.91
69.85	0.20	0.22	0.14	0.06	0.05	0.66	0.19	0.52	0.52	0.95	0.95
70.00	0.20	0.22	0.14	0.07	0.05	0.69	0.19	0.52	0.52	0.96	0.96
70.54	0.21	0.23	0.15	0.07	0.05	0.70	0.19	0.53	0.53	0.98	0.98
70.75	0.21	0.23	0.15	0.07	0.05	0.71	0.19	0.53	0.53	0.98	0.98
71.00	0.21	0.23	0.15	0.07	0.05	0.71	0.19	0.53	0.53	0.99	0.99
71.94	0.22	0.24	0.16	0.07	0.06	0.74	0.20	0.54	0.54	1.01	1.01
72.31	0.22	0.24	0.16	0.07	0.06	0.75	0.20	0.55	0.55	1.02	1.02
72.63	0.22	0.24	0.16	0.07	0.06	0.76	0.20	0.55	0.55	1.03	1.03
72.80	0.23	0.24	0.16	0.07	0.06	0.76	0.20	0.55	0.55	1.04	1.04
72.95	0.23	0.25	0.16	0.07	0.06	0.77	0.20	0.55	0.55	1.04	1.04
73.55	0.23	0.25	0.16	0.08	0.06	0.78	0.20	0.56	0.56	1.06	1.06
74.21	0.24	0.26	0.17	0.08	0.06	0.80	0.20	0.57	0.57	1.08	1.08
74.44	0.24	0.26	0.17	0.08	0.06	0.81	0.20	0.57	0.57	1.08	1.08
74.83	0.24	0.26	0.17	0.08	0.06	0.82	0.20	0.57	0.57	1.10	1.10
75.03	0.25	0.26	0.17	0.08	0.06	0.82	0.20	0.57	0.57	1.10	1.10
75.29	0.25	0.27	0.18	0.08	0.06	0.84	0.21	0.58	0.58	1.11	1.11
75.46	0.25	0.27	0.18	0.08	0.06	0.84	0.21	0.58	0.58	1.11	1.11
75.73	0.25	0.27	0.18	0.08	0.07	0.86	0.21	0.58	0.58	1.12	1.12
76.01	0.26	0.28	0.18	0.08	0.07	0.87	0.21	0.59	0.59	1.13	1.13
76.48	0.26	0.28	0.19	0.09	0.07	0.89	0.21	0.59	0.59	1.14	1.14
76.83	0.27	0.29	0.19	0.09	0.07	0.91	0.21	0.59	0.59	1.15	1.15
76.94	0.27	0.29	0.19	0.09	0.07	0.91	0.21	0.60	0.60	1.15	1.15
77.30	0.28	0.30	0.19	0.09	0.07	0.93	0.21	0.60	0.60	1.16	1.16
77.74	0.28	0.30	0.20	0.09	0.07	0.95	0.21	0.60	0.60	1.18	1.18
78.56	0.29	0.31	0.21	0.09	0.08	0.99	0.21	0.61	0.61	1.20	1.20
78.70	0.30	0.32	0.21	0.10	0.08	1.00	0.22	0.61	0.61	1.20	1.20
79.08	0.30	0.32	0.21	0.10	0.08	1.01	0.22	0.62	0.62	1.21	1.21
79.48	0.31	0.33	0.22	0.10	0.08	1.03	0.22	0.62	0.62	1.23	1.23
79.76	0.31	0.33	0.22	0.10	0.08	1.04	0.22	0.63	0.63	1.23	1.23
80.00	0.31	0.34	0.22	0.10	0.08	1.05	0.22	0.63	0.63	1.24	1.24
80.21	0.32	0.34	0.22	0.10	0.08	1.07	0.22	0.63	0.63	1.25	1.25

LAMBDA	O+(4S)	O+(2D)	O+(2P)	C+(4P)	C+(2P*)	C+(1CT)	HE	N2(ABS)	N2(ICN)	O2(ABS)	O2(ICN)
80.55	0.32	0.34	0.23	0.10	0.08	1.08	0.22	0.63	0.63	1.25	1.25
80.94	0.33	0.35	0.23	0.11	0.08	1.10	0.22	0.64	0.64	1.27	1.27
81.16	0.33	0.35	0.23	0.11	0.09	1.11	0.22	0.64	0.64	1.27	1.27
81.58	0.34	0.36	0.24	0.11	0.09	1.13	0.22	0.64	0.64	1.28	1.28
81.94	0.34	0.37	0.24	0.11	0.09	1.14	0.22	0.65	0.65	1.29	1.29
82.43	0.35	0.37	0.25	0.11	0.09	1.17	0.22	0.65	0.65	1.31	1.31
82.67	0.35	0.38	0.25	0.11	0.09	1.18	0.22	0.66	0.66	1.32	1.32
83.25	0.36	0.38	0.25	0.12	0.09	1.21	0.23	0.66	0.66	1.33	1.33
83.42	0.36	0.39	0.25	0.12	0.09	1.21	0.23	0.66	0.66	1.34	1.34
83.67	0.37	0.39	0.26	0.12	0.09	1.23	0.23	0.67	0.67	1.34	1.34
84.00	0.37	0.40	0.26	0.12	0.09	1.24	0.23	0.67	0.67	1.35	1.35
84.26	0.37	0.40	0.26	0.12	0.10	1.25	0.23	0.67	0.67	1.36	1.36
84.50	0.38	0.40	0.27	0.12	0.10	1.26	0.23	0.68	0.68	1.37	1.37
84.72	0.38	0.41	0.27	0.12	0.10	1.27	0.23	0.68	0.68	1.37	1.37
84.96	0.38	0.41	0.27	0.12	0.10	1.28	0.23	0.68	0.68	1.38	1.38
85.16	0.39	0.41	0.27	0.13	0.10	1.29	0.23	0.68	0.68	1.38	1.38
85.50	0.39	0.42	0.28	0.13	0.10	1.31	0.23	0.69	0.69	1.39	1.39
85.69	0.39	0.42	0.28	0.13	0.10	1.32	0.23	0.69	0.69	1.40	1.40
85.87	0.40	0.42	0.28	0.13	0.10	1.33	0.23	0.69	0.69	1.40	1.40
86.23	0.40	0.43	0.28	0.13	0.10	1.35	0.23	0.69	0.69	1.41	1.41
86.40	0.40	0.43	0.28	0.13	0.10	1.35	0.23	0.70	0.70	1.42	1.42
86.77	0.41	0.44	0.29	0.13	0.10	1.37	0.24	0.70	0.70	1.43	1.43
86.98	0.41	0.44	0.29	0.13	0.11	1.38	0.24	0.70	0.70	1.43	1.43
87.30	0.42	0.44	0.29	0.13	0.11	1.39	0.24	0.70	0.70	1.44	1.44
87.61	0.42	0.45	0.30	0.14	0.11	1.41	0.24	0.71	0.71	1.45	1.45
88.10	0.43	0.46	0.30	0.14	0.11	1.43	0.24	0.71	0.71	1.47	1.47
88.11	0.43	0.46	0.30	0.14	0.11	1.43	0.24	0.71	0.71	1.47	1.47
88.14	0.43	0.46	0.30	0.14	0.11	1.43	0.24	0.71	0.71	1.47	1.47
88.42	0.43	0.46	0.30	0.14	0.11	1.45	0.24	0.72	0.72	1.48	1.48
88.64	0.43	0.46	0.31	0.14	0.11	1.46	0.24	0.72	0.72	1.48	1.48
88.90	0.44	0.47	0.31	0.14	0.11	1.47	0.24	0.72	0.72	1.49	1.49
89.14	0.44	0.47	0.31	0.14	0.11	1.48	0.24	0.73	0.73	1.50	1.50
89.70	0.45	0.48	0.32	0.14	0.12	1.51	0.24	0.73	0.73	1.51	1.51
90.14	0.46	0.49	0.32	0.15	0.12	1.53	0.24	0.74	0.74	1.52	1.52
90.45	0.46	0.49	0.32	0.15	0.12	1.54	0.25	0.74	0.74	1.53	1.53
90.71	0.46	0.50	0.33	0.15	0.12	1.56	0.25	0.74	0.74	1.54	1.54
91.00	0.47	0.50	0.33	0.15	0.12	1.57	0.00	0.75	0.75	1.55	1.55
91.48	0.48	0.51	0.34	0.15	0.12	1.60	0.25	0.75	0.75	1.56	1.56
91.69	0.48	0.51	0.34	0.16	0.12	1.61	0.25	0.75	0.75	1.57	1.57
91.81	0.48	0.51	0.34	0.16	0.12	1.61	0.25	0.75	0.75	1.57	1.57

92.09	0.49	0.52	0.34	0.16	0.13	1.63	0.25	0.76	0.76	1.58	1.58
92.55	0.49	0.53	0.35	0.16	0.13	1.65	0.25	0.76	0.76	1.59	1.59
92.81	0.50	0.53	0.35	0.16	0.13	1.67	0.25	0.76	0.76	1.60	1.60
93.61	0.51	0.54	0.36	0.16	0.13	1.71	0.25	0.77	0.77	1.62	1.62
94.07	0.52	0.55	0.36	0.17	0.13	1.73	0.25	0.78	0.78	1.63	1.63
94.25	0.52	0.55	0.37	0.17	0.13	1.74	0.25	0.78	0.78	1.64	1.64
94.39	0.52	0.56	0.37	0.17	0.13	1.75	0.25	0.78	0.78	1.64	1.64
94.81	0.53	0.56	0.37	0.17	0.14	1.77	0.26	0.79	0.79	1.65	1.65
94.90	0.53	0.56	0.37	0.17	0.14	1.77	0.26	0.79	0.79	1.66	1.66
95.37	0.54	0.57	0.38	0.17	0.14	1.80	0.26	0.79	0.79	1.67	1.67
95.51	0.54	0.57	0.38	0.17	0.14	1.81	0.26	0.79	0.79	1.67	1.67
95.81	0.54	0.58	0.38	0.17	0.14	1.82	0.26	0.80	0.80	1.68	1.68
96.05	0.55	0.58	0.39	0.18	0.14	1.83	0.26	0.80	0.80	1.69	1.69
96.49	0.55	0.59	0.39	0.18	0.14	1.86	0.26	0.80	0.80	1.70	1.70
96.83	0.56	0.60	0.39	0.18	0.14	1.87	0.26	0.81	0.81	1.71	1.71
97.12	0.56	0.60	0.40	0.18	0.14	1.89	0.26	0.81	0.81	1.72	1.72
97.51	0.57	0.61	0.40	0.18	0.15	1.91	0.26	0.81	0.81	1.73	1.73
97.87	0.57	0.61	0.41	0.19	0.15	1.93	0.26	0.82	0.82	1.74	1.74
98.12	0.58	0.62	0.41	0.19	0.15	1.94	0.26	0.82	0.82	1.75	1.75
98.23	0.58	0.62	0.41	0.19	0.15	1.95	0.26	0.82	0.82	1.75	1.7[illegible]
98.50	0.58	0.63	0.41	0.19	0.15	1.96	0.27	0.82	0.82	1.76	1.76
98.88	0.59	0.63	0.42	0.19	0.15	1.98	0.27	0.83	0.83	1.77	1.77
99.44	0.60	0.64	0.42	0.19	0.15	2.01	0.27	0.83	0.83	1.78	1.78
99.71	0.60	0.64	0.43	0.19	0.15	2.02	0.27	0.84	0.84	1.79	1.79
99.99	0.61	0.65	0.43	0.20	0.16	2.04	0.27	0.84	0.84	1.80	1.80
100.54	0.62	0.66	0.44	0.20	0.16	2.07	0.28	0.87	0.87	1.84	1.84
100.96	0.62	0.67	0.44	0.20	0.16	2.09	0.28	0.89	0.89	1.86	1.86
101.57	0.63	0.68	0.45	0.20	0.16	2.12	0.28	0.93	0.93	1.90	1.90
102.15	0.64	0.69	0.45	0.21	0.16	2.15	0.29	0.96	0.96	1.94	1.94
103.01	0.65	0.70	0.46	0.21	0.17	2.19	0.30	1.01	1.01	2.00	2.00
103.15	0.66	0.70	0.46	0.21	0.17	2.20	0.30	1.01	1.01	2.01	2.01
103.17	0.66	0.70	0.46	0.21	0.17	2.20	0.30	1.02	1.02	2.01	2.01
103.58	0.66	0.71	0.47	0.21	0.17	2.22	0.31	1.04	1.04	2.04	2.04
103.94	0.67	0.71	0.47	0.22	0.17	2.24	0.31	1.06	1.06	2.06	2.06
104.23	0.67	0.72	0.47	0.22	0.17	2.26	0.31	1.08	1.08	2.08	2.08
104.76	0.68	0.73	0.48	0.22	0.17	2.29	0.32	1.11	1.11	2.11	2.11
105.23	0.69	0.74	0.49	0.22	0.18	2.31	0.32	1.13	1.13	2.14	2.14
106.25	0.71	0.76	0.50	0.23	0.18	2.37	0.33	1.19	1.19	2.21	2.21
106.57	0.71	0.76	0.50	0.23	0.18	2.39	0.33	1.21	1.21	2.23	2.23
106.93	0.72	0.77	0.51	0.23	0.18	2.42	0.34	1.23	1.23	2.26	2.26

LAMBDA	O+(4S)	O+(2D)	O+(2P)	C+(4P)	C+(2P*)	C+(1CT)	HE	N2(ABS)	N2(ION)	O2(ABS)	O2(ION)
108.05	0.74	0.79	0.52	0.24	0.19	2.49	0.35	1.29	1.29	2.33	2.33
108.46	0.75	0.80	0.53	0.24	0.19	2.51	0.35	1.31	1.31	2.36	2.36
109.50	0.77	0.82	0.54	0.25	0.20	2.58	0.36	1.37	1.37	2.43	2.43
109.98	0.78	0.83	0.55	0.25	0.20	2.61	0.37	1.39	1.39	2.46	2.46
110.56	0.79	0.84	0.56	0.25	0.20	2.64	0.37	1.43	1.43	2.50	2.50
110.62	0.79	0.84	0.56	0.25	0.20	2.65	0.37	1.43	1.43	2.50	2.50
110.76	0.79	0.85	0.56	0.25	0.20	2.66	0.38	1.44	1.44	2.51	2.51
111.15	0.80	0.85	0.56	0.26	0.20	2.68	0.38	1.46	1.46	2.54	2.54
111.25	0.80	0.86	0.56	0.26	0.20	2.69	0.38	1.47	1.47	2.54	2.54
113.60	0.85	0.91	0.60	0.27	0.22	2.85	0.40	1.61	1.61	2.71	2.71
114.09	0.86	0.91	0.60	0.28	0.22	2.87	0.41	1.62	1.62	2.73	2.73
114.24	0.86	0.92	0.61	0.28	0.22	2.87	0.41	1.63	1.63	2.74	2.74
115.39	0.88	0.94	0.62	0.28	0.22	2.95	0.42	1.70	1.70	2.82	2.82
115.82	0.89	0.95	0.63	0.29	0.23	2.97	0.42	1.72	1.72	2.84	2.84
116.75	0.90	0.97	0.64	0.29	0.23	3.03	0.43	1.77	1.77	2.90	2.90
117.20	0.91	0.98	0.64	0.29	0.23	3.06	0.44	1.80	1.80	2.93	2.93
120.40	0.97	1.04	0.69	0.31	0.25	3.26	0.47	1.97	1.97	3.15	3.15
121.15	0.99	1.05	0.70	0.32	0.25	3.31	0.48	2.02	2.02	3.20	3.20
121.79	1.00	1.07	0.70	0.32	0.26	3.35	0.48	2.05	2.05	3.24	3.24
122.70	1.01	1.09	0.72	0.33	0.26	3.40	0.49	2.10	2.10	3.30	3.30
123.50	1.03	1.10	0.73	0.33	0.26	3.45	0.50	2.15	2.15	3.35	3.35
127.65	1.11	1.18	0.78	0.36	0.28	3.71	0.54	2.38	2.38	3.63	3.63
129.87	1.13	1.22	0.81	0.37	0.29	3.82	0.56	2.50	2.50	3.77	3.77
130.30	1.14	1.23	0.81	0.37	0.29	3.84	0.56	2.47	2.47	3.92	3.92
131.02	1.15	1.24	0.82	0.37	0.30	3.88	0.57	2.51	2.51	3.96	3.96
131.21	1.15	1.24	0.82	0.37	0.30	3.88	0.57	2.52	2.52	3.97	3.97
136.21	1.21	1.33	0.88	0.40	0.32	4.12	0.62	2.79	2.79	4.26	4.26
136.28	1.21	1.33	0.88	0.40	0.32	4.13	0.62	2.79	2.79	4.27	4.27
136.34	1.21	1.33	0.88	0.40	0.32	4.13	0.62	2.80	2.80	4.27	4.27
136.45	1.21	1.33	0.88	0.40	0.32	4.14	0.62	2.80	2.80	4.28	4.28
136.48	1.21	1.33	0.88	0.40	0.32	4.14	0.63	2.80	2.80	4.28	4.28
144.21	1.30	1.46	0.96	0.43	0.35	4.51	0.70	3.25	3.25	4.79	4.79
145.00	1.31	1.48	0.97	0.44	0.35	4.55	0.71	3.29	3.29	4.85	4.85
148.38	1.35	1.53	1.01	0.45	0.36	4.71	0.75	3.50	3.50	5.09	5.09
150.10	1.37	1.56	1.02	0.46	0.37	4.79	0.76	3.61	3.61	5.21	5.21
152.15	1.39	1.59	1.04	0.47	0.38	4.87	0.78	3.73	3.73	5.34	5.34
152.84	1.39	1.60	1.05	0.47	0.38	4.89	0.79	3.78	3.78	5.38	5.38
154.28	1.40	1.62	1.06	0.47	0.38	4.94	0.80	3.86	3.86	5.46	5.46
157.73	1.43	1.67	1.09	0.49	0.39	5.07	0.83	4.07	4.07	5.66	5.66
158.38	1.44	1.68	1.10	0.49	0.40	5.10	0.84	4.11	4.11	5.70	5.70

159.94	1.45	1.70	1.11	0.50	0.40	5.16	0.85	4.20	4.20	5.80	5.80
161.13	1.46	1.76	1.15	0.51	0.41	5.31	0.88	4.42	4.42	6.08	6.08
167.50	1.51	1.80	1.18	0.52	0.43	5.44	0.90	4.61	4.61	6.32	6.32
168.17	1.51	1.81	1.18	0.53	0.43	5.46	0.91	4.64	4.64	6.37	6.37
168.55	1.52	1.82	1.19	0.53	0.43	5.48	0.91	4.66	4.66	6.40	6.40
168.92	1.52	1.82	1.19	0.53	0.43	5.49	0.91	4.69	4.69	6.42	6.42
171.06	1.54	1.85	1.21	0.54	0.44	5.57	0.93	4.81	4.81	6.58	6.58
172.12	1.55	1.87	1.22	0.54	0.44	5.61	0.93	4.88	4.88	6.65	6.65
172.92	1.55	1.88	1.23	0.54	0.44	5.64	0.94	4.93	4.93	6.71	6.71
173.10	1.55	1.88	1.23	0.54	0.44	5.65	0.94	4.94	4.94	6.72	6.72
174.53	1.57	1.90	1.24	0.55	0.45	5.70	0.95	5.04	5.04	6.82	6.82
175.24	1.57	1.91	1.25	0.55	0.45	5.73	0.96	5.08	5.08	6.87	6.87
175.47	1.57	1.91	1.25	0.55	0.45	5.74	0.96	5.10	5.10	6.89	6.89
177.22	1.59	1.94	1.26	0.56	0.46	5.80	0.97	5.22	5.22	7.01	7.01
178.02	1.59	1.95	1.27	0.56	0.46	5.83	0.98	5.27	5.27	7.06	7.06
179.74	1.61	1.97	1.29	0.57	0.46	5.89	0.99	5.38	5.38	7.18	7.18
180.40	1.61	1.98	1.29	0.57	0.47	5.92	1.00	5.37	5.37	7.22	7.22
180.71	1.61	1.99	1.30	0.57	0.47	5.93	1.00	5.38	5.38	7.24	7.24
181.14	1.62	1.99	1.30	0.57	0.47	5.95	1.00	5.40	5.40	7.27	7.27
182.16	1.62	2.01	1.31	0.58	0.47	5.98	1.01	5.45	5.45	7.33	7.33
182.39	1.63	2.01	1.31	0.58	0.47	5.99	1.01	5.45	5.45	7.34	7.34
183.91	1.64	2.03	1.32	0.58	0.47	6.05	1.03	5.52	5.52	7.44	7.44
184.10	1.64	2.03	1.33	0.59	0.47	6.06	1.03	5.53	5.53	7.45	7.45
184.57	1.64	2.04	1.33	0.59	0.47	6.07	1.03	5.55	5.55	7.47	7.47
184.76	1.64	2.04	1.33	0.59	0.47	6.08	1.04	5.56	5.56	7.49	7.49
185.21	1.65	2.05	1.34	0.59	0.48	6.10	1.04	5.58	5.58	7.52	7.52
186.60	1.66	2.07	1.35	0.60	0.48	6.15	1.05	5.64	5.64	7.60	7.60
186.87	1.66	2.07	1.35	0.60	0.48	6.16	1.06	5.65	5.65	7.62	7.62
188.23	1.67	2.09	1.36	0.60	0.48	6.21	1.07	5.71	5.71	7.70	7.70
188.70	1.67	2.10	1.37	0.60	0.48	6.22	1.08	5.74	5.74	7.72	7.72
190.00	1.68	2.11	1.38	0.61	0.49	6.27	1.09	5.80	5.80	7.80	7.80
191.29	1.69	2.13	1.39	0.62	0.49	6.32	1.11	5.87	5.87	7.87	7.87
192.38	1.70	2.15	1.40	0.62	0.49	6.36	1.13	5.93	5.93	7.93	7.93
192.60	1.71	2.15	1.40	0.62	0.49	6.37	1.13	5.95	5.95	7.96	7.96
193.50	1.71	2.16	1.41	0.62	0.50	6.40	1.14	5.99	5.99	8.00	8.00
195.14	1.72	2.19	1.42	0.63	0.50	6.46	1.16	6.09	6.09	8.09	8.09
195.63	1.73	2.21	1.44	0.64	0.50	6.51	1.19	6.18	6.18	8.18	8.18
197.41	1.74	2.22	1.44	0.64	0.50	6.54	1.20	6.23	6.23	8.23	8.23
198.53	1.75	2.23	1.45	0.64	0.51	6.58	1.22	6.30	6.30	8.30	8.30
200.00	1.76	2.25	1.47	0.65	0.51	6.64	1.24	6.40	6.40	8.40	8.40

LAMBDA	O+(4S)	O+(2D)	O+(2P)	C+(4P)	C+(2P*)	C+(ICT)	HE	N2(ABS)	N2(ICN)	O2(ABS)	O2(ICN)
201.10	1.77	2.27	1.48	0.65	0.51	6.68	1.26	6.48	6.48	8.48	8.48
202.64	1.78	2.29	1.49	0.66	0.51	6.73	1.29	6.59	6.59	8.60	8.60
203.78	1.79	2.31	1.50	0.66	0.52	6.77	1.31	6.67	6.67	8.69	8.69
204.89	1.79	2.32	1.51	0.67	0.52	6.81	1.34	6.75	6.75	8.78	8.78
206.26	1.80	2.34	1.52	0.67	0.52	6.86	1.36	6.85	6.85	8.90	8.90
206.38	1.80	2.34	1.52	0.67	0.52	6.86	1.37	6.85	6.85	8.91	8.91
207.46	1.81	2.36	1.53	0.68	0.52	6.90	1.39	6.93	6.93	9.00	9.00
208.33	1.82	2.37	1.54	0.68	0.52	6.93	1.41	6.99	6.99	9.07	9.07
209.63	1.83	2.39	1.55	0.69	0.53	6.98	1.44	7.08	7.08	9.17	9.17
209.78	1.83	2.39	1.55	0.69	0.53	6.98	1.44	7.09	7.09	9.18	9.18
209.93	1.83	2.39	1.55	0.69	0.53	6.99	1.45	7.09	7.09	9.19	9.19
211.32	1.84	2.41	1.56	0.69	0.53	7.04	1.48	7.16	7.18	9.30	9.30
212.15	1.85	2.42	1.57	0.69	0.53	7.07	1.50	7.23	7.23	9.36	9.36
214.75	1.87	2.46	1.59	0.70	0.54	7.16	1.55	7.39	7.39	9.54	9.54
215.16	1.87	2.46	1.60	0.71	0.54	7.17	1.56	7.41	7.41	9.56	9.56
216.90	1.88	2.49	1.61	0.71	0.54	7.23	1.59	7.51	7.51	9.68	9.68
218.21	1.89	2.51	1.62	0.72	0.54	7.28	1.61	7.59	7.59	9.77	9.77
219.09	1.90	2.52	1.63	0.72	0.54	7.31	1.62	7.64	7.64	9.84	9.84
220.08	1.90	2.53	1.64	0.73	0.54	7.34	1.63	7.70	7.70	9.91	9.91
221.26	1.91	2.55	1.65	0.73	0.55	7.38	1.64	7.78	7.78	9.99	9.99
221.51	1.91	2.55	1.65	0.73	0.55	7.39	1.64	7.80	7.80	10.0	10.0
223.26	1.93	2.57	1.67	0.73	0.55	7.45	1.66	7.92	7.92	10.1	10.1
223.72	1.93	2.58	1.67	0.73	0.55	7.46	1.67	7.95	7.95	10.2	10.2
224.81	1.94	2.60	1.68	0.74	0.55	7.50	1.68	8.03	8.03	10.3	10.3
225.12	1.94	2.60	1.68	0.74	0.55	7.51	1.68	8.05	8.05	10.3	10.3
227.01	1.95	2.63	1.70	0.74	0.55	7.57	1.70	8.19	8.19	10.5	10.5
227.47	1.96	2.63	1.70	0.74	0.55	7.58	1.70	8.22	8.22	10.5	10.5
228.79	1.97	2.65	1.71	0.75	0.55	7.63	1.72	8.31	8.31	10.6	10.6
230.65	1.98	2.67	1.73	0.75	0.55	7.69	1.75	8.44	8.44	10.8	10.8
231.55	1.98	2.69	1.74	0.75	0.55	7.72	1.76	8.51	8.51	10.8	10.8
232.60	1.99	2.70	1.75	0.76	0.55	7.75	1.78	8.57	8.57	10.9	10.9
233.64	2.00	2.72	1.76	0.76	0.55	7.79	1.80	8.65	8.65	11.0	11.0
234.38	2.00	2.73	1.76	0.76	0.56	7.81	1.81	8.69	8.69	11.1	11.1
235.55	2.01	2.74	1.77	0.76	0.56	7.84	1.83	8.76	8.76	11.1	11.1
237.35	2.03	2.77	1.79	0.77	0.56	7.90	1.86	8.86	8.86	11.3	11.3
239.47	2.04	2.80	1.81	0.77	0.56	7.99	1.90	8.99	8.99	11.5	11.5
240.73	2.05	2.81	1.82	0.78	0.56	8.01	1.92	9.03	9.03	11.6	11.6
243.03	2.06	2.84	1.84	0.78	0.56	8.09	1.96	9.14	9.14	11.7	11.7
245.94	2.08	2.84	1.86	0.79	0.56	8.16	2.00	9.25	9.25	12.0	12.0
246.24	2.09	2.89	1.86	0.79	0.56	8.17	2.01	9.26	9.26	12.0	12.0

246.91	2.09	2.90	1.87	0.79	0.56	8.19	2.02	9.29	9.29	12.1	12.1
247.18	2.09	2.90	1.87	0.79	0.56	8.19	2.02	9.30	9.30	12.1	12.1
249.23	2.11	2.93	1.89	0.80	0.56	8.25	2.05	9.37	9.37	12.2	12.2
251.10	2.12	2.95	1.90	0.80	0.56	8.30	2.08	9.44	9.44	12.4	12.4
251.96	2.12	2.96	1.91	0.81	0.56	8.32	2.09	9.47	9.47	12.5	12.5
252.17	2.13	2.97	1.91	0.81	0.56	8.32	2.10	9.48	9.48	12.5	12.5
253.80	2.14	2.99	1.93	0.81	0.56	8.37	2.12	9.54	9.54	12.6	12.6
256.37	2.15	3.02	1.95	0.82	0.56	8.43	2.16	9.65	9.65	12.8	12.8
256.69	2.16	3.03	1.95	0.82	0.56	8.44	2.17	9.66	9.66	12.8	12.8
257.48	2.16	3.04	1.96	0.82	0.55	8.47	2.18	9.69	9.69	12.9	12.9
258.30	2.17	3.05	1.96	0.82	0.55	8.50	2.20	9.73	9.73	13.0	13.0
259.50	2.17	3.06	1.97	0.83	0.55	8.54	2.22	9.78	9.78	13.1	13.1
261.08	2.18	3.09	1.99	0.83	0.55	8.59	2.24	9.85	9.85	13.2	13.2
262.99	2.20	3.11	2.00	0.84	0.55	8.65	2.26	9.94	9.94	13.3	13.3
264.27	2.20	3.13	2.01	0.84	0.54	8.70	2.30	10.0	10.0	13.4	13.4
264.80	2.21	3.13	2.02	0.84	0.54	8.72	2.31	10.0	10.0	13.4	13.4
270.50	2.24	3.21	2.06	0.86	0.53	8.91	2.42	10.2	10.2	13.8	13.8
271.99	2.25	3.23	2.07	0.86	0.53	8.94	2.44	10.2	10.2	13.9	13.9
272.70	2.26	3.24	2.08	0.86	0.52	8.96	2.46	10.3	10.3	14.0	14.0
274.24	2.27	3.26	2.09	0.87	0.52	9.00	2.49	10.3	10.3	14.1	14.1
275.35	2.28	3.27	2.10	0.87	0.52	9.03	2.51	10.3	10.3	14.2	14.2
275.76	2.28	3.28	2.10	0.87	0.51	9.04	2.51	10.3	10.3	14.2	14.2
276.15	2.28	3.28	2.11	0.87	0.51	9.05	2.52	10.3	10.3	14.2	14.2
276.77	2.29	3.29	2.11	0.87	0.51	9.07	2.53	10.3	10.3	14.3	14.3
277.00	2.29	3.29	2.11	0.87	0.51	9.08	2.54	10.3	10.3	14.3	14.3
277.27	2.29	3.30	2.11	0.87	0.51	9.08	2.54	10.3	10.3	14.3	14.3
278.40	2.30	3.31	2.12	0.88	0.51	9.11	2.56	10.4	10.4	14.4	14.4
281.41	2.32	3.35	2.15	0.88	0.50	9.19	2.62	10.5	10.5	14.6	14.6
284.15	2.33	3.39	2.17	0.89	0.49	9.26	2.67	10.6	10.6	14.8	14.8
285.85	2.34	3.41	2.18	0.89	0.48	9.30	2.70	10.7	10.7	14.9	14.9
288.36	2.36	3.44	2.20	0.89	0.47	9.36	2.75	10.8	10.8	15.1	15.1
289.17	2.36	3.45	2.21	0.89	0.47	9.38	2.77	10.9	10.9	15.1	15.1
290.72	2.37	3.47	2.22	0.90	0.46	9.41	2.80	10.9	10.9	15.2	15.2
291.63	2.38	3.48	2.22	0.90	0.46	9.44	2.82	11.0	11.0	15.3	15.3
292.00	2.38	3.48	2.23	0.90	0.45	9.44	2.82	11.0	11.0	15.3	15.3
292.83	2.38	3.50	2.23	0.90	0.45	9.46	2.84	11.0	11.0	15.4	15.4
295.57	2.40	3.53	2.25	0.90	0.44	9.53	2.89	11.2	11.2	15.5	15.5
296.17	2.40	3.54	2.26	0.90	0.44	9.54	2.90	11.2	11.2	15.6	15.6
299.50	2.42	3.58	2.28	0.91	0.42	9.62	2.96	11.4	11.4	15.6	15.8
303.78	2.45	3.63	2.32	0.91	0.41	9.72	3.05	11.6	11.6	16.0	16.0

LAMBDA	O+(4S)	O+(2D)	O+(2P)	O+(4P)	O+(2P*)	O+(ICT)	HE	N2(ABS)	N2(ICN)	O2(ABS)	O2(ICN)
315.02	2.51	3.76	2.39	0.92	0.00	9.57	3.26	12.4	12.4	16.5	16.5
315.05	2.51	3.76	2.39	0.92	0.00	9.57	3.26	12.4	12.4	16.5	16.5
316.20	2.51	3.77	2.40	0.92	0.00	9.60	3.28	12.5	12.5	16.6	16.6
319.63	2.54	3.82	2.42	0.93	0.00	9.70	3.35	12.8	12.8	16.7	16.7
335.05	2.63	4.01	2.54	0.94	0.00	10.12	3.67	14.7	14.7	17.3	17.3
335.39	2.64	4.01	2.54	0.94	0.00	10.13	3.70	14.7	14.7	17.3	17.3
345.13	2.69	4.12	2.60	0.94	0.00	10.35	3.88	15.9	15.9	17.7	17.7
345.74	2.69	4.13	2.61	0.94	0.00	10.36	3.90	16.0	16.0	17.7	17.7
347.42	2.70	4.15	2.62	0.94	0.00	10.40	3.95	16.1	16.1	17.7	17.7
349.65	2.71	4.17	2.63	0.94	0.00	10.46	3.97	16.4	16.4	17.8	17.8
353.66	2.73	4.22	2.65	0.93	0.00	10.54	4.03	16.8	16.8	17.9	17.9
356.07	2.75	4.24	2.67	0.93	0.00	10.59	4.10	17.0	17.0	18.0	18.0
360.76	2.77	4.29	2.70	0.93	0.00	10.68	4.20	17.4	17.4	18.1	18.1
364.80	2.79	4.34	2.72	0.92	0.00	10.77	4.30	17.7	17.7	18.3	18.3
366.07	2.81	4.37	2.74	0.92	0.00	10.84	4.35	18.0	18.0	18.4	18.4
401.70	2.93	4.63	2.87	0.83	0.00	11.27	5.10	20.1	20.1	19.1	19.1
405.00	2.94	4.65	2.88	0.82	0.00	11.30	5.16	20.3	20.3	19.2	19.2
406.00	2.94	4.66	2.89	0.82	0.00	11.31	5.20	20.4	20.4	19.2	19.2
407.00	2.95	4.66	2.89	0.82	0.00	11.32	5.22	20.4	20.4	19.3	19.3
408.00	2.95	4.67	2.89	0.82	0.00	11.33	5.25	20.5	20.5	19.3	19.3
409.00	2.95	4.68	2.90	0.81	0.00	11.34	5.28	20.5	20.5	19.3	19.3
410.00	2.96	4.69	2.90	0.81	0.00	11.35	5.30	20.6	20.6	19.3	19.3
411.00	2.96	4.69	2.90	0.81	0.00	11.36	5.31	20.6	20.6	19.3	19.3
412.00	2.96	4.70	2.91	0.80	0.00	11.37	5.33	20.7	20.7	19.3	19.3
413.00	2.97	4.71	2.91	0.80	0.00	11.38	5.35	20.7	20.7	19.3	19.3
414.00	2.97	4.71	2.91	0.80	0.00	11.39	5.37	20.8	20.8	19.3	19.3
415.00	2.97	4.72	2.91	0.79	0.00	11.40	5.39	20.8	20.8	19.3	19.3
416.00	2.98	4.73	2.92	0.79	0.00	11.41	5.41	20.9	20.9	19.4	19.4
417.00	2.98	4.73	2.92	0.79	0.00	11.43	5.43	20.9	20.9	19.4	19.4
417.24	2.98	4.74	2.92	0.79	0.00	11.43	5.41	20.9	20.9	19.4	19.4
417.71	2.98	4.74	2.92	0.79	0.00	11.43	5.45	21.0	21.0	19.4	19.4
418.00	2.98	4.74	2.92	0.79	0.00	11.44	5.45	21.0	21.0	19.4	19.4
419.00	2.99	4.75	2.93	0.78	0.00	11.44	5.48	21.0	21.0	19.4	19.4
420.00	2.99	4.75	2.93	0.78	0.00	11.45	5.50	21.1	21.1	19.4	19.4
421.00	3.00	4.76	2.93	0.77	0.00	11.47	5.52	21.2	21.2	19.4	19.4
422.00	3.00	4.77	2.94	0.77	0.00	11.48	5.55	21.2	21.2	19.4	19.4
423.00	3.00	4.78	2.94	0.77	0.00	11.49	5.57	21.3	21.3	19.5	19.5
424.00	3.01	4.78	2.94	0.76	0.00	11.50	5.59	21.4	21.4	19.5	19.5
425.00	3.01	4.79	2.95	0.76	0.00	11.51	5.61	21.5	21.5	19.5	19.5
426.00	3.02	4.80	2.95	0.75	0.00	11.52	5.63	21.6	21.6	19.5	19.5

427.00	3.02	4.80	2.95	0.75	0.00	11.53	5.65	21.6	21.6	19.5	19.5
428.00	3.02	4.81	2.96	0.75	0.00	11.54	5.68	21.7	21.7	19.6	19.6
429.00	3.03	4.82	2.96	0.74	0.00	11.55	5.70	21.8	21.8	19.6	19.6
430.00	3.03	4.82	2.96	0.74	0.00	11.56	5.72	21.8	21.8	19.6	19.6
430.50	3.03	4.83	2.97	0.74	0.00	11.56	5.74	21.8	21.8	19.6	19.6
431.00	3.03	4.83	2.97	0.74	0.00	11.57	5.75	21.8	21.8	19.6	19.6
432.00	3.04	4.84	2.97	0.73	0.00	11.58	5.78	21.9	21.9	19.6	19.6
433.00	3.04	4.84	2.97	0.73	0.00	11.59	5.80	21.9	21.9	19.6	19.6
434.00	3.05	4.85	2.98	0.72	0.00	11.60	5.80	21.9	21.9	19.6	19.6
435.00	3.05	4.86	2.98	0.72	0.00	11.61	5.83	21.9	21.9	19.6	19.6
436.00	3.05	4.86	2.98	0.00	0.00	10.90	5.86	21.9	21.9	19.6	19.6
436.10	3.05	4.86	2.98	0.00	0.00	10.90	5.86	21.9	21.9	19.6	19.6
437.00	3.06	4.87	2.99	0.00	0.00	10.91	5.88	21.9	21.9	19.7	19.7
438.00	3.06	4.88	2.99	0.00	0.00	10.92	5.90	21.9	21.9	19.7	19.7
439.00	3.06	4.88	2.99	0.00	0.00	10.94	5.93	21.9	21.9	19.7	19.7
440.00	3.07	4.89	2.99	0.00	0.00	10.95	5.95	21.9	21.9	19.7	19.7
441.00	3.07	4.89	3.00	0.00	0.00	10.96	5.97	21.9	21.9	19.7	19.7
442.00	3.07	4.90	3.00	0.00	0.00	10.97	6.00	21.9	21.9	19.7	19.7
443.00	3.08	4.91	3.00	0.00	0.00	10.98	6.02	21.9	21.9	19.8	19.8
444.00	3.08	4.91	3.00	0.00	0.00	10.99	6.04	21.9	21.9	19.8	19.8
445.00	3.08	4.92	3.01	0.00	0.00	11.01	6.06	21.9	21.9	19.8	19.8
446.00	3.09	4.93	3.01	0.00	0.00	11.02	6.08	21.9	21.9	19.9	19.9
447.00	3.09	4.93	3.01	0.00	0.00	11.03	6.10	22.0	22.0	19.9	19.9
448.00	3.09	4.94	3.01	0.00	0.00	11.04	6.13	22.0	22.0	19.9	19.9
449.00	3.10	4.94	3.02	0.00	0.00	11.05	6.15	22.0	22.0	20.0	20.0
450.00	3.10	4.95	3.02	0.00	0.00	11.06	6.17	22.0	22.0	20.0	20.0
451.00	3.10	4.95	3.02	0.00	0.00	11.08	6.20	22.0	22.0	20.0	20.0
452.00	3.11	4.96	3.02	0.00	0.00	11.09	6.22	22.0	22.0	20.0	20.0
453.00	3.11	4.97	3.03	0.00	0.00	11.10	6.25	22.0	22.0	20.1	20.1
454.00	3.17	5.06	3.08	0.00	0.00	11.31	6.27	22.0	22.0	20.1	20.1
455.00	3.33	5.23	3.24	0.00	0.00	11.90	6.29	22.0	22.0	20.1	20.1
456.00	3.30	5.27	3.20	0.00	0.00	11.77	6.31	22.0	22.0	20.1	20.1
457.00	3.25	5.20	3.16	0.00	0.00	11.61	6.33	22.0	22.0	20.1	20.1
458.00	3.22	5.15	3.13	0.00	0.00	11.50	6.35	22.0	22.0	20.2	20.2
459.00	3.20	5.12	3.11	0.00	0.00	11.43	6.37	22.0	22.0	20.2	20.2
460.00	3.19	5.09	3.09	0.00	0.00	11.37	6.40	22.0	22.0	20.2	20.2
461.00	3.18	5.08	3.09	0.00	0.00	11.35	6.43	22.0	22.0	20.2	20.2
462.00	3.17	5.07	3.08	0.00	0.00	11.32	6.45	21.9	21.9	20.3	20.3
463.00	3.17	5.06	3.07	0.00	0.00	11.29	6.47	21.9	21.9	20.3	20.3
464.00	3.16	5.05	3.06	0.00	0.00	11.27	6.50	21.9	21.9	20.3	20.3

LAMBDA	O+(4S)	O+(2D)	O+(2P)	C+(4P)	C+(2P*)	C+(TOT)	HE	N2(ABS)	N2(ION)	O2(ABS)	O2(ION)
465.00	3.16	5.04	3.06	0.00	0.00	11.26	6.52	21.8	21.8	20.4	20.4
465.22	3.15	5.04	3.06	0.00	0.00	11.25	6.53	21.8	21.8	20.4	20.4
466.00	3.15	5.04	3.05	0.00	0.00	11.24	6.54	21.8	21.8	20.4	20.4
467.00	3.13	5.01	3.03	0.00	0.00	11.17	6.56	21.8	21.8	20.5	20.5
468.00	3.11	4.97	3.01	0.00	0.00	11.08	6.58	21.7	21.7	20.5	20.5
469.00	3.10	4.95	2.99	0.00	0.00	11.04	6.60	21.7	21.7	20.6	20.6
469.80	3.09	4.93	2.98	0.00	0.00	11.01	6.62	21.7	21.7	20.6	20.6
470.00	3.09	4.93	2.98	0.00	0.00	11.00	6.63	21.7	21.7	20.6	20.6
471.00	3.06	4.90	2.96	0.00	0.00	10.92	6.65	21.7	21.7	20.6	20.6
472.00	3.03	4.84	2.92	0.00	0.00	10.78	6.68	21.7	21.7	20.7	20.7
473.00	2.96	4.73	2.86	0.00	0.00	10.55	6.70	21.7	21.7	20.7	20.7
474.00	2.80	4.48	2.71	0.00	0.00	9.99	6.72	21.7	21.7	20.8	20.8
475.00	2.64	4.22	2.55	0.00	0.00	9.41	6.90	21.7	21.7	20.8	20.8
476.00	3.21	5.14	3.10	0.00	0.00	11.45	6.76	21.7	21.7	20.8	20.8
477.00	3.29	5.25	3.17	0.00	0.00	11.70	6.78	21.7	21.7	20.9	20.9
478.00	3.65	5.83	3.52	0.00	0.00	13.00	6.81	21.7	21.7	20.9	20.9
479.00	2.81	4.49	2.70	0.00	0.00	10.00	6.83	21.7	21.7	21.0	21.0
480.00	3.23	5.16	3.11	0.00	0.00	11.50	6.85	21.7	21.7	21.0	21.0
481.00	3.41	5.45	3.28	0.00	0.00	12.15	6.88	21.7	21.7	21.0	21.0
482.00	3.38	5.40	3.25	0.00	0.00	12.02	6.90	21.7	21.7	21.1	21.1
482.10	3.38	5.39	3.24	0.00	0.00	12.01	6.90	21.7	21.7	21.1	21.1
483.00	3.35	5.34	3.21	0.00	0.00	11.90	6.93	21.7	21.7	21.1	21.1
484.00	3.33	5.31	3.19	0.00	0.00	11.83	6.95	21.7	21.7	21.2	21.2
485.00	3.31	5.28	3.17	0.00	0.00	11.77	6.97	21.7	21.7	21.2	21.2
486.00	3.30	5.27	3.16	0.00	0.00	11.73	6.99	21.7	21.7	21.3	21.3
487.00	3.29	5.25	3.15	0.00	0.00	11.69	7.02	21.7	21.7	21.3	21.3
488.00	3.28	5.23	3.14	0.00	0.00	11.65	7.04	21.7	21.7	21.4	21.4
489.00	3.28	5.23	3.14	0.00	0.00	11.64	7.06	21.7	21.7	21.4	21.4
489.50	3.27	5.23	3.13	0.00	0.00	11.64	7.07	21.7	21.7	21.5	21.5
490.00	3.27	5.23	3.13	0.00	0.00	11.63	7.08	21.7	21.7	21.5	21.5
491.00	3.27	5.22	3.13	0.00	0.00	11.62	7.10	21.7	21.7	21.6	21.6
492.00	3.27	5.22	3.12	0.00	0.00	11.61	7.13	21.7	21.7	21.6	21.6
493.00	3.28	5.23	3.13	0.00	0.00	11.64	7.15	21.8	21.8	21.7	21.7
494.00	3.29	5.24	3.13	0.00	0.00	11.66	7.18	21.8	21.8	21.7	21.7
495.00	3.29	5.25	3.14	0.00	0.00	11.68	7.20	21.8	21.8	21.8	21.8
496.00	3.30	5.26	3.14	0.00	0.00	11.71	7.22	21.9	21.9	21.9	21.9
497.00	3.31	5.27	3.15	0.00	0.00	11.73	7.25	21.9	21.9	21.9	21.9
498.00	3.32	5.28	3.15	0.00	0.00	11.76	7.27	21.9	21.9	22.0	22.0
499.00	3.32	5.30	3.16	0.00	0.00	11.78	7.30	22.0	22.0	22.0	22.0
499.27	3.33	5.30	3.16	0.00	0.00	11.79	7.30	22.0	22.0	22.1	22.1

500.00	3.33	5.31	3.17	0.00	0.00	11.80	7.32	22.0	22.0	22.1	22.1
501.00	3.33	5.31	3.17	0.00	0.00	11.81	7.34	22.0	22.0	22.2	22.2
502.00	3.34	5.32	3.17	0.00	0.00	11.82	7.36	22.1	22.1	22.2	22.2
503.00	3.34	5.32	3.17	0.00	0.00	11.83	7.38	22.1	22.1	22.3	22.3
504.00	3.34	5.32	3.17	0.00	0.00	11.84	7.42	22.1	22.1	22.4	22.4
507.90	3.36	5.34	3.17	0.00	0.00	11.87	0.00	22.4	22.4	22.7	22.7
515.60	3.38	5.36	3.17	0.00	0.00	11.91	0.00	24.0	24.0	23.6	23.6
521.10	3.39	5.37	3.17	0.00	0.00	11.93	0.00	25.2	25.2	23.9	23.9
525.60	3.40	5.39	3.17	0.00	0.00	11.96	0.00	25.6	25.6	23.9	23.9
537.03	3.43	5.41	3.16	0.00	0.00	12.01	0.00	25.3	25.3	25.2	25.2
542.80	3.46	5.43	3.16	0.00	0.00	12.05	0.00	25.2	25.2	25.7	25.7
550.00	3.48	5.46	3.16	0.00	0.00	12.10	0.00	25.1	25.1	25.4	25.4
554.51	3.50	5.47	3.16	0.00	0.00	12.13	0.00	24.7	24.7	25.6	25.6
558.60	3.51	5.47	3.15	0.00	0.00	12.14	0.00	24.3	24.3	25.8	25.8
562.80	3.52	5.48	3.14	0.00	0.00	12.14	0.00	24.0	24.0	25.7	25.7
568.50	3.54	5.48	3.13	0.00	0.00	12.15	0.00	23.8	23.8	25.4	25.4
572.30	3.55	5.48	3.13	0.00	0.00	12.15	0.00	23.6	23.6	25.3	25.3
580.40	3.57	5.49	3.11	0.00	0.00	12.16	0.00	23.2	23.2	24.0	24.0
584.33	3.58	5.49	3.10	0.00	0.00	12.17	0.00	23.2	23.2	22.0	22.0
599.60	3.63	5.51	3.07	0.00	0.00	12.21	0.00	23.1	23.1	26.6	26.6
608.00	3.67	5.51	3.05	0.00	0.00	12.23	0.00	23.1	23.1	26.6	26.6
609.00	3.67	5.51	3.05	0.00	0.00	12.23	0.00	23.1	23.1	26.3	26.3
609.65	3.67	5.51	3.05	0.00	0.00	12.23	0.00	23.1	23.1	26.1	26.1
610.00	3.67	5.51	3.05	0.00	0.00	12.23	0.00	23.1	23.1	26.1	26.1
611.00	3.68	5.51	3.04	0.00	0.00	12.23	0.00	23.1	23.1	25.9	25.9
612.00	3.68	5.51	3.04	0.00	0.00	12.23	0.00	23.1	23.1	26.1	26.1
613.00	3.68	5.51	3.04	0.00	0.00	12.23	0.00	23.1	23.1	26.1	26.1
614.00	3.69	5.51	3.03	0.00	0.00	12.23	0.00	23.1	23.1	26.1	26.1
615.00	3.69	5.51	3.03	0.00	0.00	12.23	0.00	23.2	23.2	26.0	26.0
616.00	3.69	5.51	3.03	0.00	0.00	12.23	0.00	23.2	23.2	26.0	26.0
616.60	3.70	5.51	3.03	0.00	0.00	12.23	0.00	23.2	23.2	26.0	26.0
617.00	3.70	5.51	3.02	0.00	0.00	12.23	0.00	23.2	23.2	26.0	26.0
618.00	3.70	5.51	3.02	0.00	0.00	12.23	0.00	23.2	23.2	26.0	26.0
619.00	3.70	5.51	3.02	0.00	0.00	12.23	0.00	23.2	23.2	26.0	26.0
620.00	3.71	5.51	3.01	0.00	0.00	12.23	0.00	23.2	23.2	25.9	25.9
621.00	3.71	5.51	3.01	0.00	0.00	12.23	0.00	23.2	23.2	25.9	25.9
622.00	3.71	5.51	3.01	0.00	0.00	12.23	0.00	23.2	23.2	25.9	25.9
623.00	3.72	5.51	3.00	0.00	0.00	12.23	0.00	23.2	23.2	25.9	25.9
624.00	3.72	5.51	3.00	0.00	0.00	12.23	0.00	23.2	23.2	25.9	25.9
625.00	3.72	5.51	2.99	0.00	0.00	12.23	0.00	23.2	23.2	25.9	25.9

LAMBDA	O+(4S)	O+(2D)	O+(2P)	C+(4P)	C+(2P*)	C+(1CT)	HE	N2(ABS)	N2(ION)	O2(ABS)	O2(ICN)
625.28	3.73	5.51	2.99	0.00	0.00	12.23	0.00	23.2	23.2	25.9	25.9
626.00	3.73	5.50	2.99	0.00	0.00	12.22	0.00	23.2	23.2	25.8	25.8
627.00	3.73	5.50	2.99	0.00	0.00	12.22	0.00	23.2	23.2	25.8	25.8
628.00	3.73	5.50	2.98	0.00	0.00	12.22	0.00	23.2	23.2	25.8	25.8
629.00	3.74	5.50	2.98	0.00	0.00	12.22	0.00	23.2	23.2	25.8	25.8
629.73	3.74	5.50	2.98	0.00	0.00	12.22	0.00	23.2	23.2	25.8	25.8
630.00	3.74	5.50	2.98	0.00	0.00	12.22	0.00	23.2	23.2	25.8	25.8
631.00	3.74	5.50	2.97	0.00	0.00	12.22	0.00	23.2	23.2	25.8	25.8
632.00	3.75	5.50	2.97	0.00	0.00	12.21	0.00	23.2	23.2	25.7	25.7
633.00	3.75	5.49	2.96	0.00	0.00	12.21	0.00	23.2	23.2	25.7	25.7
634.00	3.75	5.49	2.96	0.00	0.00	12.20	0.00	23.2	23.2	25.7	25.7
635.00	3.76	5.49	2.95	0.00	0.00	12.20	0.00	23.2	23.2	25.7	25.7
636.00	3.76	5.49	2.95	0.00	0.00	12.19	0.00	23.3	23.3	25.7	25.7
637.00	3.76	5.48	2.94	0.00	0.00	12.19	0.00	23.3	23.3	25.7	25.7
638.00	3.77	5.48	2.94	0.00	0.00	12.19	0.00	23.3	23.3	25.9	25.8
639.00	3.77	5.48	2.93	0.00	0.00	12.18	0.00	23.3	23.3	26.0	25.9
640.00	3.77	5.48	2.93	0.00	0.00	12.18	0.00	23.3	23.3	26.1	25.9
641.00	3.77	5.47	2.92	0.00	0.00	12.17	0.00	23.3	23.3	26.3	26.0
642.00	3.78	5.47	2.92	0.00	0.00	12.17	0.00	23.3	23.3	26.5	26.1
643.00	3.78	5.47	2.91	0.00	0.00	12.16	0.00	23.3	23.3	26.6	26.2
644.00	3.78	5.47	2.91	0.00	0.00	12.16	0.00	23.3	23.3	26.7	26.3
644.10	3.78	5.47	2.91	0.00	0.00	12.16	0.00	23.3	23.3	26.7	26.3
645.00	3.79	5.46	2.90	0.00	0.00	12.15	0.00	23.3	23.3	26.8	26.3
646.00	3.79	5.46	2.90	0.00	0.00	12.15	0.00	23.3	23.3	26.7	26.3
647.00	3.79	5.46	2.90	0.00	0.00	12.14	0.00	23.3	23.3	26.6	26.2
648.00	3.79	5.46	2.89	0.00	0.00	12.14	0.00	23.3	23.3	26.4	26.1
649.00	3.80	5.45	2.89	0.00	0.00	12.14	0.00	23.3	23.3	26.3	26.1
650.00	3.80	5.45	2.88	0.00	0.00	12.13	0.00	23.3	23.3	26.2	26.0
651.00	3.80	5.44	2.87	0.00	0.00	12.11	0.00	23.4	23.4	26.1	25.9
652.00	3.80	5.43	2.87	0.00	0.00	12.10	0.00	23.5	23.5	26.0	25.7
653.00	3.80	5.43	2.86	0.00	0.00	12.08	0.00	23.6	23.6	25.8	25.6
654.00	3.80	5.42	2.85	0.00	0.00	12.07	0.00	23.7	23.7	25.7	25.5
655.00	3.80	5.41	2.84	0.00	0.00	12.05	0.00	23.8	23.8	25.6	25.3
656.00	3.80	5.40	2.83	0.00	0.00	12.04	0.00	23.9	23.9	25.4	25.0
657.00	3.80	5.40	2.83	0.00	0.00	12.02	0.00	24.0	24.0	25.3	25.0
657.30	3.80	5.39	2.82	0.00	0.00	12.02	0.00	24.0	24.0	25.3	25.0
658.00	3.80	5.39	2.82	0.00	0.00	12.01	0.00	24.1	24.1	25.2	24.8
659.00	3.80	5.38	2.81	0.00	0.00	11.99	0.00	24.1	24.1	25.1	24.7
660.00	3.80	5.37	2.80	0.00	0.00	11.97	0.00	24.2	24.2	25.0	24.6
661.00	3.80	5.36	2.79	0.00	0.00	11.96	0.00	25.6	23.9	24.8	24.5

661.40	3.80	5.36	2.79	0.00	0.00	11.95	0.00	26.0	23.9	24.8	24.4
662.00	3.80	5.36	2.79	0.00	0.00	11.94	0.00	26.4	23.8	24.6	24.4
663.00	3.80	5.35	2.78	0.00	0.00	11.93	0.00	26.8	24.0	24.4	23.8
664.00	3.80	5.34	2.77	0.00	0.00	11.91	0.00	27.1	25.0	24.0	23.4
665.00	3.80	5.33	2.76	0.00	0.00	11.90	0.00	27.3	25.4	23.6	23.1
666.00	4.01	5.62	0.00	0.00	0.00	9.64	0.00	27.3	25.6	24.0	23.4
667.00	4.01	5.61	0.00	0.00	0.00	9.63	0.00	27.2	25.7	24.2	23.7
668.00	4.01	5.61	0.00	0.00	0.00	9.62	0.00	27.2	25.9	24.5	23.9
669.00	4.01	5.60	0.00	0.00	0.00	9.61	0.00	30.7	26.1	24.8	24.1
670.00	4.01	5.59	0.00	0.00	0.00	9.60	0.00	30.7	25.9	24.9	24.3
671.00	4.01	5.58	0.00	0.00	0.00	9.59	0.00	33.9	28.3	25.0	24.4
671.50	4.01	5.57	0.00	0.00	0.00	9.59	0.00	33.9	28.2	25.0	24.5
672.00	4.01	5.57	0.00	0.00	0.00	9.58	0.00	33.9	28.1	21.9	21.9
673.00	4.01	5.56	0.00	0.00	0.00	9.57	0.00	33.9	27.8	21.9	21.4
674.00	4.01	5.55	0.00	0.00	0.00	9.56	0.00	27.1	22.1	21.8	21.0
675.00	4.01	5.54	0.00	0.00	0.00	9.55	0.00	35.1	28.3	21.8	20.8
676.00	4.01	5.53	0.00	0.00	0.00	9.54	0.00	35.2	28.3	21.8	20.5
677.00	4.01	5.52	0.00	0.00	0.00	9.53	0.00	35.2	28.4	21.8	20.3
678.00	4.01	5.51	0.00	0.00	0.00	9.52	0.00	27.2	22.1	21.6	20.1
679.00	4.01	5.50	0.00	0.00	0.00	9.52	0.00	27.2	22.1	23.3	21.0
680.00	4.01	5.49	0.00	0.00	0.00	9.51	0.00	23.9	19.5	23.1	20.5
680.94	4.01	5.49	0.00	0.00	0.00	9.50	0.00	23.8	19.5	22.1	20.5
681.00	4.01	5.49	0.00	0.00	0.00	9.50	0.00	23.8	19.5	22.2	20.5
681.70	4.01	5.48	0.00	0.00	0.00	9.49	0.00	38.1	31.2	22.9	20.5
682.00	4.01	5.48	0.00	0.00	0.00	9.49	0.00	38.0	31.2	23.2	20.5
683.00	4.01	5.47	0.00	0.00	0.00	9.48	0.00	37.9	31.1	24.1	20.5
684.00	4.01	5.46	0.00	0.00	0.00	9.47	0.00	37.7	31.0	24.9	20.5
685.00	4.01	5.45	0.00	0.00	0.00	9.46	0.00	26.4	21.7	25.7	20.5
685.70	4.01	5.44	0.00	0.00	0.00	9.45	0.00	25.0	25.0	21.0	21.0
686.00	4.01	5.44	0.00	0.00	0.00	9.45	0.00	26.2	21.6	26.5	20.5
687.00	4.78	6.47	0.00	0.00	0.00	11.24	0.00	26.0	21.4	27.1	20.5
688.00	4.70	6.36	0.00	0.00	0.00	11.06	0.00	25.8	21.3	27.7	20.6
689.00	4.63	6.25	0.00	0.00	0.00	10.88	0.00	25.7	21.1	28.2	20.8
690.00	4.56	6.14	0.00	0.00	0.00	10.70	0.00	22.3	18.3	28.7	21.0
691.00	4.49	6.03	0.00	0.00	0.00	10.52	0.00	22.2	18.2	29.1	21.4
692.00	4.41	5.92	0.00	0.00	0.00	10.34	0.00	22.1	18.1	29.4	21.8
693.00	4.34	5.82	0.00	0.00	0.00	10.16	0.00	43.5	35.5	30.0	22.6
694.00	4.27	5.71	0.00	0.00	0.00	9.98	0.00	43.4	35.4	30.4	23.6
694.30	4.24	5.68	0.00	0.00	0.00	9.92	0.00	43.4	35.4	30.5	24.4
695.00	4.19	5.60	0.00	0.00	0.00	9.79	0.00	43.4	35.3	30.8	25.0

LAMBDA	O+(4S)	O+(2D)	O+(2P)	C+(4P)	C+(2P*)	C+(TOT)	HE	N2(ABS)	N2(ION)	O2(ABS)	O2(ION)
696.00	4.12	5.49	0.00	0.00	0.00	9.61	0.00	43.4	35.2	31.2	26.0
697.00	4.05	5.38	0.00	0.00	0.00	9.43	0.00	43.5	35.1	31.6	27.0
698.00	3.98	5.28	0.00	0.00	0.00	9.25	0.00	25.2	20.3	32.2	28.0
699.00	3.90	5.17	0.00	0.00	0.00	9.07	0.00	25.3	20.3	32.6	28.6
700.00	3.83	5.06	0.00	0.00	0.00	8.89	0.00	25.5	20.4	33.0	30.0
701.00	5.08	6.69	0.00	0.00	0.00	11.77	0.00	25.7	20.5	33.2	30.8
702.00	5.01	6.59	0.00	0.00	0.00	11.60	0.00	25.9	20.6	33.6	30.8
703.00	4.94	6.49	0.00	0.00	0.00	11.42	0.00	26.2	20.7	33.8	31.0
703.40	4.91	6.44	0.00	0.00	0.00	11.35	0.00	26.3	23.0	25.0	23.0
704.00	4.87	6.38	0.00	0.00	0.00	11.25	0.00	26.5	20.9	33.9	31.0
705.00	4.80	6.28	0.00	0.00	0.00	11.08	0.00	26.9	21.0	34.0	30.9
706.00	4.73	6.18	0.00	0.00	0.00	10.91	0.00	27.2	21.2	34.0	30.6
707.00	4.66	6.07	0.00	0.00	0.00	10.74	0.00	27.6	21.4	33.8	30.4
708.00	4.59	5.97	0.00	0.00	0.00	10.57	0.00	27.9	21.6	33.7	29.8
709.00	4.53	5.87	0.00	0.00	0.00	10.40	0.00	28.3	21.8	33.6	29.0
710.00	4.46	5.77	0.00	0.00	0.00	10.23	0.00	28.7	22.0	33.0	28.6
711.00	4.39	5.66	0.00	0.00	0.00	10.05	0.00	29.1	22.2	32.6	28.2
712.00	4.32	5.56	0.00	0.00	0.00	9.88	0.00	29.4	22.4	32.0	27.6
712.70	4.30	5.53	0.00	0.00	0.00	9.84	0.00	29.7	22.6	32.0	27.1
713.00	4.30	5.52	0.00	0.00	0.00	9.82	0.00	29.8	22.6	31.8	27.0
714.00	4.27	5.48	0.00	0.00	0.00	9.75	0.00	30.1	22.8	31.2	26.0
715.00	4.25	5.44	0.00	0.00	0.00	9.68	0.00	25.0	18.0	30.6	25.6
716.00	4.22	5.39	0.00	0.00	0.00	9.62	0.00	25.0	18.0	30.0	25.0
717.00	4.20	5.35	0.00	0.00	0.00	9.55	0.00	25.0	18.0	29.4	24.6
718.00	4.18	5.31	0.00	0.00	0.00	9.48	0.00	31.0	23.2	28.5	24.0
718.50	4.16	5.29	0.00	0.00	0.00	9.45	0.00	31.1	23.2	28.3	23.8
719.00	4.15	5.27	0.00	0.00	0.00	9.42	0.00	31.1	23.2	28.0	23.6
720.00	4.13	5.22	0.00	0.00	0.00	9.35	0.00	31.1	23.1	27.3	23.0
721.00	4.10	5.18	0.00	0.00	0.00	9.28	0.00	31.0	23.0	27.0	22.4
722.00	4.08	5.14	0.00	0.00	0.00	9.22	0.00	57.2	42.4	26.4	22.0
723.00	4.06	5.10	0.00	0.00	0.00	9.15	0.00	56.9	42.1	26.0	21.8
724.00	4.03	5.05	0.00	0.00	0.00	9.09	0.00	56.6	41.8	27.0	21.8
725.00	4.01	5.01	0.00	0.00	0.00	9.02	0.00	56.1	41.5	29.4	22.0
726.00	3.99	4.98	0.00	0.00	0.00	8.97	0.00	55.5	41.0	30.6	22.5
727.00	3.97	4.94	0.00	0.00	0.00	8.91	0.00	54.8	40.5	31.4	23.8
728.00	3.95	4.91	0.00	0.00	0.00	8.86	0.00	27.7	20.5	32.2	25.0
729.00	3.93	4.87	0.00	0.00	0.00	8.81	0.00	26.7	19.8	32.6	26.4
730.00	3.92	4.84	0.00	0.00	0.00	8.76	0.00	25.5	19.0	33.0	28.0
731.00	3.90	4.80	0.00	0.00	0.00	8.70	0.00	24.2	18.0	33.4	29.0
732.00	3.88	4.77	0.00	0.00	0.00	8.65	0.00	22.8	17.0	33.6	30.0

733.00	4.18	0.00	0.00	0.00	0.00	4.18	0.00	21.3	16.0	33.9	31.0
734.00	4.18	0.00	0.00	0.00	0.00	4.18	0.00	27.1	20.4	34.0	31.4
735.00	4.18	0.00	0.00	0.00	0.00	4.18	0.00	34.0	29.2	34.0	31.6
736.00	4.18	0.00	0.00	0.00	0.00	4.18	0.00	26.6	24.0	33.6	31.2
737.00	4.18	0.00	0.00	0.00	0.00	4.18	0.00	33.0	30.1	33.6	30.4
738.00	4.18	0.00	0.00	0.00	0.00	4.18	0.00	28.7	26.3	33.2	29.8
739.00	4.18	0.00	0.00	0.00	0.00	4.18	0.00	29.3	26.4	32.2	28.0
740.00	4.18	0.00	0.00	0.00	0.00	4.18	0.00	29.3	25.8	30.8	26.0
741.00	4.18	0.00	0.00	0.00	0.00	4.18	0.00	29.3	24.9	28.4	25.0
742.00	4.18	0.00	0.00	0.00	0.00	4.18	0.00	21.0	17.1	27.6	24.0
743.00	4.18	0.00	0.00	0.00	0.00	4.18	0.00	29.5	22.8	26.6	22.0
744.00	4.18	0.00	0.00	0.00	0.00	4.18	0.00	29.5	21.5	25.6	20.0
745.00	4.18	0.00	0.00	0.00	0.00	4.18	0.00	29.5	20.3	24.6	16.7
746.00	4.18	0.00	0.00	0.00	0.00	4.18	0.00	29.5	19.2	23.4	11.5
747.00	4.18	0.00	0.00	0.00	0.00	4.18	0.00	29.6	18.3	22.3	10.3
748.00	4.18	0.00	0.00	0.00	0.00	4.18	0.00	28.3	16.8	21.1	9.1
749.00	4.18	0.00	0.00	0.00	0.00	4.18	0.00	28.9	16.7	19.8	7.8
750.00	4.18	0.00	0.00	0.00	0.00	4.18	0.00	24.7	14.2	18.4	6.4
751.00	4.18	0.00	0.00	0.00	0.00	4.18	0.00	24.7	14.5	20.6	8.6
752.00	4.18	0.00	0.00	0.00	0.00	4.18	0.00	17.7	11.0	21.3	8.6
753.00	4.18	0.00	0.00	0.00	0.00	4.18	0.00	17.7	11.9	21.9	8.5
754.00	4.18	0.00	0.00	0.00	0.00	4.18	0.00	32.0	19.6	22.4	8.5
755.00	4.18	0.00	0.00	0.00	0.00	4.18	0.00	32.0	19.7	22.8	8.4
756.00	4.18	0.00	0.00	0.00	0.00	4.18	0.00	32.0	19.9	23.2	8.4
757.00	4.18	0.00	0.00	0.00	0.00	4.18	0.00	32.2	20.2	23.4	8.4
758.00	4.18	0.00	0.00	0.00	0.00	4.18	0.00	32.2	20.3	23.6	8.4
758.70	4.18	0.00	0.00	0.00	0.00	4.18	0.00	26.1	16.5	23.7	8.4
759.00	4.18	0.00	0.00	0.00	0.00	4.18	0.00	26.1	16.5	23.7	8.4
759.40	4.18	0.00	0.00	0.00	0.00	4.18	0.00	26.1	16.6	23.7	8.4
760.00	4.18	0.00	0.00	0.00	0.00	4.18	0.00	30.3	0.0	23.7	8.4
760.40	4.18	0.00	0.00	0.00	0.00	4.18	0.00	40.0	22.0	20.0	10.0
761.00	4.18	0.00	0.00	0.00	0.00	4.18	0.00	30.3	19.6	23.6	8.4
762.00	4.18	0.00	0.00	0.00	0.00	4.18	0.00	30.3	19.6	23.5	8.4
762.06	4.18	0.00	0.00	0.00	0.00	4.18	0.00	30.3	19.8	23.5	8.4
763.00	4.18	0.00	0.00	0.00	0.00	4.18	0.00	18.6	12.3	23.3	8.4
764.00	4.18	0.00	0.00	0.00	0.00	4.18	0.00	18.6	0.0	22.9	8.5
764.60	4.18	0.00	0.00	0.00	0.00	4.18	0.00	85.0	66.0	23.0	12.0
765.00	4.18	0.00	0.00	0.00	0.00	4.18	0.00	35.5	23.7	22.5	8.5
766.00	4.18	0.00	0.00	0.00	0.00	4.18	0.00	35.5	23.8	22.0	8.6
767.00	4.18	0.00	0.00	0.00	0.00	4.18	0.00	9.7	6.6	21.5	8.7

LAMBDA	O+(4S)	O+(2D)	O+(2P)	C+(4P)	C+(2P*)	C+(TOT)	HE	N2(ABS)	N2(ION)	O2(ABS)	O2(ION)
768.00	4.18	0.00	0.00	0.00	0.00	4.18	0.00	9.7	6.6	20.8	8.7
769.00	.18	0.00	0.00	0.00	0.00	4.18	0.00	9.7	6.6	20.1	8.8
770.00	4.18	0.00	0.00	0.00	0.00	4.18	0.00	9.7	0.0	19.2	8.9
770.40	4.18	0.00	0.00	0.00	0.00	4.18	0.00	15.0	8.0	18.0	11.0
771.00	4.18	0.00	0.00	0.00	0.00	4.18	0.00	26.9	18.4	25.2	9.7
772.00	4.18	0.00	0.00	0.00	0.00	4.18	0.00	26.9	18.4	25.6	9.8
773.00	4.18	0.00	0.00	0.00	0.00	4.18	0.00	26.9	18.3	26.0	9.8
774.00	4.18	0.00	0.00	0.00	0.00	4.18	0.00	26.9	18.3	26.4	9.9
775.00	4.18	0.00	0.00	0.00	0.00	4.18	0.00	36.2	24.6	26.8	10.0
776.00	4.18	0.00	0.00	0.00	0.00	4.18	0.00	47.1	31.9	27.2	10.0
776.00	4.18	0.00	0.00	0.00	0.00	4.18	0.00	47.1	31.8	27.2	10.0
777.00	4.18	0.00	0.00	0.00	0.00	4.18	0.00	47.1	29.5	27.5	10.0
778.00	4.18	0.00	0.00	0.00	0.00	4.18	0.00	47.1	29.2	27.9	10.0
779.00	4.18	0.00	0.00	0.00	0.00	4.18	0.00	24.7	15.2	28.2	10.0
780.00	4.18	0.00	0.00	0.00	0.00	4.18	0.00	24.7	0.0	28.5	10.0
780.30	4.18	0.00	0.00	0.00	0.00	4.18	0.00	19.0	13.0	28.0	11.0
781.00	4.18	0.00	0.00	0.00	0.00	4.18	0.00	40.8	24.8	28.8	10.0
782.00	4.18	0.00	0.00	0.00	0.00	4.18	0.00	40.8	24.8	29.1	9.9
783.00	4.18	0.00	0.00	0.00	0.00	4.18	0.00	64.8	39.3	29.4	9.9
784.00	4.20	0.00	0.00	0.00	0.00	4.20	0.00	64.8	39.3	29.6	9.8
785.00	4.21	0.00	0.00	0.00	0.00	4.21	0.00	64.8	39.3	29.8	9.8
786.00	4.23	0.00	0.00	0.00	0.00	4.23	0.00	16.3	9.8	30.1	9.7
786.48	4.24	0.00	0.00	0.00	0.00	4.24	0.00	16.3	9.9	30.2	9.6
787.00	4.24	0.00	0.00	0.00	0.00	4.24	0.00	16.3	0.0	30.3	9.6
787.71	4.25	0.00	0.00	0.00	0.00	4.25	0.00	9.0	8.0	24.0	13.0
788.00	4.26	0.00	0.00	0.00	0.00	4.26	0.00	16.3	9.9	30.5	9.4
789.00	4.27	0.00	0.00	0.00	0.00	4.27	0.00	25.0	17.7	30.7	9.3
790.00	4.29	0.00	0.00	0.00	0.00	4.29	0.00	29.2	0.0	31.0	9.7
790.21	4.30	0.00	0.00	0.00	0.00	4.30	0.00	25.0	11.5	28.0	10.0
791.00	4.34	0.00	0.00	0.00	0.00	4.34	0.00	59.9	33.3	31.9	9.5
792.00	4.39	0.00	0.00	0.00	0.00	4.39	0.00	59.9	26.6	32.7	9.4
793.00	4.43	0.00	0.00	0.00	0.00	4.43	0.00	59.9	17.0	33.5	9.3
794.00	4.48	0.00	0.00	0.00	0.00	4.48	0.00	27.0	7.7	34.3	9.2
795.00	4.52	0.00	0.00	0.00	0.00	4.52	0.00	27.0	0.0	35.1	9.1
796.00	4.57	0.00	0.00	0.00	0.00	4.57	0.00	27.0	0.0	35.8	9.0
797.00	4.62	0.00	0.00	0.00	0.00	4.62	0.00	2.2	0.0	36.6	9.0
798.00	4.66	0.00	0.00	0.00	0.00	4.66	0.00	7.3	0.0	37.3	9.0
799.00	4.71	0.00	0.00	0.00	0.00	4.71	0.00	5.9	0.0	38.0	9.0
800.00	4.76	0.00	0.00	0.00	0.00	4.76	0.00	8.7	0.0	38.7	9.0
801.00	4.81	0.00	0.00	0.00	0.00	4.81	0.00	45.1	0.0	39.3	9.1

802.00	4.87	0.00	0.00	0.00	0.00	4.87	0.00	45.1	0.0	40.0	9.1
803.00	5.32	0.00	0.00	0.00	0.00	5.32	0.00	0.0	0.0	40.6	9.2
804.00	6.49	0.00	0.00	0.00	0.00	6.49	0.00	29.6	0.0	41.2	9.4
805.00	25.00	0.00	0.00	0.00	0.00	25.00	0.00	0.0	0.0	41.8	9.5
806.00	2.92	0.00	0.00	0.00	0.00	2.92	0.00	31.8	0.0	42.4	9.7
807.00	3.90	0.00	0.00	0.00	0.00	3.90	0.00	44.6	0.0	42.9	9.8
808.00	4.03	0.00	0.00	0.00	0.00	4.03	0.00	44.6	0.0	43.5	10.0
809.00	4.16	0.00	0.00	0.00	0.00	4.16	0.00	23.4	0.0	44.0	10.3
810.00	4.29	0.00	0.00	0.00	0.00	4.29	0.00	0.0	0.0	44.5	10.5
811.00	4.93	0.00	0.00	0.00	0.00	4.93	0.00	0.0	0.0	48.1	11.9
812.00	11.00	0.00	0.00	0.00	0.00	11.00	0.00	0.0	0.0	45.8	11.5
813.00	2.92	0.00	0.00	0.00	0.00	2.92	0.00	35.9	0.0	43.6	11.1
814.00	3.75	0.00	0.00	0.00	0.00	3.75	0.00	35.9	0.0	41.5	10.7
815.00	3.68	0.00	0.00	0.00	0.00	3.68	0.00	35.9	0.0	39.5	10.3
816.00	4.00	0.00	0.00	0.00	0.00	4.00	0.00	0.0	0.0	37.6	10.0
817.00	4.03	0.00	0.00	0.00	0.00	4.03	0.00	0.0	0.0	35.8	9.6
818.00	4.05	0.00	0.00	0.00	0.00	4.05	0.00	0.0	0.0	34.1	9.3
819.00	4.07	0.00	0.00	0.00	0.00	4.07	0.00	49.8	0.0	32.5	8.9
820.00	4.10	0.00	0.00	0.00	0.00	4.10	0.00	49.8	0.0	31.0	8.6
821.00	4.12	0.00	0.00	0.00	0.00	4.12	0.00	0.0	0.0	29.6	8.3
822.00	4.13	0.00	0.00	0.00	0.00	4.13	0.00	16.0	0.0	28.4	7.9
823.00	4.15	0.00	0.00	0.00	0.00	4.15	0.00	16.0	0.0	27.2	7.6
824.00	4.17	0.00	0.00	0.00	0.00	4.17	0.00	9.3	0.0	26.1	7.3
825.00	4.18	0.00	0.00	0.00	0.00	4.18	0.00	9.3	0.0	25.2	7.0
826.00	4.18	0.00	0.00	0.00	0.00	4.18	0.00	15.7	0.0	24.3	6.7
827.00	4.18	0.00	0.00	0.00	0.00	4.18	0.00	15.7	0.0	23.5	6.4
828.00	4.18	0.00	0.00	0.00	0.00	4.18	0.00	15.7	0.0	22.9	6.2
829.00	4.18	0.00	0.00	0.00	0.00	4.18	0.00	0.0	0.0	22.3	5.9
830.00	4.18	0.00	0.00	0.00	0.00	4.18	0.00	0.0	0.0	21.9	5.6
831.00	4.18	0.00	0.00	0.00	0.00	4.18	0.00	0.0	0.0	25.7	6.9
832.00	4.18	0.00	0.00	0.00	0.00	4.18	0.00	0.0	0.0	25.0	6.7
833.00	4.18	0.00	0.00	0.00	0.00	4.18	0.00	0.0	0.0	24.2	6.5
834.00	4.18	0.00	0.00	0.00	0.00	4.18	0.00	0.0	0.0	23.5	6.4
834.20	4.18	0.00	0.00	0.00	0.00	4.18	0.00	15.0	0.0	13.0	5.0
835.00	4.18	0.00	0.00	0.00	0.00	4.18	0.00	32.0	0.0	22.8	6.2
836.00	4.18	0.00	0.00	0.00	0.00	4.18	0.00	32.0	0.0	22.1	6.1
837.00	4.18	0.00	0.00	0.00	0.00	4.18	0.00	32.0	0.0	21.5	5.9
838.00	4.18	0.00	0.00	0.00	0.00	4.18	0.00	8.3	0.0	20.8	5.8
839.00	4.18	0.00	0.00	0.00	0.00	4.18	0.00	8.3	0.0	20.2	5.6
840.00	4.18	0.00	0.00	0.00	0.00	4.18	0.00	8.3	0.0	19.6	5.5

LAMBDA	C+(4S)	C+(2D)	C+(2P)	C+(4P)	C+(2P*)	C+(ICI)	ME	N2(ABS)	N2(ICN)	O2(ABS)	O2(ICN)
841.00	4.18	0.00	0.00	0.00	0.00	4.18	0.00	21.5	0.0	19.1	5.3
842.00	4.18	0.00	0.00	0.00	0.00	4.18	0.00	21.5	0.0	18.5	5.2
843.00	4.18	0.00	0.00	0.00	0.00	4.18	0.00	21.5	0.0	18.0	5.1
844.00	4.18	0.00	0.00	0.00	0.00	4.18	0.00	21.5	0.0	17.5	4.9
845.00	4.18	0.00	0.00	0.00	0.00	4.18	0.00	11.0	0.0	17.0	4.8
846.00	4.18	0.00	0.00	0.00	0.00	4.18	0.00	11.0	0.0	16.5	4.7
847.00	4.18	0.00	0.00	0.00	0.00	4.18	0.00	11.0	0.0	16.1	4.6
848.00	4.18	0.00	0.00	0.00	0.00	4.18	0.00	3.1	0.0	15.7	4.5
849.00	4.18	0.00	0.00	0.00	0.00	4.18	0.00	3.1	0.0	15.3	4.4
850.00	4.18	0.00	0.00	0.00	0.00	4.18	0.00	13.8	0.0	14.9	4.3
851.00	4.18	0.00	0.00	0.00	0.00	4.18	0.00	13.8	0.0	14.6	4.2
852.00	4.18	0.00	0.00	0.00	0.00	4.18	0.00	13.8	0.0	14.2	4.1
853.00	4.18	0.00	0.00	0.00	0.00	4.18	0.00	13.8	0.0	13.9	4.0
854.00	4.18	0.00	0.00	0.00	0.00	4.18	0.00	36.4	0.0	13.6	3.9
855.00	4.18	0.00	0.00	0.00	0.00	4.18	0.00	36.4	0.0	13.4	3.8
856.00	4.18	0.00	0.00	0.00	0.00	4.18	0.00	36.4	0.0	13.1	3.7
857.00	4.18	0.00	0.00	0.00	0.00	4.18	0.00	53.0	0.0	12.9	3.7
858.00	4.18	0.00	0.00	0.00	0.00	4.18	0.00	29.8	0.0	12.7	3.6
859.00	4.18	0.00	0.00	0.00	0.00	4.18	0.00	29.8	0.0	12.5	3.5
860.00	4.18	0.00	0.00	0.00	0.00	4.18	0.00	29.8	0.0	12.4	3.4
861.00	4.18	0.00	0.00	0.00	0.00	4.18	0.00	9.9	0.0	12.2	3.4
862.00	4.18	0.00	0.00	0.00	0.00	4.18	0.00	9.9	0.0	12.1	3.0
863.00	4.18	0.00	0.00	0.00	0.00	4.18	0.00	9.9	0.0	12.0	3.1
864.00	4.18	0.00	0.00	0.00	0.00	4.18	0.00	16.0	0.0	12.0	3.1
865.00	4.18	0.00	0.00	0.00	0.00	4.18	0.00	16.0	0.0	11.9	3.1
866.00	4.18	0.00	0.00	0.00	0.00	4.18	0.00	54.0	0.0	11.9	3.1
867.00	4.18	0.00	0.00	0.00	0.00	4.18	0.00	42.0	0.0	11.9	3.1
868.00	4.18	0.00	0.00	0.00	0.00	4.18	0.00	42.0	0.0	11.9	3.1
869.00	4.18	0.00	0.00	0.00	0.00	4.18	0.00	42.0	0.0	11.9	3.2
870.00	4.18	0.00	0.00	0.00	0.00	4.18	0.00	42.0	0.0	12.0	4.6
871.00	4.18	0.00	0.00	0.00	0.00	4.18	0.00	36.9	0.0	12.1	4.6
872.00	4.18	0.00	0.00	0.00	0.00	4.18	0.00	36.0	0.0	10.5	4.6
873.00	4.18	0.00	0.00	0.00	0.00	4.18	0.00	36.0	0.0	9.0	4.6
874.00	4.18	0.00	0.00	0.00	0.00	4.18	0.00	36.0	0.0	7.5	3.2
875.00	4.18	0.00	0.00	0.00	0.00	4.18	0.00	36.0	0.0	6.0	3.3
876.00	4.18	0.00	0.00	0.00	0.00	4.18	0.00	47.9	0.0	5.8	3.3
877.00	4.18	0.00	0.00	0.00	0.00	4.18	0.00	47.9	0.0	5.6	3.3
878.00	4.18	0.00	0.00	0.00	0.00	4.18	0.00	47.9	0.0	5.5	5.6
879.00	4.18	0.00	0.00	0.00	0.00	4.18	0.00	47.9	0.0	5.3	5.6
880.00	4.18	0.00	0.00	0.00	0.00	4.18	0.00	47.9	0.0	5.2	5.5

881.00	4.18	0.00	0.00	0.00	0.00	4.18	0.00	63.2	0.0	9.0	5.6
882.00	4.18	0.00	0.00	0.00	0.00	4.18	0.00	63.2	0.0	8.9	5.9
883.00	4.18	0.00	0.00	0.00	0.00	4.18	0.00	63.2	0.0	8.8	5.9
884.00	4.18	0.00	0.00	0.00	0.00	4.18	0.00	63.2	0.0	11.4	5.8
885.00	4.18	0.00	0.00	0.00	0.00	4.18	0.00	0.0	0.0	11.4	5.8
886.00	4.18	0.00	0.00	0.00	0.00	4.18	0.00	49.7	0.0	11.3	5.8
887.00	4.18	0.00	0.00	0.00	0.00	4.18	0.00	176.2	0.0	11.3	5.8
888.00	4.18	0.00	0.00	0.00	0.00	4.18	0.00	176.2	0.0	11.3	5.9
889.00	4.18	0.00	0.00	0.00	0.00	4.18	0.00	9.4	0.0	11.3	5.9
890.00	4.18	0.00	0.00	0.00	0.00	4.18	0.00	9.4	0.0	11.3	5.9
891.00	4.18	0.00	0.00	0.00	0.00	4.18	0.00	45.7	0.0	7.6	5.3
892.00	4.18	0.00	0.00	0.00	0.00	4.18	0.00	45.7	0.0	7.6	5.3
893.00	4.18	0.00	0.00	0.00	0.00	4.18	0.00	45.7	0.0	7.6	5.3
894.00	4.18	0.00	0.00	0.00	0.00	4.18	0.00	10.3	0.0	7.7	5.5
895.00	4.18	0.00	0.00	0.00	0.00	4.18	0.00	10.3	0.0	7.7	5.5
896.00	4.18	0.00	0.00	0.00	0.00	4.18	0.00	10.3	0.0	7.7	5.5
897.00	4.18	0.00	0.00	0.00	0.00	4.18	0.00	61.9	0.0	4.8	3.5
898.00	4.18	0.00	0.00	0.00	0.00	4.18	0.00	106.1	0.0	4.8	3.5
899.00	4.18	0.00	0.00	0.00	0.00	4.18	0.00	106.1	0.0	4.8	3.5
900.00	4.18	0.00	0.00	0.00	0.00	4.18	0.00	18.1	0.0	17.6	8.3
901.00	4.18	0.00	0.00	0.00	0.00	4.18	0.00	18.1	0.0	17.6	8.3
902.00	4.18	0.00	0.00	0.00	0.00	4.18	0.00	22.8	0.0	17.6	8.3
903.00	4.18	0.00	0.00	0.00	0.00	4.18	0.00	19.2	0.0	17.6	8.3
904.00	4.18	0.00	0.00	0.00	0.00	4.18	0.00	20.4	0.0	17.6	8.2
904.10	4.18	0.00	0.00	0.00	0.00	4.18	0.00	6.3	0.0	11.0	6.3
905.00	4.18	0.00	0.00	0.00	0.00	4.18	0.00	18.0	0.0	17.6	8.2
906.00	4.18	0.00	0.00	0.00	0.00	4.18	0.00	18.0	0.0	4.8	3.4
907.00	4.18	0.00	0.00	0.00	0.00	4.18	0.00	18.0	0.0	17.8	10.9
908.00	4.18	0.00	0.00	0.00	0.00	4.18	0.00	11.6	0.0	17.7	10.9
909.00	4.18	0.00	0.00	0.00	0.00	4.18	0.00	11.6	0.0	17.7	10.8
910.00	4.18	0.00	0.00	0.00	0.00	4.18	0.00	11.6	0.0	17.6	10.8
911.00	0.00	0.00	0.00	0.00	0.00	0.00	0.00	14.5	0.0	17.6	10.8
912.00	0.00	0.00	0.00	0.00	0.00	0.00	0.00	14.5	0.0	17.6	10.8
913.00	0.00	0.00	0.00	0.00	0.00	0.00	0.00	40.9	0.0	17.5	10.7
914.00	0.00	0.00	0.00	0.00	0.00	0.00	0.00	40.9	0.0	17.4	11.3
915.00	0.00	0.00	0.00	0.00	0.00	0.00	0.00	40.9	0.0	4.4	3.2
916.00	0.00	0.00	0.00	0.00	0.00	0.00	0.00	40.9	0.0	4.4	3.1
917.00	0.00	0.00	0.00	0.00	0.00	0.00	0.00	10.0	0.0	14.4	9.1
918.00	0.00	0.00	0.00	0.00	0.00	0.00	0.00	10.0	0.0	14.3	9.0
919.00	0.00	0.00	0.00	0.00	0.00	0.00	0.00	10.0	0.0	14.2	9.0

LAMBDA	O+(4S)	O+(2D)	O+(2P)	C+(4P)	C+(2P*)	C+(ICT)	HE	N2(ABS)	N2(ION)	O2(ABS)	O2(ION)
920.00	0.00	0.00	0.00	0.00	0.00	0.00	0.00	95.8	0.0	14.2	9.0
921.00	0.00	0.00	0.00	0.00	0.00	0.00	0.00	95.8	0.0	14.1	8.9
922.00	0.00	0.00	0.00	0.00	0.00	0.00	0.00	55.6	0.0	14.1	8.9
923.00	0.00	0.00	0.00	0.00	0.00	0.00	0.00	31.9	0.0	4.0	2.9
23.10	0.00	0.00	0.00	0.00	0.00	0.00	0.00	31.9	0.0	4.0	2.9
924.00	0.00	0.00	0.00	0.00	0.00	0.00	0.00	31.9	0.0	13.5	10.8
925.00	0.00	0.00	0.00	0.00	0.00	0.00	0.00	31.9	0.0	13.5	10.8
926.00	0.00	0.00	0.00	0.00	0.00	0.00	0.00	19.0	0.0	13.4	10.8
926.20	0.00	0.00	0.00	0.00	0.00	0.00	0.00	19.0	0.0	13.4	10.8
927.00	0.00	0.00	0.00	0.00	0.00	0.00	0.00	19.0	0.0	13.4	10.8
928.00	0.00	0.00	0.00	0.00	0.00	0.00	0.00	19.0	0.0	13.3	10.7
929.00	0.00	0.00	0.00	0.00	0.00	0.00	0.00	64.5	0.0	13.2	10.7
930.00	0.00	0.00	0.00	0.00	0.00	0.00	0.00	64.5	0.0	3.6	2.8
930.70	0.00	0.00	0.00	0.00	0.00	0.00	0.00	4.8	0.0	26.0	17.0
931.00	0.00	0.00	0.00	0.00	0.00	0.00	0.00	64.5	0.0	25.7	18.6
932.00	0.00	0.00	0.00	0.00	0.00	0.00	0.00	3.1	0.0	25.7	18.6
933.00	0.00	0.00	0.00	0.00	0.00	0.00	0.00	3.1	0.0	25.6	18.5
933.40	0.00	0.00	0.00	0.00	0.00	0.00	0.00	3.1	0.0	25.6	18.5
934.00	0.00	0.00	0.00	0.00	0.00	0.00	0.00	3.1	0.0	25.6	18.5
935.00	0.00	0.00	0.00	0.00	0.00	0.00	0.00	3.1	0.0	25.6	18.5
936.00	0.00	0.00	0.00	0.00	0.00	0.00	0.00	2.9	0.0	25.5	18.5
937.00	0.00	0.00	0.00	0.00	0.00	0.00	0.00	0.0	0.0	3.3	2.6
937.80	0.00	0.00	0.00	0.00	0.00	0.00	0.00	10.0	0.0	5.0	2.5
938.00	0.00	0.00	0.00	0.00	0.00	0.00	0.00	3.1	0.0	23.6	14.1
939.00	0.00	0.00	0.00	0.00	0.00	0.00	0.00	120.8	0.0	23.5	14.1
940.00	0.00	0.00	0.00	0.00	0.00	0.00	0.00	120.8	0.0	23.5	14.1
941.00	0.00	0.00	0.00	0.00	0.00	0.00	0.00	120.8	0.0	23.5	14.0
942.00	0.00	0.00	0.00	0.00	0.00	0.00	0.00	120.8	0.0	23.4	14.0
943.00	0.00	0.00	0.00	0.00	0.00	0.00	0.00	39.8	0.0	23.4	14.0
944.00	0.00	0.00	0.00	0.00	0.00	0.00	0.00	39.8	0.0	23.4	13.9
944.50	0.00	0.00	0.00	0.00	0.00	0.00	0.00	39.8	0.0	23.4	13.9
945.00	0.00	0.00	0.00	0.00	0.00	0.00	0.00	39.8	0.0	30.2	19.9
946.00	0.00	0.00	0.00	0.00	0.00	0.00	0.00	39.8	0.0	30.1	19.8
947.00	0.00	0.00	0.00	0.00	0.00	0.00	0.00	5.2	0.0	30.1	19.8
948.00	0.00	0.00	0.00	0.00	0.00	0.00	0.00	0.0	0.0	30.1	19.8
949.00	0.00	0.00	0.00	0.00	0.00	0.00	0.00	0.0	0.0	30.1	19.8
949.74	0.00	0.00	0.00	0.00	0.00	0.00	0.00	0.0	0.0	6.3	3.2
950.00	0.00	0.00	0.00	0.00	0.00	0.00	0.00	7.2	0.0	30.1	19.7
951.00	0.00	0.00	0.00	0.00	0.00	0.00	0.00	7.2	0.0	30.1	19.7
952.00	0.00	0.00	0.00	0.00	0.00	0.00	0.00	7.2	0.0	3.0	2.2

953.00	0.00	0.00	0.00	0.00	0.00	0.00	0.00	7.2	0.0	2.9	2.2
954.00	0.00	0.00	0.00	0.00	0.00	0.00	0.00	7.2	0.0	2.9	2.2
955.00	0.00	0.00	0.00	0.00	0.00	0.00	0.00	7.2	0.0	28.5	23.0
956.00	0.00	0.00	0.00	0.00	0.00	0.00	0.00	15.9	0.0	28.5	22.9
957.00	0.00	0.00	0.00	0.00	0.00	0.00	0.00	15.9	0.0	28.5	22.9
958.00	0.00	0.00	0.00	0.00	0.00	0.00	0.00	15.9	0.0	28.5	22.9
959.00	0.00	0.00	0.00	0.00	0.00	0.00	0.00	260.8	0.0	28.5	22.9
960.00	0.00	0.00	0.00	0.00	0.00	0.00	0.00	260.8	0.0	28.5	22.9
961.00	0.00	0.00	0.00	0.00	0.00	0.00	0.00	56.9	0.0	27.1	19.6
962.00	0.00	0.00	0.00	0.00	0.00	0.00	0.00	56.9	0.0	27.1	19.6
963.00	0.00	0.00	0.00	0.00	0.00	0.00	0.00	56.9	0.0	27.1	19.6
964.00	0.00	0.00	0.00	0.00	0.00	0.00	0.00	56.9	0.0	27.0	19.6
965.00	0.00	0.00	0.00	0.00	0.00	0.00	0.00	56.9	0.0	27.0	19.6
966.00	0.00	0.00	0.00	0.00	0.00	0.00	0.00	63.4	0.0	27.0	19.6
967.00	0.00	0.00	0.00	0.00	0.00	0.00	0.00	63.4	0.0	27.0	19.6
968.00	0.00	0.00	0.00	0.00	0.00	0.00	0.00	63.4	0.0	26.9	19.6
969.00	0.00	0.00	0.00	0.00	0.00	0.00	0.00	63.4	0.0	26.9	19.6
970.00	0.00	0.00	0.00	0.00	0.00	0.00	0.00	63.4	0.0	26.9	19.6
971.00	0.00	0.00	0.00	0.00	0.00	0.00	0.00	63.4	0.0	26.9	19.5
972.00	0.00	0.00	0.00	0.00	0.00	0.00	0.00	68.1	0.0	22.0	16.0
972.50	0.00	0.00	0.00	0.00	0.00	0.00	0.00	370.0	0.0	32.0	16.0
973.00	0.00	0.00	0.00	0.00	0.00	0.00	0.00	68.1	0.0	21.9	16.0
974.00	0.00	0.00	0.00	0.00	0.00	0.00	0.00	0.1	0.0	21.9	16.0
975.00	0.00	0.00	0.00	0.00	0.00	0.00	0.00	68.1	0.0	21.9	16.0
976.00	0.00	0.00	0.00	0.00	0.00	0.00	0.00	68.1	0.0	21.8	16.0
977.00	0.00	0.00	0.00	0.00	0.00	0.00	0.00	68.1	0.0	21.6	16.0
977.03	0.00	0.00	0.00	0.00	0.00	0.00	0.00	0.7	0.0	4.0	2.5
978.00	0.00	0.00	0.00	0.00	0.00	0.00	0.00	68.1	0.0	21.8	16.0
979.00	0.00	0.00	0.00	0.00	0.00	0.00	0.00	44.2	0.0	21.7	15.9
980.00	0.00	0.00	0.00	0.00	0.00	0.00	0.00	44.2	0.0	21.7	15.9
981.00	0.00	0.00	0.00	0.00	0.00	0.00	0.00	44.2	0.0	21.7	15.9
982.00	0.00	0.00	0.00	0.00	0.00	0.00	0.00	44.2	0.0	21.6	15.9
983.00	0.00	0.00	0.00	0.00	0.00	0.00	0.00	44.2	0.0	22.9	16.8
984.00	0.00	0.00	0.00	0.00	0.00	0.00	0.00	44.2	0.0	22.8	16.7
985.00	0.00	0.00	0.00	0.00	0.00	0.00	0.00	44.2	0.0	22.8	16.7
986.00	0.00	0.00	0.00	0.00	0.00	0.00	0.00	0.0	0.0	22.8	16.7
987.00	0.00	0.00	0.00	0.00	0.00	0.00	0.00	0.0	0.0	22.7	16.7
988.00	0.00	0.00	0.00	0.00	0.00	0.00	0.00	0.0	0.0	22.7	16.6
989.00	0.00	0.00	0.00	0.00	0.00	0.00	0.00	0.0	0.0	22.7	16.6
990.00	0.00	0.00	0.00	0.00	0.00	0.00	0.00	0.0	0.0	22.6	16.6

LAMBDA	O+(4S)	O+(2D)	O+(2P)	C+(4P)	C+(2P*)	C+(TCT)	HE	N2(ABS)	N2(ICN)	O2(ABS)	O2(ICN)
991.00	0.00	0.00	0.00	0.00	0.00	0.00	0.00	1.5	0.0	1.9	1.1
991.00	0.00	0.00	0.00	0.00	0.00	0.00	0.00	0.0	0.0	1.6	1.1
992.00	0.00	0.00	0.00	0.00	0.00	0.00	0.00	0.0	0.0	1.9	1.6
993.00	0.00	0.00	0.00	0.00	0.00	0.00	0.00	0.0	0.0	1.9	1.6
994.00	0.00	0.00	0.00	0.00	0.00	0.00	0.00	0.0	0.0	13.1	11.1
995.00	0.00	0.00	0.00	0.00	0.00	0.00	0.00	0.0	0.0	13.0	11.0
996.00	0.00	0.00	0.00	0.00	0.00	0.00	0.00	0.0	0.0	13.0	11.0
997.00	0.00	0.00	0.00	0.00	0.00	0.00	0.00	0.0	0.0	13.0	11.0
998.00	0.00	0.00	0.00	0.00	0.00	0.00	0.00	0.0	0.0	1.7	1.5
999.00	0.00	0.00	0.00	0.00	0.00	0.00	0.00	0.0	0.0	1.7	1.4
1000.00	0.00	0.00	0.00	0.00	0.00	0.00	0.00	0.0	0.0	1.7	1.4
1001.00	0.00	0.00	0.00	0.00	0.00	0.00	0.00	0.0	0.0	1.6	1.4
1002.00	0.00	0.00	0.00	0.00	0.00	0.00	0.00	0.0	0.0	1.6	1.4
1003.00	0.00	0.00	0.00	0.00	0.00	0.00	0.00	0.0	0.0	1.6	1.4
1004.00	0.00	0.00	0.00	0.00	0.00	0.00	0.00	0.0	0.0	3.8	3.4
1005.00	0.00	0.00	0.00	0.00	0.00	0.00	0.00	0.0	0.0	3.8	3.4
1006.00	0.00	0.00	0.00	0.00	0.00	0.00	0.00	0.0	0.0	3.7	3.3
1007.00	0.00	0.00	0.00	0.00	0.00	0.00	0.00	0.0	0.0	3.7	3.3
1008.00	0.00	0.00	0.00	0.00	0.00	0.00	0.00	0.0	0.0	1.5	1.3
1009.00	0.00	0.00	0.00	0.00	0.00	0.00	0.00	0.0	0.0	1.4	1.3
1010.00	0.00	0.00	0.00	0.00	0.00	0.00	0.00	0.0	0.0	1.4	1.3
1010.20	0.00	0.00	0.00	0.00	0.00	0.00	0.00	0.0	0.0	1.4	1.3
1011.00	0.00	0.00	0.00	0.00	0.00	0.00	0.00	0.0	0.0	1.4	1.2
1012.00	0.00	0.00	0.00	0.00	0.00	0.00	0.00	0.0	0.0	1.4	1.2
1013.00	0.00	0.00	0.00	0.00	0.00	0.00	0.00	0.0	0.0	1.4	1.2
1014.00	0.00	0.00	0.00	0.00	0.00	0.00	0.00	0.0	0.0	1.3	1.2
1015.00	0.00	0.00	0.00	0.00	0.00	0.00	0.00	0.0	0.0	1.3	1.2
1016.00	0.00	0.00	0.00	0.00	0.00	0.00	0.00	0.0	0.0	1.3	1.2
1017.00	0.00	0.00	0.00	0.00	0.00	0.00	0.00	0.0	0.0	1.3	1.2
1018.00	0.00	0.00	0.00	0.00	0.00	0.00	0.00	0.0	0.0	1.3	1.2
1019.00	0.00	0.00	0.00	0.00	0.00	0.00	0.00	0.0	0.0	1.2	1.2
1020.00	0.00	0.00	0.00	0.00	0.00	0.00	0.00	0.0	0.0	1.2	1.1
1021.00	0.00	0.00	0.00	0.00	0.00	0.00	0.00	0.0	0.0	1.2	1.1
1021.00	0.00	0.00	0.00	0.00	0.00	0.00	0.00	0.0	0.0	1.2	1.1
1022.00	0.00	0.00	0.00	0.00	0.00	0.00	0.00	0.0	0.0	1.2	1.1
1023.00	0.00	0.00	0.00	0.00	0.00	0.00	0.00	0.0	0.0	1.1	1.1
1024.00	0.00	0.00	0.00	0.00	0.00	0.00	0.00	0.0	0.0	1.1	1.1
1025.00	0.00	0.00	0.00	0.00	0.00	0.00	0.00	0.0	0.0	1.1	1.1
1025.72	0.00	0.00	0.00	0.00	0.00	0.00	0.00	0.0	0.0	1.6	1.0
1026.00	0.00	0.00	0.00	0.00	0.00	0.00	0.00	0.0	0.0	1.0	1.0

1027.00	0.00	0.00	0.00	0.00	0.00	0.00	0.00	0.0	0.0	1.0	1.0
1028.00	0.00	0.00	0.00	0.00	0.00	0.00	0.00	0.0	0.0	1.0	0.0
1029.00	0.00	0.00	0.00	0.00	0.00	0.00	0.00	0.0	0.0	1.0	0.0